Improving building energy efficiency: biomimetic adaptive façade and computational data-driven approach

Dac Khuong Bui
ORCID: orcid.org/0000-0001-9105-7157

Submitted in total fulfillment of the requirements of the degree of
Doctor of Philosophy

Department of Infrastructure Engineering
THE UNIVERSITY OF MELBOURNE

October 2020

Abstract

The urbanisation and population growth are resulting in a significant increase in energy consumption in buildings, leading to a substantial increase in greenhouse gas (GHG) emissions. During the operation of buildings, a massive amount of GHG emissions are released due to the process of building heating, cooling, and lighting, which accounts for the most significant proportion in building energy consumption. Therefore, energy-efficiency design and operation will play an essential role in reducing GHG emissions in buildings.

Façade systems are one of the most critical aspects regarding the efficient management of heating, cooling, and lighting energy in buildings. A façade system is a barrier and exchanger (simultaneously) for temperature, light, and air between the building indoor environment and the outside environment. Therefore, the proper design and operation of the façade can effectively save substantial energy. For decades, engineers and researchers from all over the world have been in search for the intelligent design and operation of the façade systems to improve energy efficiency and sustainability in buildings, and to not compromise a pleasant indoor environment for building occupants. Subsequently, they have found that many natural systems have developed a highly efficient biological structure to adapt to dynamic and extreme environments over millions of years. These natural systems now have become great inspirations for the research community in the quest for building energy efficiency solutions, and the biomimetic adaptive façade (BAF) system is one of those remarkable examples of adopting bioinspiration in buildings.

The BAF system is considered as a potential solution to improve the performance of conventional façade systems. The BAF system has an ability to adapt its functions, features, or

behaviour for dynamically varying climatic conditions, providing buildings with the operational flexibility to act in response to different climate scenarios. Nonetheless, the practical application of a BAF in buildings remains limited due to the absence of a comprehensive design platform that can facilitate the widespread adoption of BAF systems. Most studies on BAFs remain at a conceptual stage of development, and an effective platform that can effectively assist the design and operation of BAF is still lacking.

This thesis proposes and develops a methodology for enhancing building energy efficiency using the design of BAF systems, and thereby supports the transition to next-generation façades. Specifically, the objective of this thesis is to develop, test, and evaluate a computational data-driven optimisation approach in assisting the BAF design. The thesis presents a multidisciplinary approach that combines building energy modelling, metaheuristic optimisation, and data-driven methods. The goal of the proposed approach is to minimise the total energy consumption in buildings, including heating, cooling, and lighting energy, but still maintain the indoor environmental quality in terms of thermal and visual performance. A comprehensive analysis of the proposed computational data-driven optimisation approach is provided in the thesis.

In summary, this study has proposed a computational data-driven approach based on building energy simulations, optimisation processes, and machine learning algorithms. The proposed approach is used to assist the design and operation of BAFs for building energy efficiency and analyse the interactions between energy-saving and indoor environmental quality. These significant findings demonstrate the potential of BAFs to enhance the energy efficiency of buildings, and the developed platform can be used as an effective tool to support BAFs in both design and product development.

Declaration

This is to certify that:

i. the thesis comprises only my original work toward the PhD,
ii. due acknowledgement has been made in the text to all other material used,
iii. the thesis is fewer than 100,000 words in length, exclusive of tables, maps, bibliographies, and appendices.

Khuong

Dac Khuong Bui, October 2020

Acknowledgements

I would like to express my special appreciation and thanks to my supervisors, Professor Tuan Ngo and Dr Tuan Nguyen, from the Department of Infrastructure Engineering at The University of Melbourne. I would like to thank you for the guidance, support, and encouragement throughout my candidature. I appreciate all your contributions to make my PhD journey productive and stimulating.

I have been blessed with great fellow members of the Advanced Protective Technologies for Engineering Structures (APTES) group. Thank you for all the knowledge sharing, insightful discussions, and encouragement. Thanks to Dr Steven Linforth, Dr Abdallah Ghazlan, Dr Philip Christopher, Tu Le, and other great members of my research group.

Last but not least, I would like to express my love and thanks to my wife and family, who have always helped and encouraged me. Thank you for supporting me with everything.

Preface

I hereby confirm that the works presented in this thesis are based on my original research during my PhD candidature at the University of Melbourne (September 2016 – July 2020). I was the investigator and was responsible for all the works in the thesis.

The works in Chapter 3, Chapter 5 and appendix A in this thesis have been published in three journals, while the works in Chapter 4 is ready to submit to a journal. My PhD supervisors, Prof Tuan Ngo, Dr Tuan Nguyen supervised my works and contributed to the published articles. My co-authors, Dr Abdallah Ghazlan, Dr H. Nguyen-Xuan from Ho Chi Minh City University of Technology (Hutech), Prof Jui-Sheng Chou from National Taiwan University of Science and Technology, and Dr Ngoc-Tri Ngo from The University of Danang – University of Science and Technology supported with the revision and evaluation of the published articles. The amount of my contribution towards each published chapter is listed below:

Chapter 3: Published in Applied Energy 265 (2020)

Journal Impart Factor: 8.426, Rank 1/408 in Civil Engineering

Personal contribution: 70%

Reference: **Bui, D.-K**., T.N. Nguyen, A. Ghazlan, N.-T. Ngo, and T.D. Ngo, *Enhancing building energy efficiency by adaptive façade: A*

computational optimization approach. Applied Energy, 2020. 265: p. 114797.

Chapter 4: Ready to submit in Applied Energy

Personal contribution: 70%

Reference: **Bui, D.-K.**, T.N. Nguyen, A. Ghazlan, and T.D. Ngo, *The computational design of biomimetic adaptive façade for energy efficiency building*. (in-progress)

Chapter 5: Published in Energy 190 (2020)

Journal Impart Factor: 5.537, Rank 8/408 in Civil Engineering

Personal contribution: 70%

Reference: **Bui, D.-K**., T.N. Nguyen, T.D. Ngo, and H. Nguyen-Xuan, *An artificial neural network (ANN) expert system enhanced with the electromagnetism-based firefly algorithm (EFA) for predicting the energy consumption in buildings*. Energy, 2020. 190: p. 116370.

Appendix A: Published in Construction and Building Materials 180 (2018)

Journal Impart Factor: 4.046, Rank 28/408 in Civil Engineering

Personal contribution: 70%

Reference**: Bui, D.-K.**, T. Nguyen, J.-S. Chou, H. Nguyen-Xuan, and T.D. Ngo, *A modified firefly algorithm-artificial neural network expert system for predicting compressive and tensile strength of high-performance concrete*. Construction and Building Materials, 2018. 180: p. 320-333.

Publications

These publications are not mentioned in the Preface:

1. Le, D.T., **D.-K. Bui**, T.D. Ngo, Q.-H. Nguyen, and H. Nguyen-Xuan, *A novel hybrid method combining electromagnetism-like mechanism and firefly algorithms for constrained design optimization of discrete truss structures*. Computers & Structures, 2019. 212: p. 20-42.
2. **D.-K. Bui**, T. Nguyen., T.D. Ngo, *Predicting forest fires by using modified firefly algorithm-artificial neural network*. in 7th International Conference on Protection of Structures against Hazards. 2018. Hanoi, Vietnam **(Highly Recommendable Paper awards)**
3. **D.-K. Bui**, T. Nguyen., H. Nguyen-Xuan, T.D. Ngo, An electromagnetism - firefly algorithm for structural optimisation. in 25th Australasian Conference on Mechanics of Structures and Materials (ACMSM25). 2018. Brisbane, Australia

Table of Contents

List of Figures

List of Tables

Chapter 1
Introduction

1.1 Research Background

World energy consumption is from three major economic sectors, namely transportation, industry, and building [1]. A substantial share of global energy consumption is from buildings, which is expected to increase to 32.4% of total energy consumption by 2040 [2]. Moreover, by 2050, the population of all cities in the worlds will welcome more than 2.5 billion additional people, which means around two-thirds of the world's population will live in cities in the next three decades [3]. The growth of population in urban areas will result in higher energy consumption in buildings. The energy is derived from both electricity and fossil fuels (gas, coal, and oil). Electricity and fossil fuels account for 54% and 43% of total building energy, respectively [4]. As a result, buildings will release a massive amount of GHG emissions when consuming energy when operating. It is known that an increase in GHG emissions will escalate climate change, which has adversely affected many aspects of the natural environment. Therefore, it is urgently important to improve energy efficiency in buildings.

Energy consumption in buildings occurs through building services, including heating, cooling, lighting, ventilation, cooking, transport, appliances, and equipment. Generally, heating, cooling, and lighting energy accounts for the most significant proportion of building energy consumption [5]. The efficiency of energy consumption for heating, cooling, and lighting is affected by the façade system of buildings. The façade system is responsible for visible light transmittance, heat transmission, solar heat gain coefficient, and air ventilation between a building and the environment. Hence the total energy consumption in a building can

significantly be reduced by improving the performance of the façade system [6]. Many efforts have been carried out to demonstrate the significant role of façade systems in building energy efficiency. For example, the effect of different façade types on the cooling energy of a multistorey building in Brisbane, Australia, was compared by Rafat [7]. The results show that the best overall energy consumption is achieved for a moderate performance glazing, but not the higher or smaller performance glazing, and the use of an effective façade can reduce energy consumption by 6% - 20% [7].

Recently, a biomimetic adaptive façade (BAF) is considered as a potential solution to improve the energy performance of buildings. A BAF has an ability to adapt its functions, features, or behaviour to dynamically varied climatic conditions, which can provide buildings the flexibility to act in response to different climate scenarios. BAFs also allow for individual building components to adapt to climatic change rather than one single solution for all operational situations. They are increasingly becoming a promising solution for low-energy building operations while still maintaining high levels of indoor environmental quality.

From a technical point of view, the design of BAF systems for building energy efficiency is an optimisation problem (i.e., minimising energy consumption) with dynamically varying constraints (i.e., climatic and outdoor conditions). As a result, traditional approaches for façade design with only a single design solution (i.e., static façade design), which is irresponsive to the changes of climatic conditions, fail to address the problem. Therefore, a BAF, which is responsive to the change of climatic conditions, is needed to improve energy efficiency in building. A BAF has an ability to change its properties to adapt to variable climatic conditions, thereby achieving the best optimal operational stage for reducing the total energy consumption. In this way, the BAF system is optimised to react to the changes of climatic conditions, and the BAF system enables the adaptation of individual building component such as a single-window rather than one single solution for all operational scenarios [8].

1.2 Problem Statement

Despite the many advantages of BAFs, the application of BAFs in existing and future buildings is still limited, and it is a lack of solutions facilitating the widespread adoption of BAF systems [9]. There are several reasons which hinder the wide adoption of BAF. First of all, the process of design and operation of BAFs require a multidisciplinary approach, which combines diverse expertise and skills such as building energy simulation, optimisation, and data analysis. The next reason is the ability of current building energy simulation software to model the adaptive response of BAFs accurately. Finally, the implementation of control strategies on BAFs during these simulations remains challenging [10]. These difficulties have limited the potential of adaptive façades. As a result, most of the current studies on BAFs remain at a conceptual stage of development and have not resolved the mentioned difficulties.

This thesis aims to contribute to the development and application of BAF systems in terms of design and operation. Specifically, the goal is to propose a computational, data-driven platform to assist the design and operation of a BAF to reduce the energy consumption in buildings. To archive this goal, firstly, a computational approach is developed to support and improve the performance of BAF during the operation. A biomimetic approach, which mimics the strategies found in nature to solve human problems, is then incorporated to create a new concept of BAF design in this study. The goal is to find new insights into the evolution and operation of biological systems in nature and then apply these insights to BAF design. Finally, the data-driven approach is proposed in this study to enhance the capacity of building energy simulation. Overall, this thesis investigates the potential of BAF to improve the energy efficiency in buildings, thereby reducing GHG emissions.

1.3 Objective and scope of the thesis

In order to provide an energy-efficient building, the main aim of this research is to develop, test, and evaluate a computational data-driven approach that can be used to support the design and operation of BAFs in buildings. Four objectives directly related to the research aim are as below:

- To develop and test a computational approach, based on simulation and optimisation techniques, to explore the performance potential of BAFs in enhancing the energy efficiency of office buildings.
- To investigate a biomimetic approach in the development of a BAF design for using in locations that have variable climates such as Melbourne and Texas.
- To develop and evaluate a data-driven approach for prediction of energy consumption in office buildings.
- To propose an integrated computational, data-driven platform to design the BAF system for improving energy efficiency in office buildings.

The BAFs is a multi-disciplinary research area that covers many aspects of façade systems. This thesis focuses on a specific sub-area within the broader field of adaptive façades. A clarification of the specific scope of the thesis is given below:

- Performance of buildings: this thesis focuses on saving energy of buildings by minimising the total lighting, heating, and cooling load while keeping the indoor environmental quality in terms of thermal and visual comfort.
- Type of adaptability: the focus of this research is on façade adaption with the hourly time step.

- BAF: the term BAF used in this thesis refers to a façade that has an ability to change its functions (i.e., thermotical, structural) over time in response to weather fluctuations, daily cycles, or seasonal patterns.
- BAF property type: the thesis concentrates on the thermophysical and optical properties of the exterior façade.
- The role in the building design process: the proposed approach is developed with the target of assessing the viability of adaptive façades as a design strategy in general. The results of this research can be used as a guide for future research and development processes. Therefore, the work is not necessarily limited to currently available materials but intends to facilitate the exploration of next-generation BAF concepts.

1.4 Outline of the thesis

The thesis is divided into seven chapters, which are briefly highlighted as follows:

- **Chapter 1** presents an introduction to the research background, motivation, research methodology, objectives, and scope of the thesis.
- **Chapter 2** provides the background and characteristics of the BAF and the application of the data-driven and computational approach in energy-efficient buildings.
- **Chapter 3** is an article that was published in Applied Energy journal, with the title of **"**Enhancing building energy efficiency by adaptive façade: A computational optimisation approach". This chapter develops and tests a computational approach based on simulation and optimisation techniques to explore the performance potential of the adaptive façade.

- **Chapter 4** proposes the concept of an BAF for energy efficiency in buildings. This chapter presents the second research objective of this thesis by investigating and transferring the biological features found in chameleons into designing façade systems. The works in this chapter is ready to submit to Applied Energy journal, with the title of "Computational design of adaptive, biomimetic electrochromic windows for enhancing building energy efficiency".
- **Chapter 5** is an article that was published in the *Energy* journal, with the title of "An artificial neural network (ANN) expert system enhanced with electromagnetism-based firefly algorithm (EFA) for predicting energy consumption in building". This chapter develops a data-driven approach and shows its applications in predicting energy consumption in buildings. Two case studies were investigated in this work.
- **Chapter 6** proposes an integrated computational, data-driven platform to design the BAF system for improving building energy efficiency. This chapter demonstrates that the data-driven approach can predict the energy consumption in buildings, including heating, cooling and lighting energy with high accuracy. Therefore, it can complement the building energy simulation software in the computational optimisation approach and improve the effectiveness of the BAFs.
- **Chapter 7** presents the key conclusions of the thesis and provides recommendations for future research**.**

The thesis structure and the connections between the chapters are illustrated by in Figure 1.1.

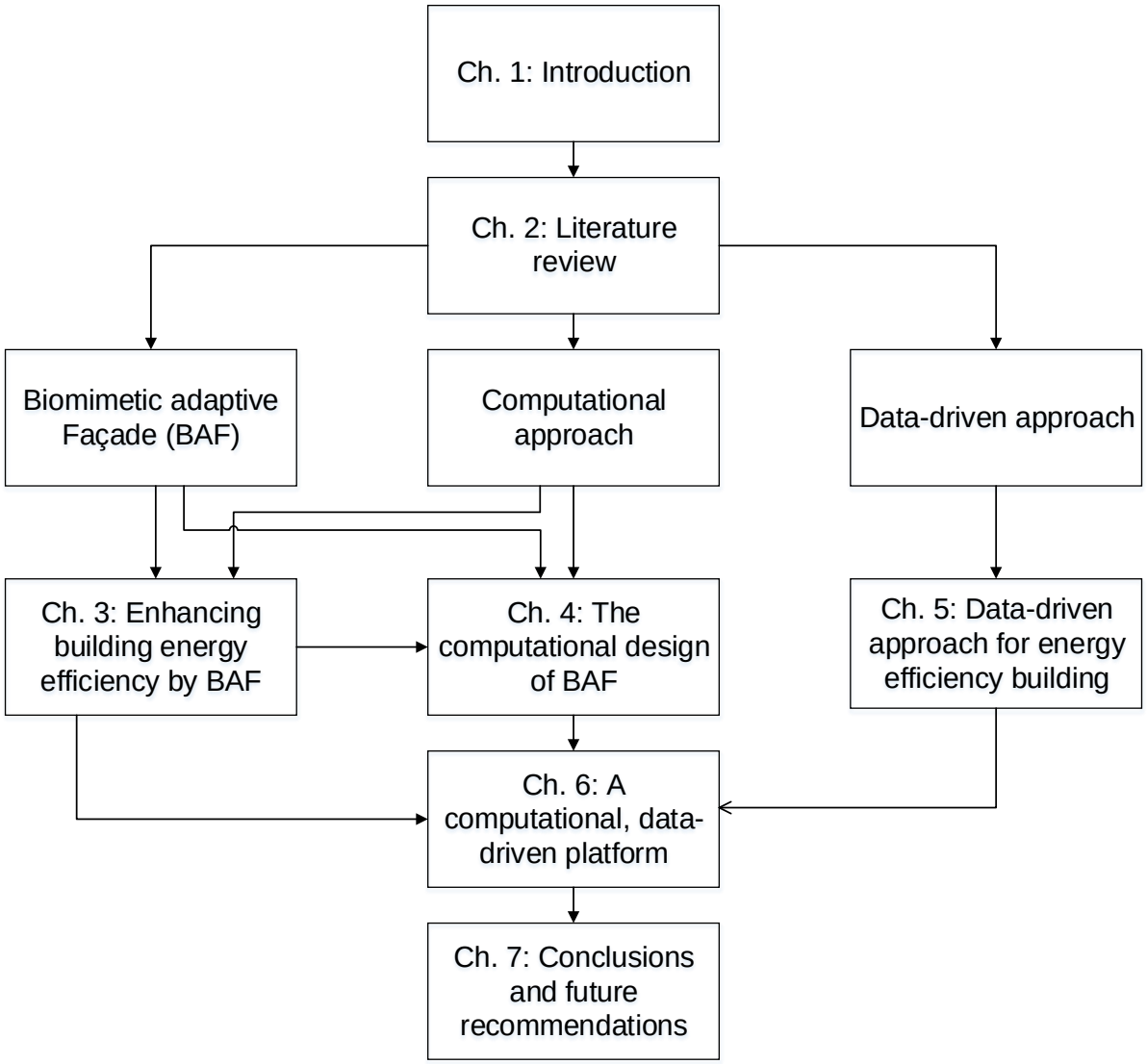

Figure 1-1. Thesis layout and structure

References

1. Al-Homoud, M.S., *Computer-aided building energy analysis techniques.* Building and Environment, 2001. 36(4): p. 421-433.

2. IEA, *World Energy Outlook 2015*. 2015.

3. Ritchie, H. and M.J.O.W.i.D. Roser, *Urbanization.* 2018.

4. Ürge-Vorsatz, D., L.F. Cabeza, S. Serrano, C. Barreneche, and K. Petrichenko, *Heating and cooling energy trends and drivers in buildings.* Renewable and Sustainable Energy Reviews, 2015. 41: p. 85-98.

5. Pérez, G., J. Coma, S. Sol, and L.F. Cabeza, *Green facade for energy savings in buildings: The influence of leaf area index and facade orientation on the shadow effect.* Applied Energy, 2017. 187: p. 424-437.

6. Kim, K. and C. Jarrett, *Energy performance of an adaptive façade system*. 2014. 2014.

7. Al Waked, R., *Effect of Façade Type on the Cooling Load of a Multi-Storey Building.* Cambridge Young Scientist Journal, 2010. 1(1): p. 9-14.

8. Lee, C.-s., *Simulation-based performance assessment of climate adaptive greenhouse shells*. 2017, PhD Thesis, TU Eindhoven.

9. Loonen, R.C.G.M., M. Trčka, D. Cóstola, and J.L.M. Hensen, *Climate adaptive building shells: State-of-the-art and future challenges.* Renewable and Sustainable Energy Reviews, 2013. 25: p. 483-493.

10. de Klijn-Chevalerias, M., R. Loonen, A. Zarzycka, D. De Witte, M. Sarakinioti, and J. Hensen. *Assisting the development of innovative responsive façade elements using building performance simulation*. in *Proceedings of SimAUD2017, Symposium on Simulation for Architecture and Urban Design*. 2017.

Chapter 2
Literature review

2.1 Introduction

This chapter provides a range of literature reviews on the research background related to improving façade system performance in buildings. There are three approaches of improving façade system, including biomimetic adaptive façades (BAF) approach, computational approach and data-driven approach, are investigated in the Thesis. The comprehensive background of each approach is reviewed and discussed in a sub section and a summary of the literature review is presented at the end of this chapter. These approaches are then discussed in more details in Chapter 3, 4 and 5 when each chapter focuses on an approach, respectively.

2.2 Overview of biomimetic adaptive façade

2.2.1 Adaptive characteristic of façade

In building, façade systems play an essential role owing to its multi-functionalities. In fact, the façade system provides safety, privacy for building occupants and also protects them against harsh weather such as wind, rain, and hot/cold temperature. The façade system is considered as a boundary between inside and outside environments; therefore, it affects the comfort of building occupants and the energy performance of buildings. Conventional façades are designed as static components. That means they cannot adapt to weather fluctuations, daily cycles, or seasonal patterns. On the other hand, BAF which recently emerge as an exciting development in building design can proactively change its functions (i.e., thermotical, structural) over time in response to dynamic weather conditions. Within the design concept of

BAF, many different definitions, including smart [1], intelligent [2], dynamic [3], responsive [4], advanced [5], and kinetic [6] façades, were used by the engineer, architect and researchers. Nonetheless, there are two main research directions for BAF that can be discerned.

The first direction involves façade systems that have active components with the actuation of movable parts via a mechanical system [7, 8]. For example, Ahmed *et al.* [7] proposed a smart kinetic shading system, which can change its opening angle through a sensor-based computer controlling system. Ahmed *et al.* proved that the system could consume less energy than to the reference building by 18-20% [7]. In another study, Mahmoud and Elghazi validated and compared the rotational and translational motion for hexagonal façade patterns [8]. They proved that the rotational motion gained a better daylight level than translational motion, and the proposed façade improved daylight from 30% to 50% compared to the static façade system.

The second direction focuses on the use of responsive materials, which can change its physical properties (e.g. U-value) in response to dynamic climatic conditions, for the BAF system. This direction can be categorized into two sub-directions, which are the passively adaptive control strategy (using photochromic and thermochromic windows) and the actively adaptive control strategy (using electrochromic windows). For the first group, the photochromic and thermochromic windows change their properties with the fluctuation of solar radiation and temperature, respectively, and the adaptation ais uncontrollable. In contrast, the active adaptation of electrochromic windows can be achieved by adjusting small voltage inputs, which enables a more active and controllable method.

The effectiveness of photochromic and thermochromic windows has been proven in several studies. Wu *et al.* developed a cost-effective photochromic window that can reduce the visible light transmittance and solar transmittance by 25% - 65% and 12% - 25%, respectively, compared to double glazed low-E [9]. Zhang *et al.* proposed a perovskite thermochromic

window to obtain not only a high solar modulation ability but also a low transition temperature and high luminous transmittance [10]. Runqi *et al.* investigated the energy and visual performance of several types of thermochromic windows, and the results showed that the thermochromic windows can save building energy and improve the optical performance, compared to traditional clear double windows [11].

The electrochromic windows have been attracting more attention than the passive adaptive type because of their controllability. Lee *et al.* [12] provided a full-scale outdoor field test to validate the performance of an electrochromic window. In their study, the solar heat gain coefficient and visible transmittance (Tvis) of the adaptive window can vary in a range of [0.09-0.41] and [0.01-0.6], respectively, by using a small voltage (3-5 Volts). The electrochromic window was subdivided into three zones, and the solar heat gain coefficient and the visible transmittance of each zone were controllable [12]. Lee *et al.* [12] found the room with the electrochromic window saved 50% energy consumption compared to a benchmark room with a conventional low-emittance window. Ajaji and Andre investigated a control strategy for the electrochromic windows of a building in Brussels [13]. They proved that the annual energy consumption of an office, equipped with electrochromic glazing, reduced by approximately 70%.

From the literature, it was found that BAF systems can improve the total energy consumption of buildings. Nevertheless, it should be noticed that the relationships between the operational stage of BAF systems, either changing the topology of façade systems by dynamic controlling shading devices or changing the material properties, and the building energy consumption are complex non-linear problems [14, 15]. The operation of the BAF must correctly represent a sequence of time-varying façade system stages corresponding to climatic conditions. It means that the status of BAF, such as the position of controlling components or material properties, needs to dynamically change to correctly adapt to various scenarios and

account for short-term heat transfer and energy storage effects in buildings [16]. Therefore, the performance of the BAF primarily depends on its adapted status during the operation, which requires a thorough design of the BAF to achieve the desired performance. For example, the selection of materials for electrochromic windows requires prior knowledge of the time-varying sequence of material properties such as U-value and Tvis concerning climate data at building locations. However, this complicated task is still challenging because there is a lack of a reliable computational design approach to assist this process. Most of the previous studies mainly focused on the concept design phase of BAF, and there is no comprehensive study on the operation of BAF. It is essential to have a tool that can support BAF during the operation to improve the performance of BAF.

2.2.2 Biomimetic approach

Biological systems can adapt to harsh environments in nature because they have unique integration geometries, characteristics, and strategies. The term biomimetic, firstly introduced by Otto Schmidt, is related to the solutions obtained by mimicking functional analogies, processes, and mechanisms from nature [18]. Biomimetic can be called with other words, including bio-inspired and biomimicry, but they are all about the transfer strategies found in nature into engineering and technology. Biomimetic is not a new idea as people always are looking for solutions from nature for innovation. However, it is never too late to seek the solution from nature as the living organisms change in every moment.

In the foretime, people have a connection with nature when they used to use animal skins, bamboo, or timber as envelopes of houses. The relationship with nature was gradually lost because modern buildings prefer to use concrete, glass, and steel as a building envelope. However, the connection has steadily come back with many new façade designs inspired by nature. There are many biomimetic approaches in the development of building envelope systems, and they can be classified into two groups: (1) form and (2) function [19].

The first group is to mimic the morphological appearance, visual shape of the organism or biological system in nature. For instance, Sheikh and Asghar, inspired by the shape of Oxalis oregana leaf, proposed a two-axes, foldable shading device which can be folded along both horizontal and vertical axes [20]. The device can enable shading under several angles of sunlight, thereby reducing the sun-glare and overheating in the building during the hot season. They validated the performance of the biomimicry shading device by applying to a 20-story commercial building in Lahore, Pakistan. The results showed that the proposed device can reduce the energy consumption in the building by 32% and keep a haft of floor area with the naturally, satisfactory light level of 500 – 750 lux [20]. In another study, Han *et al.* studied the particular retro-reflecting property of the flower petals, then modelled a bio-inspired retro-reflective building envelope [21]. In addition, many applications inspired by Strelitzia reginae flower, spruce cones are presented [22].

The second group of biomimetic approaches is to mimic the underlying biological mechanism. This group focuses on what a natural system behaves rather than how it looks, and they inspire from nature by direct approach and indirect approach. The direct approach explicitly mimics the functional fundamentals of the organism or biological system into the same-role elements of the façade system. In contrast, the indirect method take the conceptual inspiration from natural systems into the mimicry transformation. This group is more popular than the other group because of the similarity between the building envelope and the skins of living organisms.

Many ideas inspired by biological principles have been proposed and investigated [23-27]. For example, Webb *et al.* investigated the heat transfer of animal fur and then transferred that distinctive performance characteristic to building façades [23]. The results from this study showed that the fur-lined façade could reduce the heat gains and heat losses by 50% during summer and winter, respectively, when comparing with a conventional lightweight façade. In

another study, Taghizade and Taraz focused on the effect of the pattern of bird feathers on the energy consumption of the bird. They then proposed a design of a mobile surface inspired by bird feathers to reduce energy consumption and increase the shade for buildings [24]. In addition, various biological principles have been reviewed in other studies, such as seeds and leaves of a plant [25], tree bark [26], polar bear hair [27]. Most of studies focus on developing a kinetic façade, which can move and change the position, but the study on adaptive thermal material is limited. Moreover, most of all published BAF remain at a conceptual stage of development, and there are under ten percentage of studies that having energy analysis [29]. Studies of BAF is still limited while the potential of BAF in improving the energy efficiency of buildings is undisputed. It needs to have a comprehensive study on BAF elicit other potentials of BAF, especially on the design and operation phases.

2.3 Overview of the computational approach in enhancing energy efficiency in buildings

Nowadays, building energy simulation programs have been widely used in building design. They help to evaluate the energy performance of the building in the design stage by analysing the energy consumption, system operation, and weather conditions of the building. The early energy assessment of energy usage can significantly help to reduce energy consumption and improve system efficiency [30]. Therefore, building energy simulation programs have enormous potential in building design.

There are several effective building energy simulation programs, including EnergyPlus, DOE-2, Window, HAM, TRNSYS, and eQUEST. They have several different features, which make them distinctive, in terms of engine algorithms, ease of use, modelling resolution, and modelling options. They can help designers to simulate the building with their design and predict the energy consumption, thereby quickly validating the designs. Moreover, the software

is also useful for retrofitting buildings and improving the system. Hence, they are used by many engineering and designer during the past decade.

For instance, Dahanayake and Chow used EnergyPlus to simulate the thermal effect of vertical greenery systems [31]. The energy management system feature of EnergyPlus was used to predict the vertical greenery system on indoor air temperature and surface temperature of façades. Guarino *et al.* investigated the importance of life cycle step of building on the energy consumption and global warming potential by TRNSYS [32]. Also, Song and Meng used eQUEST software to simulate the energy consumption of the actual university library [33]. Many variables, including summer air supply temperature, summer indoor temperature, indoor personnel density and lighting power density, were used in the simulation.

There are many building energy simulation programs with various applications. Therefore, it is important to choose suitable software for each application. However, Crawley *et al.* provided a detailed comparison of many building performance simulation tools in terms of their features and capabilities [34]. This review showed that EnergyPlus is one of the most effective building energy simulation software with the capacity of calculating heating and cooling energy in a variable time step. In another study, Loonen compared the capabilities of several building energy simulation software in assisting six applications of adaptive façade, as shown in Table 2-1 [35]. The comparison indicated that EnergyPlus can support most of the applications related to BAF.

Table 2-1. Comparison of the capability of several building energy simulation software.

Applications	Software			
	EnergyPlus	TRNSYS	eQUEST	ESP-r
Thermochromic glazing	Y	E	N	Y
Electrochromic glazing	Y	E	Y	Y
Phase change materials	Y	Y	N	Y
Insulating solar shading	Y	E	N	N
Movable insulation	Y	E	N	N

Green walls and roofs	Y	Y	N	N

Y: The capability is available to use by advanced users.
E: The capability is available, but an expert experience is required.
N: The capability is not available.

Therefore, EnergyPlus was selected for this study because it provides the ability to assist the design and operation process of the BAF system, and it was successfully used in many previous studies. EnergyPlus is open-source software and is developed by the U.S. Department of Energy (DOE), Building Technologies Office (BTO) [36]. This program can be used for simulating energy consumption from lighting, HVAC, and plug and process loads in buildings. EnergyPlus is a console-based program and thereby users have to deal with text-based inputs and outputs (e.g., .html, .txt, .cvs). Therefore, EnergyPlus has been considered as a rigorous program by many users.

However, EnergyPlus has no graphical user interface, so it is hard to operate the software. Fortunately, there are some graphical user interface software that can be integrated into EnergyPlus for model creation, including DesignBuilder, OpenStudio, AECOsim Energy Simulator, Google SketchUp, gEnergy, and Simergy. The building models can be generated in these software, which is more accurate and efficient than the text-based approach. Similar to other building energy simulation softwares, EnergyPlus does not provide any built-in functions for advanced analyses such as automation, parametric analysis, and optimisation. In other words, all manipulation in EnergyPlus, including changes in material properties, running time, and thermostat setting, must be manually developed by a user. It will be difficult for many users to use EnergyPlus because it is too complicated. EnergyPlus requires many expert's experiences to use, so it needs a methodology to support the use of EnergyPlus.

2.4 Overview of data-driven in enhancing energy efficiency in buildings

Data-driven approaches apply machine learning (ML) and statistical tools to solve problems, which are hard to handle by traditional computational techniques [37]. Three main

reasons support the development of ML in recent years [40]. First, the improvement of ML-oriented techniques, including tensor processing units and graphic processor units, help people access easily to computational resources. Second, the speedy development of the internet of things technologies provides the opportunity to obtain a massive amount of data for everyone. Third, more and more state-of-the-art ML algorithms have been developed to enhance the capacity of ML in a wide range of fields. Notably, many ML techniques have been applied to improve energy performance in building [41-43].

In data-driven approaches, ML algorithms learn from the provided data and try to understand the relationship among all variables in the data. The self-learning process of ML can be categorised into three groups, including supervised, unsupervised, and reinforcement. In supervised learning, all the input and output variables are identified before training the ML model, or in other words, all variables in data are labelled. Then, the ML model learns and understands the relationship between the inputs and outputs. Regarding building energy, the inputs can be properties of windows or the outdoor air temperature, while the outputs are the heating and cooling energy in buildings. Most of ML applications in improving energy efficiency in buildings used supervised learning. For example, Kumar *et al.* used an ML algorithm to estimate the heating and cooling energy in buildings [44]. In this study, the input variables were used are structural attributes of buildings, such as surface area, relative compactness, glazing area of the building, while the heating and cooling load were used as the output variables. The results of this study showed that the ML approach could find the relationship between the structural attributes and the total energy consumption of buildings. In another study, Naji *et al.* validated the effects of the properties of the façade system on the total energy consumption by using the ML approach [45]. The inputs, in this case, were the properties of the façade system, including the thermal conductivity, thickness, and type of façade, and the only output was the total heating and cooling energy.

Unsupervised learning is used when there is no specified prediction output, and the main goal is to explore data analysis to categorise all the variables. This approach is useful when analyse data with a high number of variables (e.g., big data) because it can help to identify important variables, thereby reducing unnecessary variables and simplifying the data. The unsupervised learning tries to find the relationship among unlabelled variable in a dataset. Applications of unsupervised learning in building energy include identification of occupant's behaviour, data analytics, and anomaly detection [46, 47]. For instance, Tang *et al.* applied an unsupervised approach to choose the most critical inputs that affect the heating and cooling demand [48]. The results showed that the unsupervised approach improved the accuracy by 11% compared to the model without an unsupervised approach.

The last group of ML is reinforcement learning. In this group, the output is the intended target, and the main goal is to find the inputs using the try and error method. The ML model generates random inputs and grades these inputs based on their relationship with the output. The most popular application of reinforcement learning is the self-driving vehicle, which can drive without the control of humans. Within the scope of this thesis, reinforcement learning is not investigated much, but it still has some applications in this field. For example, Mocanu *et al.* proposed two reinforcement algorithms, which are the state-action-reward-state-action and Q-learning, and an unsupervised deep belief network to predict energy consumption using unlabelled historical data [49]. The study proved that the combining model between Q-learning and deep belief networks obtained the best accuracy when predicting the energy consumption problem in this study.

Recently, among many ML techniques, artificial neural network (ANN) has been widely used in optimising the design for energy-efficient building [50-52]. ANN simulates the function of the biological neuron by imitating the working principles of the human brain in a simplified manner. ANN can be useful for many problems with linear or with non-linear patterns. Many

advantages of ANN were demonstrated in several studies. For instance, Jin *et al.* used an ANN-based thermal control logic model to optimise initial conditions and heating system operations for energy-efficient [50]. Also, Chung *et al.* proposed an ANN model to design a comfortable indoor thermal environment in an energy-efficient manner [53]. However, there are not many studies on applying ANN to enhance the façade system's performance, especially BAF. It can be explained that both BAF and ML (i.e., ANN) are new research areas, so not many researchers are trying to incorporate them.

2.5 Summary

The literature review shows that BAF is a potential solution to enhance energy efficiency in buildings. The main advantage of BAF is the ability to change its functions (i.e., thermotical, structural) over time in response to weather fluctuations, daily cycles, or seasonal patterns. The capacity of BAF has been validated in many studies in the literature. Still, most of the studies focused on the active components with the actuation of movable parts and there is lack of research on responsive materials. It also was found that BAFs are required proper designs and operations to obtain the maximum performance and reach their full potential. Therefore, this thesis proposed a computational optimisation approach to support BAF design and validated the potential of the BAF design with several case studies in Chapter 3. In addition, a biomimetic approach is proposed and analysed in Chapter 4 to find new insights into the evolution and operation of biological systems in nature. Adaptation is one of the most crucial factors in the development of biological systems. Analysing and investigating these adaptation strategies are crucial for the success of transferring these strategies to BAF design.

Many studies in the literature have proven the capabilities of ML algorithms in building energy simulations. Hence, this study proposes a data-driven approach to study energy efficiency in buildings. This data-driven approach is based on the ANN model, and an in-house

optimisation tool is used to enhance the performance of the ANN model. The development and validation of the data-driven approach is presented in Chapter 5. Finally, a computational data-driven platform for the design of BAF is presented in chapter 6.

References

1. Iken, O., S.e.-D. Fertahi, M. Dlimi, R. Agounoun, I. Kadiri, and K. Sbai, *Thermal and energy performance investigation of a smart double skin facade integrating vanadium dioxide through CFD simulations.* Energy Conversion and Management, 2019. 195: p. 650-671.

2. Liu, M., K.B. Wittchen, and P.K. Heiselberg, *Control strategies for intelligent glazed façade and their influence on energy and comfort performance of office buildings in Denmark.* Applied Energy, 2015. 145: p. 43-51.

3. Johnsen, K. and F.V. Winther, *Dynamic Facades, the Smart Way of Meeting the Energy Requirements.* Energy Procedia, 2015. 78: p. 1568-1573.

4. Taveres-Cachat, E., S. Grynning, J. Thomsen, and S. Selkowitz, *Responsive building envelope concepts in zero emission neighborhoods and smart cities - A roadmap to implementation.* Building and Environment, 2019. 149: p. 446-457.

5. Taveres-Cachat, E., S. Grynning, O. Almas, and F. Goia, *Advanced transparent facades: market available products and associated challenges in building performance simulation.* Energy Procedia, 2017. 132: p. 496-501.

6. Hosseini, S.M., M. Mohammadi, and O. Guerra-Santin, *Interactive kinetic façade: Improving visual comfort based on dynamic daylight and occupant's positions by 2D and 3D shape changes.* Building and Environment, 2019. 165: p. 106396.

7. Ahmed, M., A. Abdel-Rahman, M. Bady, and E.K. Mahrous, *The thermal performance of residential building integrated with adaptive kinetic shading system.* International Energy Journal, 2016. 16: p. 97-106.

8. Mahmoud, A.H.A. and Y. Elghazi, *Parametric-based designs for kinetic facades to optimize daylight performance: Comparing rotation and translation kinetic motion for hexagonal facade patterns.* Solar Energy, 2016. 126: p. 111-127.

9. Wu, L.Y.L., Q. Zhao, H. Huang, and R.J. Lim, *Sol-gel based photochromic coating for solar responsive smart window.* Surface and Coatings Technology, 2017. 320: p. 601-607.

10. Zhang, Y., et al., *Perovskite thermochromic smart window: Advanced optical properties and low transition temperature.* Applied Energy, 2019. 254: p. 113690.

11. Liang, R., Y. Sun, M. Aburas, R. Wilson, and Y. Wu, *Evaluation of the thermal and optical performance of thermochromic windows for office buildings in China.* Energy and Buildings, 2018. 176: p. 216-231.

12. Lee, E.S., C. Gehbauer, B.E. Coffey, A. McNeil, M. Stadler, and C. Marnay, *Integrated control of dynamic facades and distributed energy resources for energy cost minimization in commercial buildings.* Solar Energy, 2015. 122: p. 1384-1397.

13. Ajaji, Y. and P. André. *Support for energy and comfort management in an office building using smart electrochromic glazing: dynamic simulations*. in *Proceedings of BS2015: 14th conference of IBPSA*. 2016. BS publications.

14. Ngo, N.-T., *Early predicting cooling loads for energy-efficient design in office buildings by machine learning.* Energy and Buildings, 2019. 182: p. 264-273.

15. Lee, S.W. and J.S. Park, *Evaluating thermal performance of double-skin facade using response factor.* Energy and Buildings, 2019: p. 109657.

16. Loonen, R., *Shaping the next generation of adaptive facade concepts with the use of simulations*. 2014.

17. Benyus, J.M., *Biomimicry: Innovation inspired by nature*. 1997, Morrow New York.

18. Vincent, J.F., O.A. Bogatyreva, N.R. Bogatyrev, A. Bowyer, and A.-K.J.J.o.t.R.S.I. Pahl, *Biomimetics: its practice and theory.* 2006. 3(9): p. 471-482.

19. Zari, M.P., *Biomimetic design for climate change adaptation and mitigation.* Architectural Science Review, 2010. 53(2): p. 172-183.

20. Sheikh, W.T. and Q. Asghar, *Adaptive biomimetic facades: Enhancing energy efficiency of highly glazed buildings.* Frontiers of Architectural Research, 2019. 8(3): p. 319-331.

21. Han, Y., J.E. Taylor, and A.L. Pisello, *Toward mitigating urban heat island effects: Investigating the thermal-energy impact of bio-inspired retro-reflective building envelopes in dense urban settings.* Energy and Buildings, 2015. 102: p. 380-389.

22. López, M., R. Rubio, S. Martín, and C. Ben, *How plants inspire façades. From plants to architecture: Biomimetic principles for the development of adaptive architectural envelopes.* Renewable and Sustainable Energy Reviews, 2017. 67: p. 692-703.

23. Webb, M., E. Hertzsch, and R. Green. *Modelling and optimisation of a biomimetic façade based on animal fur*. in *Proceedings of building simulation*. 2011.

24. Taghizade, K. and M.J.A.J.M.E.T. Taraz, *Designing a mobile facade using bionic approach.* 2013. 1(2): p. 22-29.

25. Fernández, M.L., R. Rubio, and S.M. González. *Architectural envelopes that interact with their environment*. in *2013 International Conference on New Concepts in Smart Cities: Fostering Public and Private Alliances (SmartMILE)*. 2013. IEEE.

26. Yowell, J. and N. Oklahoma, *Biomimetic building skin: A phenomenological approach using tree bark as model*. 2011, Citeseer.

27. Stegmaier, T., M. Linke, H.J.P.T.o.t.R.S.A.M. Planck, Physical, and E. Sciences, *Bionics in textiles: flexible and translucent thermal insulations for solar thermal applications.* 2009. 367(1894): p. 1749-1758.

28. Corp, S. *StoColor Lotusan*. 2019; 2019:[Available from: https://www.stocorp.com/coatings-us/.

29. Kuru, A., P. Oldfield, S. Bonser, and F. Fiorito, *Biomimetic adaptive building skins: Energy and environmental regulation in buildings.* Energy and Buildings, 2019. 205: p. 109544.

30. Trčka, M. and J.L.M. Hensen, *Overview of HVAC system simulation.* Automation in construction, 2010. 19(2): p. 93-99.

31. Dahanayake, K.W.D.K.C. and C.L. Chow, *Studying the potential of energy saving through vertical greenery systems: Using EnergyPlus simulation program.* Energy and Buildings, 2017. 138(Supplement C): p. 47-59.

32. Guarino, F., et al., *Integration of Building Simulation and Life Cycle Assessment: A TRNSYS Application.* Energy Procedia, 2016. 101(Supplement C): p. 360-367.

33. Song, J., X. Zhang, and X. Meng, *Simulation and Analysis of a University Library Energy Consumption based on EQUEST.* Procedia Engineering, 2015. 121(Supplement C): p. 1382-1388.

34. Crawley, D.B., J.W. Hand, M. Kummert, and B.T. Griffith, *Contrasting the capabilities of building energy performance simulation programs.* Building and Environment, 2008. 43(4): p. 661-673.

35. Loonen, R., *Approaches for computational performance optimization of innovative adaptive façade concepts*, in *Department of the Built Environment*. 2018, Eindhoven University of Technology: Netherlands.

36. (DOE), U.S.D.o.E. *Commercial Reference Buildings*. Available from: https://www.energy.gov/.

37. Flood, I., *Towards the next generation of artificial neural networks for civil engineering.* Advanced Engineering Informatics, 2008. 22(1): p. 4-14.

38. Mousavi, S.M., P. Aminian, A.H. Gandomi, A.H. Alavi, and H. Bolandi, *A new predictive model for compressive strength of HPC using gene expression programming.* Advances in Engineering Software, 2012. 45(1): p. 105-114.

39. Platon, R., V.R. Dehkordi, and J. Martel, *Hourly prediction of a building's electricity consumption using case-based reasoning, artificial neural networks and principal component analysis.* Energy and Buildings, 2015. 92: p. 10-18.

40. Hong, T., Z. Wang, X. Luo, and W. Zhang, *State-of-the-art on research and applications of machine learning in the building life cycle.* Energy and Buildings, 2020. 212: p. 109831.

41. Pham, A.-D., N.-T. Ngo, T.T. Ha Truong, N.-T. Huynh, and N.-S. Truong, *Predicting energy consumption in multiple buildings using machine learning for improving energy efficiency and sustainability.* Journal of Cleaner Production, 2020. 260: p. 121082.

42. Robinson, C., et al., *Machine learning approaches for estimating commercial building energy consumption.* Applied Energy, 2017. 208: p. 889-904.

43. Yang, S., M.P. Wan, W. Chen, B.F. Ng, and S. Dubey, *Model predictive control with adaptive machine-learning-based model for building energy efficiency and comfort optimization.* Applied Energy, 2020. 271: p. 115147.

44. Kumar, S., S.K. Pal, and R.P. Singh, *A novel method based on extreme learning machine to predict heating and cooling load through design and structural attributes.* Energy and Buildings, 2018. 176: p. 275-286.

45. Naji, S., et al., *Estimating building energy consumption using extreme learning machine method.* Energy, 2016. 97(Supplement C): p. 506-516.

46. Fan, C., F. Xiao, Z. Li, and J. Wang, *Unsupervised data analytics in mining big building operational data for energy efficiency enhancement: A review.* Energy and Buildings, 2018. 159: p. 296-308.

47. Miller, C., Z. Nagy, and A. Schlueter, *A review of unsupervised statistical learning and visual analytics techniques applied to performance analysis of non-residential buildings.* Renewable and Sustainable Energy Reviews, 2018. 81: p. 1365-1377.

48. Tang, F., A. Kusiak, and X. Wei, *Modeling and short-term prediction of HVAC system with a clustering algorithm.* Energy and Buildings, 2014. 82: p. 310-321.

49. Mocanu, E., P.H. Nguyen, W.L. Kling, and M. Gibescu, *Unsupervised energy prediction in a Smart Grid context using reinforcement cross-building transfer learning.* Energy and Buildings, 2016. 116: p. 646-655.

50. Moon, J.W., J.-H. Lee, J.D. Chang, and S. Kim, *Preliminary performance tests on artificial neural network models for opening strategies of double skin envelopes in winter.* Energy and Buildings, 2014. 75: p. 301-311.

51. Asadi, E., M.G.d. Silva, C.H. Antunes, L. Dias, and L. Glicksman, *Multi-objective optimization for building retrofit: A model using genetic algorithm and artificial neural network and an application.* Energy and Buildings, 2014. 81: p. 444-456.

52. Magnier, L. and F. Haghighat, *Multiobjective optimization of building design using TRNSYS simulations, genetic algorithm, and Artificial Neural Network.* Building and Environment, 2010. 45(3): p. 739-746.

53. Chung, M.H., Y.K. Yang, K.H. Lee, J.H. Lee, and J.W. Moon, *Application of artificial neural networks for determining energy-efficient operating set-points of the VRF cooling system.* Building and Environment, 2017. 125: p. 77-87.

54. Lee, A., W.Z. Geem, and K.-D. Suh, *Determination of Optimal Initial Weights of an Artificial Neural Network by Using the Harmony Search Algorithm: Application to Breakwater Armor Stones.* Applied Sciences, 2016. 6(6).

55. Yam, Y.F. and T.W.S. Chow, *Determining initial weights of feedforward neural networks based on least squares method.* Neural Processing Letters, 1995. 2(2): p. 13-17.

56. Chang, Y.-T., J. Lin, J.-S. Shieh, and M.F. Abbod, *Optimization the Initial Weights of Artificial Neural Networks via Genetic Algorithm Applied to Hip Bone Fracture Prediction.* Advances in Fuzzy Systems, 2012. 2012: p. 9.

57. Liu, Q., X. Cui, Y.-C. Chou, M.F. Abbod, J. Lin, and J.-S. Shieh, *Ensemble artificial neural networks applied to predict the key risk factors of hip bone fracture for elders.* Biomedical Signal Processing and Control, 2015. 21: p. 146-156.

Chapter 3
Enhancing building energy efficiency by adaptive façade: A computational optimisation approach

[PUBLISHED JOURNAL[1]]

3.1 Introduction to the paper

This chapter is a published article in *Applied Energy journal (Journal Impart Factor: 8.426, Rank 1/408 in Civil Engineering)*, titled "Enhancing building energy efficiency by adaptive façade: A computational optimisation approach". The article presents the first research objective of this thesis, which are proposing a strategy for building energy simulation and exploring the performance potential of adaptive façade for improving building energy efficiency. The highlights of this study are:

- A computational optimisation approach is proposed to support adaptive façade design.
- Two case studies are used to validate the capacity of the proposed computational optimisation approach.
- The effects of the adaptive façade on heating, cooling, and lighting energy are analysed and discussed.
- The study facilitates the exploration of next-generation adaptive façade concepts.

The key findings in this study are:

- The computational optimisation approach, which uses a combination of building energy modelling software (EnergyPlus), the metaheuristic optimisation algorithm and Eppy

[1] Bui, D.-K., T.N. Nguyen, A. Ghazlan, N.-T. Ngo, and T.D. Ngo, *Enhancing building energy efficiency by adaptive façade: A computational optimization approach*. Applied Energy, 2020. 265: p. 114797.

toolkit, can effectively assist the design and operation of adaptive façades systems.

- The adaptive façade, which is assisted by the computational optimisation approach can reduce from 14.2% - 29.0% of the total energy consumption in building compared to the non-adaptive façades.
- The properties of adaptive façade (i.e., U-value and Tvis) are reasonably responsive to dynamic climatic conditions.

3.2 Abstract

The energy consumption in buildings, which accounts for approximately one-third of the total energy used in the world, can be reduced significantly by employing adaptive façades. In this study, a computational optimisation approach is proposed to enhance the energy efficiency of buildings based on the design of an adaptive façade system, which can adapt its thermal and visible transmittance for dynamically varying climatic conditions. The engine of the adaptive façade design approach is an automated optimisation process, which combines the building energy simulation program (EnergyPlus) with an optimisation technique through Eppy, a powerful Python toolkit. The modified firefly algorithm, an in-house optimisation tool, is employed to design the adaptive façade system in this study. However, our proposed method is not tied to any particular optimisation tool and does not impose any restrictions on a type of building. To this end, the capability of the proposed method for enhancing building energy efficiency is validated by two case studies, namely a typical single office room and a medium office building. We found that the proposed adaptive façade system can reduce the energy consumption by 14.9% - 29.0% and 14.2% - 22.3% for the first and second case study, respectively, compared to the static façades. These significant findings demonstrate the potential of adaptive façades to enhance the energy efficiency of buildings.

3.3 Introduction

The International Energy Agency reported that transportation, industry (i.e., energy-intensive manufacturing, nonenergy-intensive manufacturing, and nonmanufacturing), and building sectors account for the highest energy consumption in the global economy [1]. In fact, the building sector is expected to consume more than one-third of the global energy consumption by 2040 [2]. The energy used by the building sector is expected to grow by 1.5% and 2.1% per year from 2012 to 2040 in member countries of the Organization for Economic Cooperation and Development (OECD) and developing countries, respectively [3]. The energy consumed during the operational stage of a building (e.g., for lighting, heating, and cooling) accounts for a large proportion of the energy consumption in a building during its life cycle [4]. Therefore, it is crucial to reduce the energy used during the operational stage of buildings to achieve the Net Zero Energy Buildings (NZEB) target [5].

According to Sun *et al.* [6], the solutions to NZEB during the operational stage of a building can be categorized into active or passive solutions. Active solutions involve improving lighting systems, heating, ventilation, air conditioning (HVAC) systems, and other service energy-intensive systems. Passive solutions aim to improve the energy efficiency of building envelopes (e.g., façade systems) [6]. The potential energy saved through active solutions was widely recognized in many studies [7, 8]. In contrast, passive solutions have attracted the attention of researchers in recent years in the context of improving the energy efficient design of façade systems. For example, Andjelkovic *et al.* showed that the transmittance of a double-skin façade can reduce both heat losses and gains in a building compared to a single-skin façade [9]. Passive solutions are more cost-effective, i.e., they incur lower investment costs compared to their energy-saving potential.

Various methods were proposed to improve the façade system for NZEB, which can be divided into two common strategies. The first strategy involves the instrumentation of shading devices to reduce the heat gained from sunlight through a façade system. For example, Gao *et al.* proposed a sun-tracking photovoltaic shading element that not only reduces annual energy generation but also provides better protection against glare [10]. The second strategy aims to investigate the effect of thermal transmittance (U-value) or thermal resistance (R-value) of façade systems on energy efficiency. For instance, Rodrigues *et al.* studied the impact of U-value on the energy consumption of buildings with different thermal masses. They concluded that the thermal mass affects the energy usage and U-value scale differently [11]. The two strategies share the same objective in terms of reducing the energy for lighting, heating and cooling in buildings.

Furthermore, reducing the heat gained from sunlight by using shading devices or low thermal transmittance materials may affect the visual comfort of building occupants, which is associated with the transparency and intensity of natural light [12]. In fact, the variations of climatic conditions (e.g., daylighting, natural ventilation, heat gain from sunlight) pose significant challenges to the design of an effective façade system for NZEB. The energy efficiency of façade systems is sensitive to climatic and outdoor conditions, which hinder their applications for NZEB [13].

It can be stated that the design of façade systems for building energy efficiency is an optimisation problem (i.e., minimizing energy consumption) with dynamically varying constraints (i.e., climatic and outdoor conditions). As a result, traditional approaches for façade design with only a single design solution (i.e., static façade systems), which is irresponsive to the changes of climatic conditions, fail to address the problem completely. Therefore, an adaptive façade system, which is responsive to the change of climatic conditions, is needed to improve NZEB. The adaptive façade has the ability to change its properties to adapt to variable

climatic conditions, which can achieve the best optimal operational stage for reducing the total energy consumption. In this way, the adaptive façade system is optimized to react to the changes of climatic conditions. The adaptive façade system also allows for individual building components (e.g., a single-window) to adapt to climatic change rather than one single solution for all operational scenarios [14].

In this study, we aim to develop a computational optimisation approach, which is built upon building energy modeling (BEM) and optimisation techniques, to explore the potential performance of the adaptive façade system for reducing the energy consumption of buildings. EnergyPlus, a BEM software, is used to evaluate the energy consumption of buildings subjected to varying climatic conditions. There are several BEM software packages for evaluating the energy consumption and occupant comfort in buildings such as EnregyPlus [15], TRNSYS [16], ESP-r [17] and eQuest [18]. These software packages have been used by architects, engineers and researchers to evaluate the energy efficiency and occupant comfort in buildings during the operational stage. Crawley *et al.* [19] reported that EnergyPlus has been employed in many studies as it can efficiently analyze the effect of façade systems on energy consumption as well as occupant comfort (e.g., visual comfort). For example, Chong *et al.* developed a continuous calibration framework, which uses EnergyPlus as an engine, to utilize different sources of information [20]. In another study, Kamal *et al.* used EnergyPlus to model thermal energy storage in a standard reference large office building and then developed a control strategy to reduce operating costs [21]. Therefore, we use EnergyPlus to evaluate the energy consumption of buildings in this study. We then propose a new computational optimisation approach using Eppy, a Python toolkit, to integrate EnergyPlus and optimisation algorithms to design the adaptive façade system, which accounts for the dynamic change of climatic conditions. We prove that the adaptive façade system can significantly reduce the total energy consumption of buildings.

3.4 Literature Review

Adaptive façade (AF) is a building envelope that can frequently change its functions (i.e., thermotical, structural) over time in response to weather fluctuations, diurnal cycles or seasonal patterns to reduce the energy consumption of a building. Several variations of AF, including smart [22], intelligent [23], dynamic [24], responsive [25], advanced [26] and kinetic [27] façades, have been used by engineers, architects and researchers. There are two main research directions for AF that can be discerned, which are reviewed hereafter.

The first direction involves façade systems that have active components, which operate via the actuation of movable parts in a mechanical system [28, 29]. For example, Ahmed *et al.* [28] proposed a smart kinetic shading system, which can change its opening angle through a sensor-based computer controlled system. Ahmed *et al.* showed that AF can reduce the energy consumption of a reference building by 18-20% [28]. Mahmoud and Elghazi validated and compared the rotational and translational motion of hexagonal façade patterns [29]. They reported that the proposed façade improved daylight from 30% to 50% compared to the static façade system through rotational motion.

The second direction focuses on the use of responsive materials in AF, which can change their physical properties (e.g., U-value) in response to dynamic climatic conditions. This direction can be categorized into two sub-directions, which involve passive-adaptive (photochromic and thermochromic) and active-controllable adaptive (EC) windows. Photochromic and thermochromic glazing change their properties in response to fluctuations of solar radiation and temperature, respectively, and the property changes cannot be controlled. In contrast, EC glazing can change their properties by applying and adjusting a small voltage, which is a more active and controllable method.

The effectiveness of photochromic and thermochromic windows has been proven in several studies. Wu *et al.* developed a cost-effective photochromic window that can reduce the visible light transmittance and solar transmittance by 25% - 65% and 12% - 25%, respectively, compared to a normal glass [30]. Zhang *et al.* proposed a perovskite thermochromic window to obtain high solar modulation, a low transition temperature and high luminous transmittance [31]. Runqi *et al.* reported that several types of thermochromic windows reduced building energy consumption and improved visual performance, compared to traditional clear double glazed windows [32].

EC windows have been attracting more attention than their passive-adaptive counterpart due to their controllability. Lee *et al.* [33] conducted a full-scale outdoor field test to validate the performance of an EC window for which they varied the solar heat gain coefficient and visible transmittance (Tvis) between [0.09-0.41] and [0.01-0.6], respectively, by applying a small voltage (3-5 Volts). The EC window is subdivided into three zones, and the solar heat gain coefficient and the visible transmittance of each zone are controllable [33]. After one week, Lee *et al.* [33] found that the room with the EC window reduced energy consumption by 50% compared to a benchmark room with a conventional low-emittance window. Ajaji and Andre investigated a control strategy for the EC windows of a building in Brussels [34]. They proved that the annual energy consumption of a floor equipped with EC glazing reduced energy consumption by approximately 70%. Lee *et al.* proposed an optimized EC glazing control to enhance the energy efficiency of a commercial building in different climates [35]. Four control parameters, including outdoor air temperature, room air temperature, solar radiation incident on window and global horizontal irradiance, were optimized to minimize the annual energy consumptions of the building. The results showed that EC glazing reduced the annual energy consumption by 17.4% compared to the typical static window case [35].

From the literature, we found that AF systems have achieved a positive impact on the total energy consumption of buildings. Nevertheless, we also noticed that predicting the energy consumption of buildings in the operational stage of AF systems involves complex and nonlinear problems, which are obtained by either changing the topology of façade systems by dynamic controlling shading devices or changing the material properties of windows [36, 37]. The operation of the AF must correctly represent a sequence of time-varying stages corresponding to climatic conditions. This implies that the status of AF, such as the position of the controlling components or material properties, need to dynamically change to correctly adapt to various scenarios, and account for short-term heat transfer and energy storage effects in buildings [38]. Therefore, the performance of the AF primarily depends on its adapted status during the operation stage, which requires a thorough design to achieve the desired performance. For example, the selection of materials for EC windows requires prior knowledge of the time-varying sequence of material properties such as U-value and Tvis with respect to climate data. However, this complicated task is still challenging because a reliable computational design approach is lacking.

For the AF in this study, we assume that adaptation is achieved by adjusting its U-value, which is the rate of heat transferred through a material, and Tvis, which is a ratio of visible light transmitted through a material in response to dynamic climatic conditions. The assumption is aligned with the EC windows of the adaptive façade system reported by Lee *et al.* [33]. We propose a computational optimisation approach for designing the AF, which will provide a time-varying sequence of desired material properties (U-value and Tvis) for enhancing the energy performance of buildings. We use the proposed approach, which is powered by the Eppy toolkit, to integrate optimisation techniques with EnergyPlus for obtaining the optimal time-varying sequence, which can inform the design of the AF system. The proposed computational optimisation approach is detailed in Section 3. Section 4

introduces two case studies in the paper. Section 5 presents the results and discussions of the two case studies. Section 6 provides concluding remarks and recommendations for future work.

3.5 Methodology

3.5.1 EnergyPlus

EnergyPlus is an open-source, BEM software and has been considered as the first choice for modeling the energy performance of buildings by researchers, engineers and architects [15]. The development of EnergyPlus is funded by the U.S. Department of Energy (DOE), Building Technologies Office (BTO). This program can be used for simulating energy consumption from lighting, HVAC, and plug and process loads in buildings. EnergyPlus is a console-based program and thereby processes text-based inputs and returns the results in different text formats (e.g., .html, .txt, .cvs). Therefore, EnergyPlus has been considered as a difficult program by many users. Fortunately, there are several graphical user interfaces that EnergyPlus can be linked with, including Autodesk Revit, DesignBuilder, OpenStudio, AECOsim Energy Simulator, Google SketchUp, gEnergy, and Simergy. These software packages can be used to create the geometry of the building and extract the required EnergyPlus Input Data File (.idf) for simulation.

In this study, Autodesk Revit [39] is used to generate the geometry of a building for the performance simulation in EnergyPlus, which is more accurate and efficient than the text-based approach. After creating the geometry of the building in Autodesk Revit, the model is transferred to another Autodesk program called Green Building Studio to convert the building geometry into an EnergyPlus Input Data File (.idf), which is ready to perform the energy simulation. However, EnergyPlus does not provide any built-in functions for advanced analyzes such as automation, parametric analysis and optimisation. In other words, all manipulation in EnergyPlus, including changes in material properties, running time and

thermostat setting, must be manually applied by a user. This arduous process thereby has many limitations of applications. This issue limits the efficiency of the program and causes difficulties for designing the adaptive façade system, which requires an automatic optimisation approach.

3.5.2 Eppy

Eppy, developed by Philip *et al.* [40], is an open-source package in the Python programming language, which provides a powerful toolkit for controlling and manipulating EnergyPlus in a systematic and programmatic way. Eppy is a scripting language for EnergyPlus input and output files, which is used as an interpreter between EnergyPlus and Python. As depicted in Figure 3-1, this package is a bridge to transfer data between two programs. Eppy can change the properties of any EnergyPlus objects for energy simulation, read the output files and transfer the results back to Python for further analysis (e.g., optimisation and design of the AF system in this study).

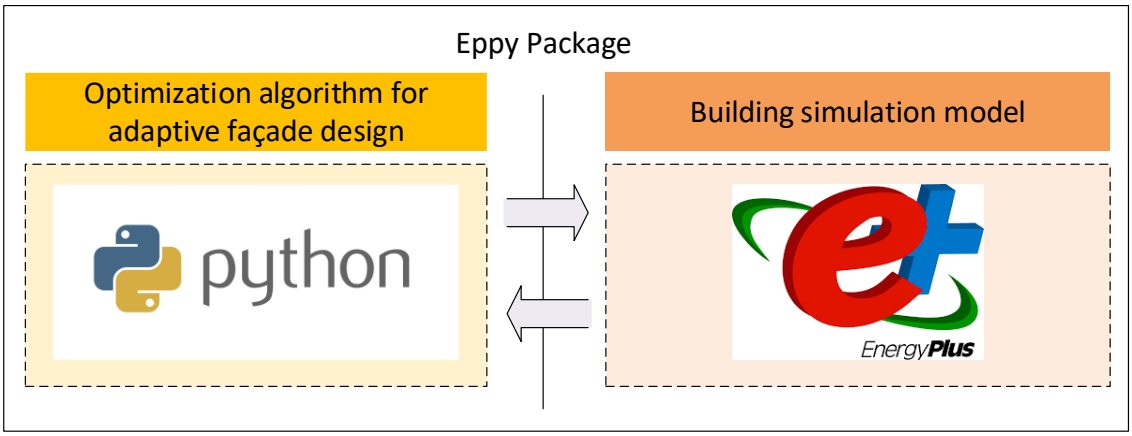

Figure 3-1. The role of the Eppy package as an interpreter between EnergyPlus and Python.

Figure 3-2 shows a schematic of the design process, which includes three main steps for the adaptive façade. In step 1, a building is modelled in Revit, which generates the geometry profiles and the material properties of all objects (e.g., wall, roof, ground and window system).

The building model is then transferred to Green Building Studio to create an EnergyPlus input file in step 2. In step 3, other settings of the building, including a period of running time, time step, thermostat setting and climatic conditions, will be added to EnergyPlus by using the Eppy toolkit as shown in Figure 3.1 and Figure 3-2. The building energy simulation and optimisation process will be conducted on the Python using the Eppy toolkit to obtain the design of the adaptive façade. In this study, we use an in-house code for the optimisation process in Python, which is presented in the next section.

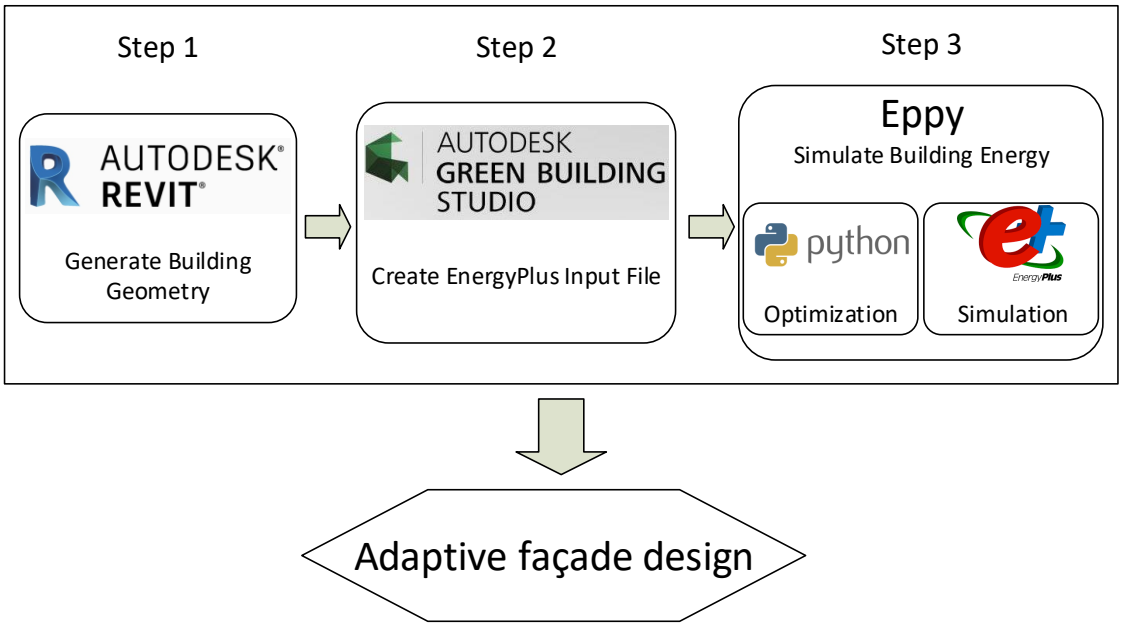

Figure 3-2. Schematic of the adaptive façade design process.

3.5.3 Modified firefly algorithm

This section briefly presents the development of the modified firefly algorithm (MFA) for the optimisation component in step 3 of the adaptive façade design (Figure 2). Interested readers are encouraged to refer to [41, 42] for the detailed development of MFA. MFA is an enhanced version of the Firefly algorithm (FA), which is inspired by the behavior of tropical fireflies and first proposed by Yang [43]. This stochastic, swarm-based metaheuristic algorithm follows three primary rules:

(1) Fireflies are attracted together.

(2) Attractiveness decreases when distance increases, and vice versa.

(3) An objective function is defined to control the attractiveness of the fireflies.

When a firefly (i^{th}) is attracted to a brighter firefly (j^{th}), it will fly to another location calculated by Eq.3.1 as follows:

$$x_i^{t+1} = x_i^t + \beta^t (x_j^t - x_i^t) + \alpha \times \varepsilon \times s \tag{3.1}$$

where x is the location of a firefly; t is the iteration; β is the attractiveness of a firefly (Eq. 3.2); α is a trade-off constant used to decide the random behavior of firefly (Eq. 4); ε is a vector of random numbers (Eq. 5); *s* is a number generated by a Lévy distribution (Eq. 6).

$$\beta^t = \beta_{\min} e^{-\gamma r^2} \tag{3.2}$$

where *r* is the distance between two fireflies (Eq.3.3), $\beta_{\min}$ is the attractiveness of a firefly at $r = 0$, e is a constant coefficient, and γ is the absorption coefficient ($0 \leq \gamma \leq 1$).

$$r_{ij} = \left\| x_i - x_j \right\| = \sqrt{\sum (x_i - x_j)^2} \tag{3.3}$$

$$\alpha^t = \alpha_0 \theta^t \tag{3.4}$$

where α_0 is the initial trade-off coefficient; θ is the adaptive parameter ($0 < \theta < 1$).

$$\varepsilon = rand - 1/2 \tag{3.5}$$

where $rand$ is a random number in the range [0, 1], which is generated by a uniform distribution.

$$s = \frac{u}{|v|^{2/3}} \tag{3.6}$$

where v and u are created by a normal distribution, as shown in Eq. 3.7 and Eq. 3.8, respectively, as follows:

$$v \sim N(0,1) \tag{3.7}$$

$$u \sim N(0,\left\{\frac{\Gamma(1+\tau)\sin(\pi\tau/2)}{\Gamma[(1+\tau)/2]\tau 2^{(\tau-1)/2}}\right\}^{2/\tau}) \tag{3.8}$$

where τ is a constant value; $\Gamma(z)$ is the Gamma function determined by Eq. 3.9 as follows:

$$\Gamma(z) = \int_0^\infty t^{z-1}e^{-t}dt \tag{3.9}$$

3.5.4 The computational optimisation approach for adaptive façade design

In this section, we present the detailed structure of the computational optimisation approach for designing an adaptive façade based on EnergyPlus, MFA and Eppy. The framework of the approach is shown in Figure 3-3. In the proposed framework, the building geometry, thermal and visual properties of windows and weather conditions are used as input data, which are used by EnergyPlus and MFA to find the optimal design of the adaptive façade system. The optimal results, which are the best sequence of U-values and Tvis, can be used to select the best materials and operational stages for adaptive façade systems such as EC windows.

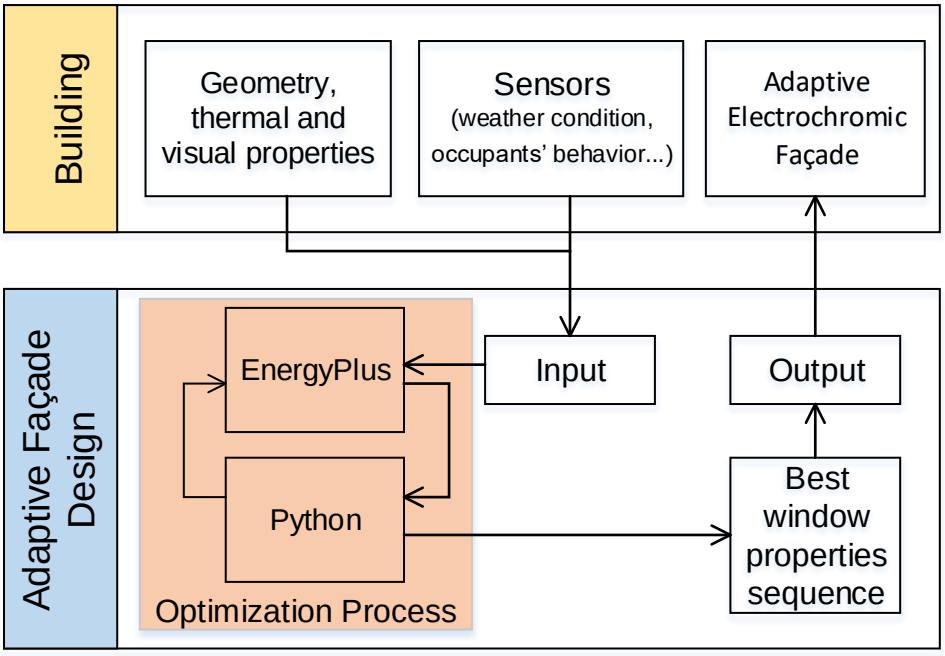

Figure 3-3. The framework of the computational optimisation approach for adaptive façade design.

The engine of the approach is the optimisation process, which combines the energy performance prediction (EnergyPlus) with an MFA optimisation technique. The process is implemented in the Python environment, where the Eppy toolkit is used as a middleware tool to exchange data between EnergyPlus and MFA in this process. The target of the optimisation process is to find the best window properties sequence to minimize energy consumption and satisfy visual comfort requirements, thereby providing a preliminary design of an adaptive façade system. The design of the adaptive façade in this study can be formulated as an optimisation problem as follows:

Input: Building geometry and dynamic climatic conditions

Controlled variable: U-value and Tvis

Objective: minimize $E_{total} = E_{heating} + E_{cooling} + E_{lighting}$

Constraint: Glare index ≤ 22

The design of the adaptive façade is subjected to dynamic climatic conditions and the glare index constraint, which is associated with the visual comfort of building occupants. It is established that a glare index higher than 22 is too bright for building occupants [44].

Figure 3-4 shows the flowchart of the optimisation process for the adaptive façade design. At the beginning of this process, MFA generates an initial population of U-values and Tvis of the façade system. EnergyPlus will be used to simulate the energy consumption in the building. The outputs of the simulation (e.g., the total energy consumption E_{total} and glare index) are sent back to MFA to find the optimal properties sequence that takes into account the multiple performance criteria of interest, which include minimizing the total energy consumption and satisfying the visual performance condition (Glare index ≤ 22). In this study, a maximum generation constant of 10 is chosen as the termination criterion in Figure 3-4.

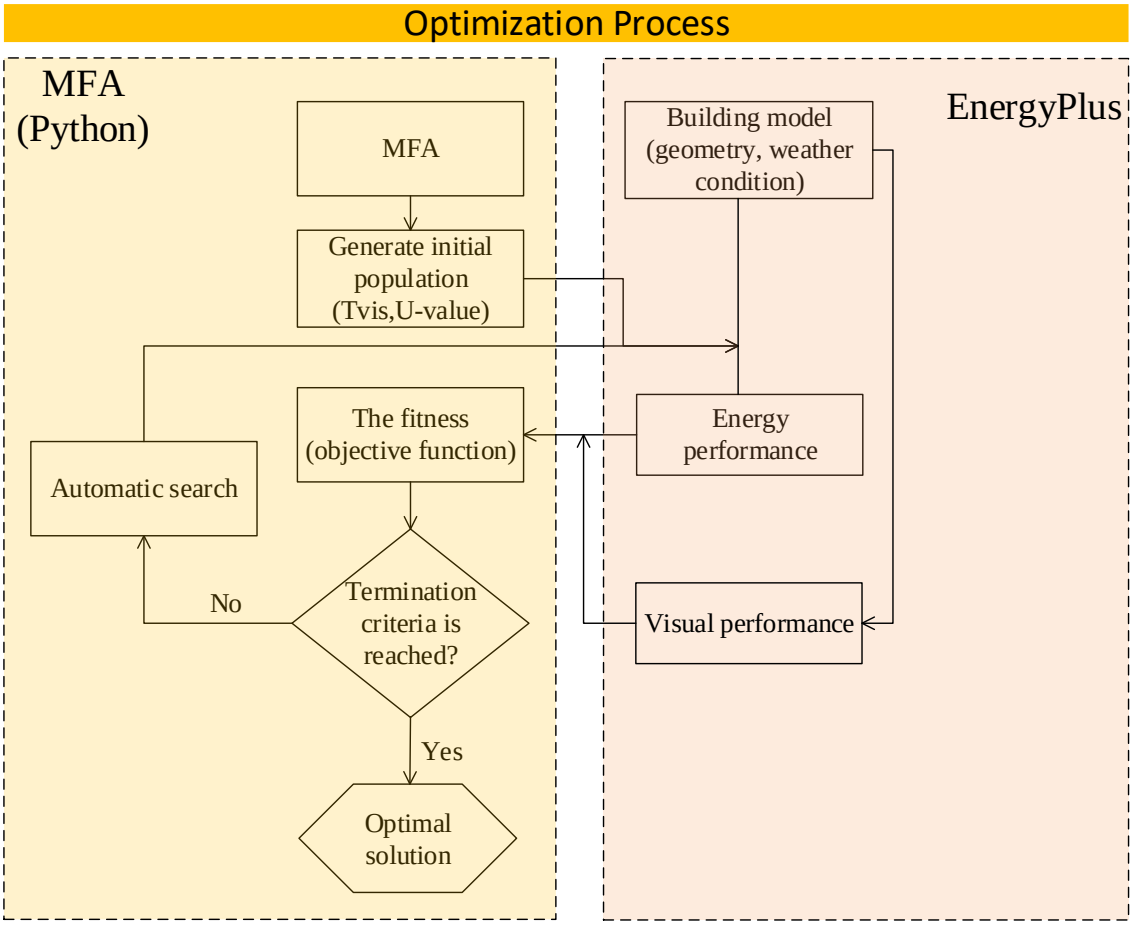

Figure 3-4. Flowchart of the optimisation process for adaptive façade design.

3.6 The energy performance of adaptive façades – case study

This study develops two case studies to demonstrate the capability of the proposed computational optimisation approach to design the adaptive façade for enhancing building energy efficiency. The first case study is a typical single-zone office model, as shown in Figure 3-5a. This case study was experimentally conducted by Lee *et al.* [33] through a full-scale outdoor field test to validate the effects of an adaptive EC façade. The dimensions of the model are 3.00m x 4.57m x 2.50m (LxWxH), and the window-to-wall ratio is 59% as shown in Figure 3-5a. The U-value and Tvis of the windows of the adaptive façades can vary in a range of [0.1-10 W/m^{2}K] and [0.05-0.9], respectively. The material properties of other parts of the façade are given in Table 3-1. These material properties are assumed in accordance with the material

library in Revit [39] as they were missing in the study of Lee *et al.* [33]. The windows of this case study are subdivided into three zones in the same manner as reported by Lee *et al.* [33], and the adaptation of the adaptive façade (e.g., Tvis and U-value) can be controlled separately for each zone.

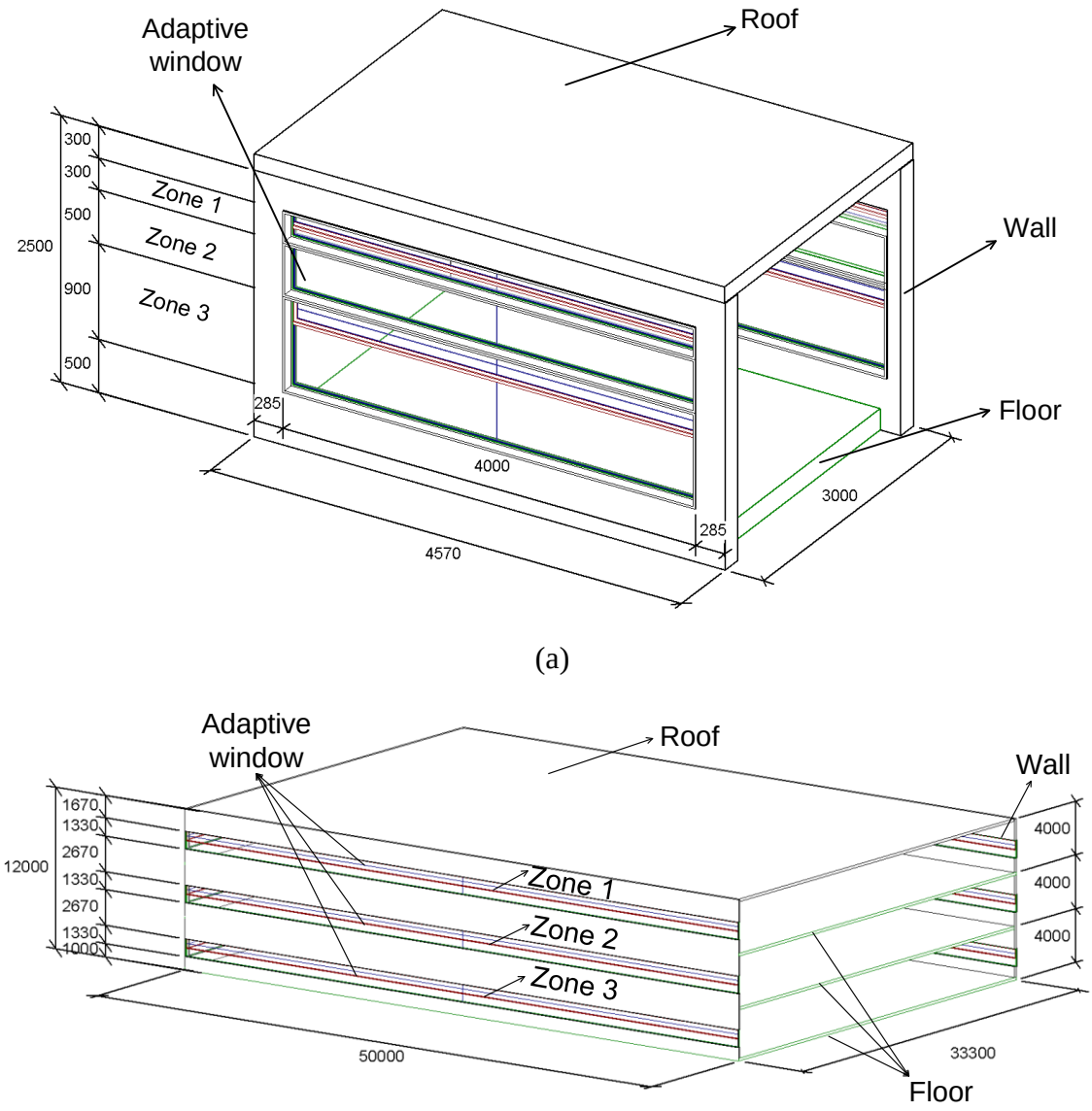

Figure 3-5. (a) Case study 1: a typical single-zone office space model; (b) Case study 2: a medium office model

Table 3-1. Material properties of the adaptive and static components in case study 1

Type	Components	Material	Thickness (mm)	Specific Heat (J/g.°C)	Density (kg/m^3)	U-value ($W/(m^2k)$)	T-vis (-)
Static/Fixed	Floor [39]	Floor tiles	6	0.85	1700	133.3	N/A
		Concrete	200	0.657	2300	5.2	N/A
	Roof [39]	Concrete	200	0.657	2300	5.2	N/A
	Wall [39]	Lightweight concrete	200	0.657	950	1.0	N/A
		Gypsum wall board	12	0.84	1100	54.2	N/A
Adaptive	Window	Glass	6	N/A	N/A	0.1 - 10	0.05-0.9

To demonstrate that the proposed computational optimisation approach can also be applied to an actual office building, we conducted a second case study of a medium office, which has three floors with a total floor area of 4982 m^2. This model was used by the DOE as a building benchmark model [45]. All four sides of the building have windows with an equal window-to-wall ratio of 33% as shown in Figure 3-5b. The building has a rectangular shape with an aspect ratio of 1.5. The windows of this case study are also subdivided into three zones (i.e., each floor is one zone). The details of the material properties of the office building are listed in Table 3-2.

Table 3-2. Material properties of the adaptive façade in case study 2

Type	Components	Material	Thickness (mm)	Specific Heat (J/g.°C)	Density (kg/m^3)	U-value ($W/(m^2k)$)	T-vis (-)
Static/Fixed	Floor [45]	Concrete	100	0.837	2240	13.1	N/A
	Roof [45]	Membrane	9.5	1.46	1121	16.8	N/A
		Insulation	125	0.837	265	0.4	N/A

		Metal Decking	1.5	0.418	7680	300.0	N/A
		Concrete	200	0.837	2240	6.6	N/A
	Wall [45]	Insulation	50	0.837	265	1.0	N/A
		Gypsum wall board	12	0.83	785	13.3	N/A
Adaptive	Window	Glass	6	N/A	N/A	0.1 - 10	0.05-0.9

For the energy simulations in EnergyPlus, it is assumed that there are six occupants occupying the office for the two case studies, and they start working from 8:00 to 17:00 on weekdays. The heat gain per floor area from lighting and electric equipment are 4.7 (W/m^2) and 14.4 (W/m^2), respectively. The temperature setpoints of the HVAC system for heating and cooling are 18°C and 25°C, respectively, during the occupied hours. For non-working hours, these temperature setpoints are adjusted to 15°C and 28°C, respectively. Besides, a minimum workplace illuminance of 500 lux is maintained, and an illuminance sensor is placed at the center of the room at the work plan height (0.8 m). The location of the office is Melbourne, Australia, and a typical meteorological year of Melbourne is used for the energy simulation. The two case studies focus on two typical weeks in summer and winter, and the time step for the simulation is 15 minutes. Figure 6 shows an example of setting the U-value and Tvis in the EnergyPlus model. U-value is modified by changing the thermal conductivity (K-value) of materials, and the relationship between U-value and K-value is represented by Eq. 3.10:

$$U = \frac{K}{d} \tag{3.10}$$

where d is the thickness of the material.

```
WindowMaterial:Glazing,
    Glaze-Zone 1,             !- Name
    SpectralAverage,          !- Optical Data Type
    ,                         !- Window Glass Spectral Data Set Name
    0.006,                    !- Thickness
    0.05,                     !- Solar Transmittance at Normal Incidence
    0.071,                    !- Front Side Solar Reflectance at Normal Incidence
    0.071,                    !- Back Side Solar Reflectance at Normal Incidence
    0.05,                     !- Visible Transmittance at Normal Incidence
    0.08,                     !- Front Side Visible Reflectance at Normal Incidence
    0.08,                     !- Back Side Visible Reflectance at Normal Incidence
    0.0,                      !- Infrared Transmittance at Normal Incidence
    0.84,                     !- Front Side Infrared Hemispherical Emissivity
    0.84,                     !- Back Side Infrared Hemispherical Emissivity
    0.06;                     !- Conductivity

WindowMaterial:Glazing,
    Glaze-Zone 2,             !- Name
    SpectralAverage,          !- Optical Data Type
    ,                         !- Window Glass Spectral Data Set Name
    0.006,                    !- Thickness
    0.05,                     !- Solar Transmittance at Normal Incidence
    0.071,                    !- Front Side Solar Reflectance at Normal Incidence
    0.071,                    !- Back Side Solar Reflectance at Normal Incidence
    0.05,                     !- Visible Transmittance at Normal Incidence
    0.08,                     !- Front Side Visible Reflectance at Normal Incidence
    0.08,                     !- Back Side Visible Reflectance at Normal Incidence
    0.0,                      !- Infrared Transmittance at Normal Incidence
    0.84,                     !- Front Side Infrared Hemispherical Emissivity
    0.84,                     !- Back Side Infrared Hemispherical Emissivity
    0.06;                     !- Conductivity

WindowMaterial:Glazing,
    Glaze-Zone 3,             !- Name
    SpectralAverage,          !- Optical Data Type
    ,                         !- Window Glass Spectral Data Set Name
    0.006,                    !- Thickness
    0.05,                     !- Solar Transmittance at Normal Incidence
    0.071,                    !- Front Side Solar Reflectance at Normal Incidence
    0.071,                    !- Back Side Solar Reflectance at Normal Incidence
    0.05,                     !- Visible Transmittance at Normal Incidence
    0.08,                     !- Front Side Visible Reflectance at Normal Incidence
    0.08,                     !- Back Side Visible Reflectance at Normal Incidence
    0.0,                      !- Infrared Transmittance at Normal Incidence
    0.84,                     !- Front Side Infrared Hemispherical Emissivity
    0.84,                     !- Back Side Infrared Hemispherical Emissivity
    0.06;                     !- Conductivity
```

Figure 3-6. The setting of U-value and Tvis in the EnergyPlus model.

Table 3-3 lists the input parameters for MFA to the optimisation process in this paper. In addition to the adaptive façade presented in Tables 1 and 2, we also analyze five reference benchmarks of static façades (i.e., fixed U-value and Tvis), which are listed in Table 3-4 for comparison. The five reference benchmarks have the same properties as the adaptive façade i.e., components, climatic conditions and other settings.

Table 3-3. The initial parameters of MFA in both case studies.

Parameter	Description	Value
β_{min}	The minimum attractiveness	0.1
γ	The absorption coefficient	1
α_o	The initial trade-off coefficient	0.2
θ	The adaptive parameter	$(10^{-2} / 0.9)^{1/MaxGeneration}$
τ	The constant value	1.5
Number of populations		20
Maximum of generations		10

Table 3-4. Details value of U-value and Tvis in the reference cases.

Case	1	2	3	4	5
U-Value (W/m^2K)	0.1	0.1	2.5	5	10
Tvis	0.05	0.9	0.25	0.75	0.05

3.7 Numerical results and Discussion

In this section, we present the outcomes of the adaptive façade design and compare its performance with the five reference benchmarks to demonstrate its potential to enhance the energy efficiency in buildings. A comparison of the energy and visual performance between several design options in a week in summer is shown in Table3- 5 for the two case studies. The visual performance is calculated as the percentage of time that the glare index is equal to or smaller than 22 during working hours. This implies that a visual performance of 100% meets the visual comfort requirements and vice versa. In Figure 3-7, the first five columns represent the performance of five reference benchmarks with a non-adaptive, static façade, while the last column shows the energy consumption of the adaptive case.

Table 3-5. Detailed energy and visual performance of the two case studies in the summer week for adaptive façade and reference benchmarks.

	Unit	Reference benchmark					Adaptive façade
		1	2	3	4	5	
Case study 1							
Lighting	10^5 kJ	0.13	0.08	0.08	0.08	0.13	0.08
Heating	10^5 kJ	0.28	0.22	0.25	0.21	0.26	0.20
Cooling	10^5 kJ	1.66	1.04	1.38	1.02	1.42	1.19
Total	10^5 kJ	2.07	1.34	1.71	1.31	1.81	1.47
Energy save*	%	29.0	-	-	-	18.8	-
Visual performance	%	100	51	83	61	100	100
Case study 2							
Lighting	10^7 kJ	0.36	0.19	0.21	0.19	0.36	0.21
Heating	10^7 kJ	0.33	0.30	0.31	0.30	0.33	0.30
Cooling	10^7 kJ	2.03	1.73	1.83	1.76	1.99	1.79
Total	10^7 kJ	2.72	2.22	2.35	2.25	2.68	2.30
Energy save*	%	15.4	-	-	-	14.2	-
Visual performance	%	100	60	83	63	100	100

*Energy save = (energy of the reference benchmark –energy of the adaptive façade)/ energy of the reference benchmark

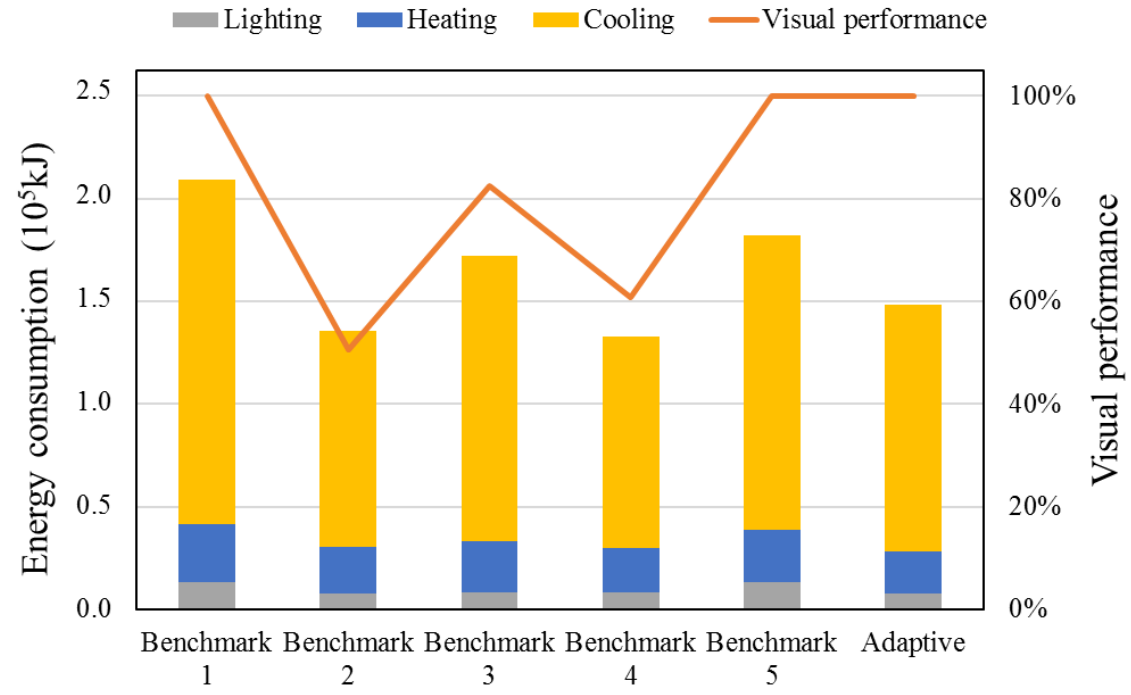

(a)

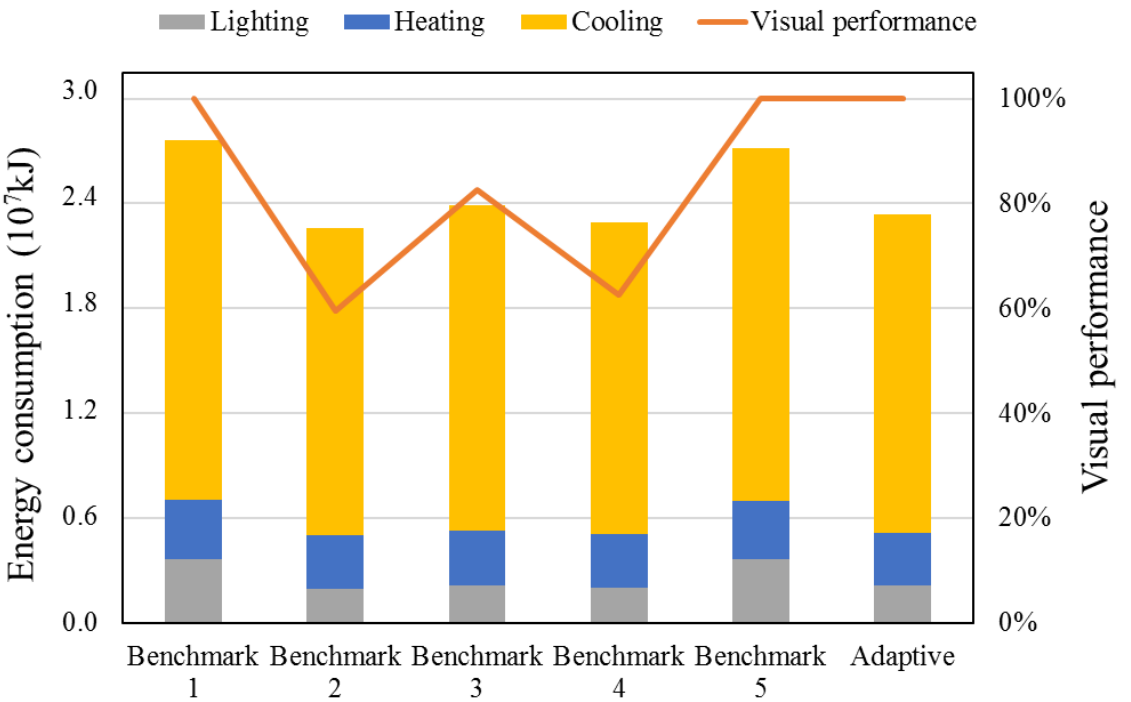

(b)

Figure 3-7. Comparison of results in the summer week for (a) case study 1 and (b) case study 2.

For case study 1, the office with the adaptive façade system has consumed the smallest total energy (1.47E+5 kJ) for heating, cooling and lighting, and has a visual performance of 100%. The reference benchmarks 2, 3, and 4 do not satisfy the visual comfort requirements as the visual performances are 51%, 83% and 61%, respectively, as shown in Table 5. The results also indicate that the benchmark façade 1, which has high insulated windows (U-value = 0.1 W/m^2K, Tvis = 0.05), has higher energy consumption for cooling than the benchmark façades 5 (low insulated windows: U-value = 10 W/m^2K, Tvis = 0.05) as shown in Table 5 (1.66 E+5 kJ for benchmark 1 and 1.42 E+5 kJ for benchmark 5). This can be attributed to the fact that it is difficult for internal heat to be released to the environment for benchmark 1, which thereby requires a noticeable amount of cooling energy to maintain a comfortable interior condition.

Besides, when comparing the two benchmark cases with the same U-value (the benchmark 1 and 2), it is clear that benchmark 2 with Tvis = 0.9 consumed less energy than benchmark 1 with Tvis=0.05, as the high Tvis of benchmark 2 allows more solar light to travel through the office, which reduces the lighting energy. Overall, the adaptive façade can save 18.8-29.0% of the total energy consumption compared to other reference offices (benchmark 1 and 5). Benchmarks 2, 3, and 4 are not comparable because they do not satisfy the visual comfort requirement. It can be observed from Figure 3-7 that most of the energy in this period is used for cooling due to summer weather conditions.

The same tendency is noticed for case study 2 when the adaptive façade office and benchmark 1 and 5 satisfy the visual performance requirement, and the adaptive façade office has consumed a minimum amount of energy for heating, cooling and lighting among these models, with a total energy consumption of 2.30E+7 kJ. Compared to benchmarks 1 and 5, the adaptive façade system can help to save 14.2-15.4% of the total energy consumption. Although benchmarks 2 and 4 have a lower energy consumption than the adaptive façade system, they

do not satisfy the visual comfort, as they have visual performances of 60% and 63%, respectively, as shown in Table 3-5.

The compared results between the adaptive façade system and reference benchmarks over a winter week are shown in Table 3-6 for the two case studies. In case study 1, the office with the adaptive façade also consumes the smallest total energy compared to the reference benchmarks. However, the office with a high insulated façade (the benchmark 1: U-value = 0.1 W/m^2K,) consumed less energy (1.48E+5 kJ) than the case with a low insulated façade (the benchmark 5: U-value = 10 W/m^2K, 1.63E+5 kJ). It can be explained that the internal heat of the office benchmark 5 can easily escape to the external environment because of the low insulated façade, so it requires more heating energy to warm up the room on cold winter days. The same trend of visual performance was observed in summer when a higher Tvis results in lower energy consumption because of the reduction of lighting energy for benchmarks 1 and 2. Benchmarks 2, 3, and 4 once again do not satisfy the visual comfort for which the visual performances are smaller than 100%, as shown in Figure 3-8. The office with the adaptive façade can save 14.9-22.7% (for the case study 1) and 18.1-22.3% (for the case study 2) of the total energy consumption, compared to the static, non-adaptive façade systems. As opposed to the summer week, the most significant amount of energy is used for heating during the winter week as depicted in Figure 3-8.

Table 3-6. Detailed energy and visual performance of the two case studies in the winter week between the adaptive façade and reference benchmarks.

	Unit	Reference benchmark					Adaptive façade
		1	2	3	4	5	
Case study 1							
Lighting	10^5 kJ	0.14	0.10	0.11	0.10	0.14	0.10

Heating	10^5 kJ	0.88	0.94	0.98	1.02	1.09	0.82
Cooling	10^5 kJ	0.46	0.34	0.39	0.32	0.40	0.34
Total	10^5 kJ	1.48	1.38	1.48	1.44	1.63	1.26
Energy save*	%	14.9	-	-	-	22.7	-
Visual performance	%	100	67	91	79	100	100
Case study 2							
Lighting	10^7 kJ	0.19	0.12	0.14	0.12	0.19	0.12
Heating	10^7 kJ	0.90	0.83	0.92	0.88	0.99	0.79
Cooling	10^7 kJ	0.40	0.36	0.37	0.37	0.39	0.31
Total	10^7 kJ	1.49	1.31	1.43	1.37	1.57	1.22
Energy save*	%	18.1	-	-	-	22.3	-
Visual performance	%	100	70	95	73	100	100

*Energy save = (energy of the reference benchmark – energy of the adaptive façade)/ energy of the reference benchmark

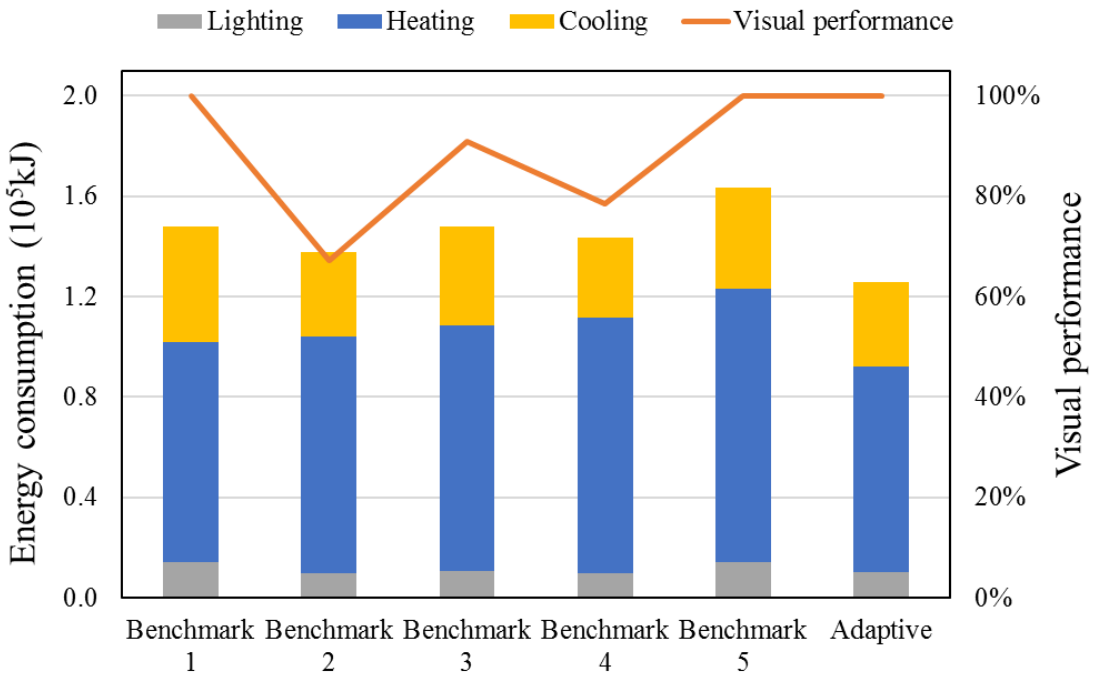

(a)

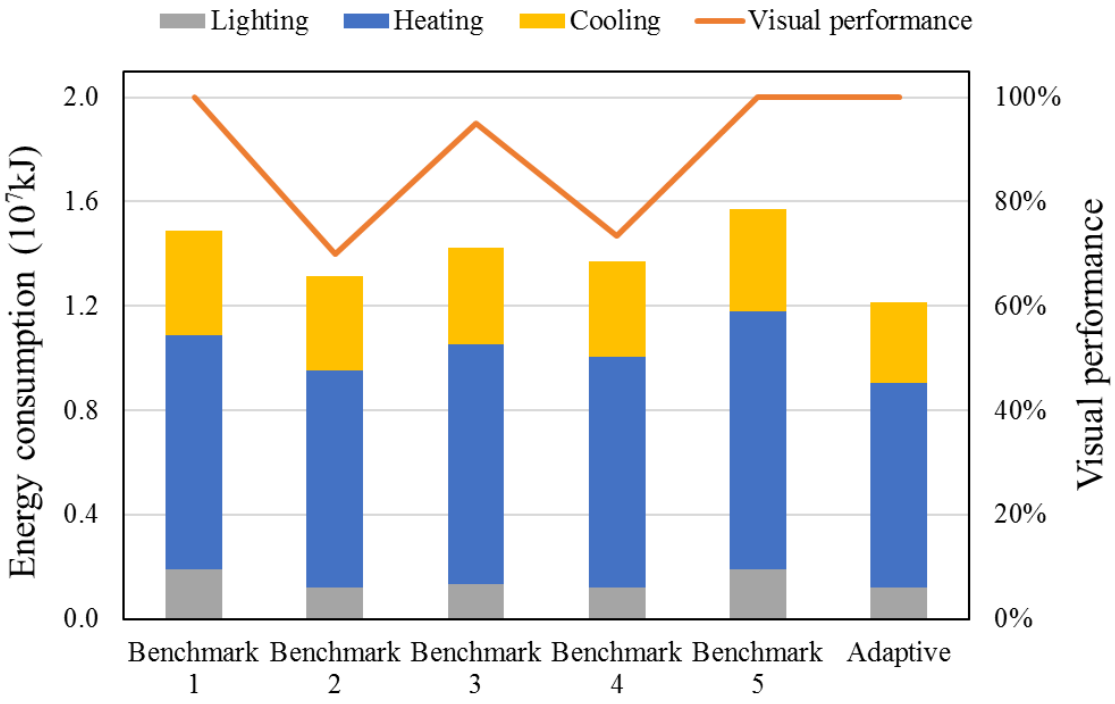

(b)

Figure 3-8. Comparison of results in the winter week for (a) case study 1 and (b) case study 2.

In this study, we also analyze the optimal sequence of U-value and Tvis for the designed adaptive component, which can inform the design and operation of the adaptive façade system (EC windows, for example). For a better understanding of the design and performance of the adaptive façade system, we plot the climatic conditions in this study in Figure 3-9, which shows the average temperature and direct normal radiation for one week in summer and winter in Melbourne. Direct normal radiation (Wh/m^2) is the amount of solar radiation that a surface received directly from the solar disk. It can be noticed that the temperature and direct normal radiation on most days in the summer week are significantly higher than those in the winter week.

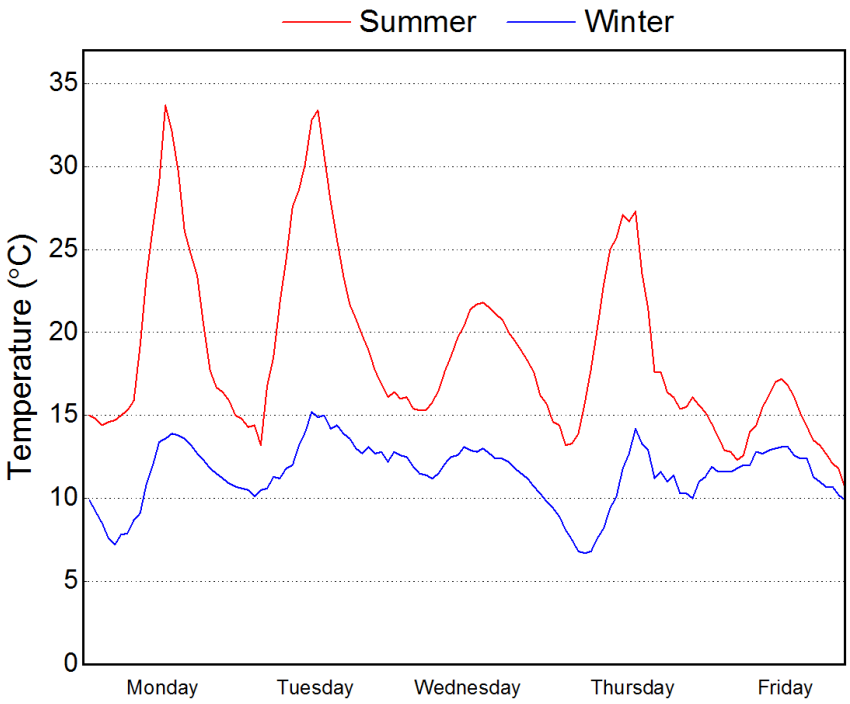

(a)

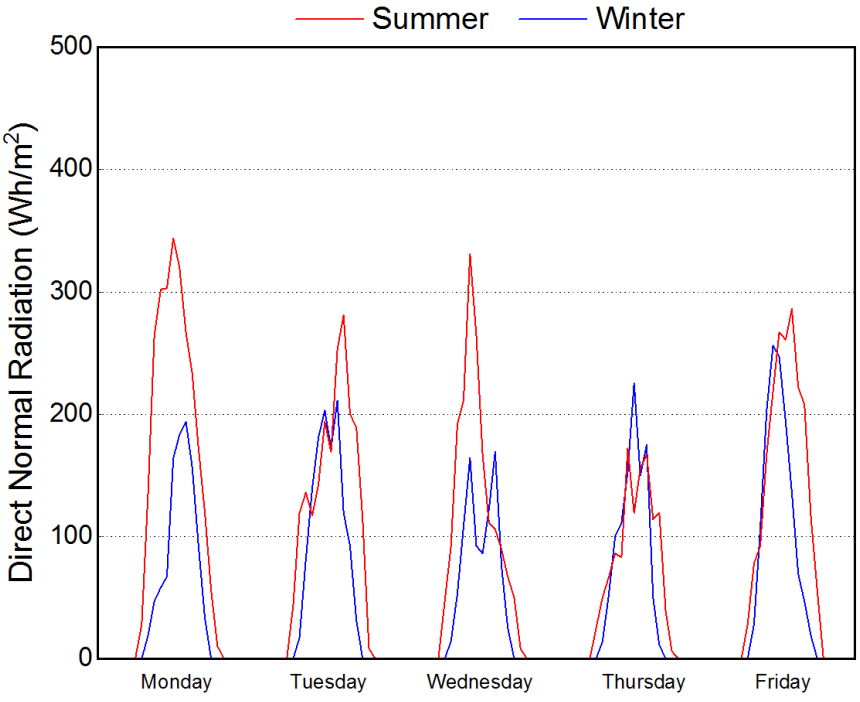

(b)

Figure 3-9. Weather data profile of the summer week and winter week: (a) Temperature and (b) Direct Normal Radiation

Figure 3-10 illustrates the averaged optimal Tvis and U-value for each hour of the adaptive façade in case study 1 for the summer week. Figure 10a shows that the U-value of the adaptive façade system is optimized to a high value (i.e., low insulation) during the morning and night to allow for temperature exchange between the internal and external environment because the external temperature in this period is in the range of the temperature setpoints of a HVAC system. As shown in Figures 10a and 10b, the minimum U-value values (0.1 W/m^2K) are recommended by the proposed approach during midday on Monday, Tuesday and Thursday. As depicted in Figure 3-9a, the temperature at midday on Monday, Tuesday and Thursday is very high. The low U-value (i.e., high insulation) is required to block the hot airflow from the outside environment, and thereby reduce the cooling demand. It is also observed that the low U-values are not recommended at midday on Wednesday and Friday (Figure 3-10a) because the temperature is low (Figure 3-9a). For analyzing the visual performance, the Tvis value is set to a high value in the early morning (before 8:00) and the late afternoon (after 16:00) as shown in Figure 3-10b to have more access to sunlight, thereby reducing lighting energy. The Tvis value is then reduced to a low value (around 0.2 for Tuesday in Figure 10b) between 8:00-16:00 to satisfy the visual comfort (i.e., glare index is smaller than 22) when the direct normal radiation is high during daylight as shown in Figure 3-9b. In particular, for Wednesday afternoon and Thursday, when the direct normal radiation is low (Figure 3-9b), the Tvis values are clustered together in the range of [0.4-0.6] (Figure 3-10a), which is not observed for the other days when the direct normal radiation is high.

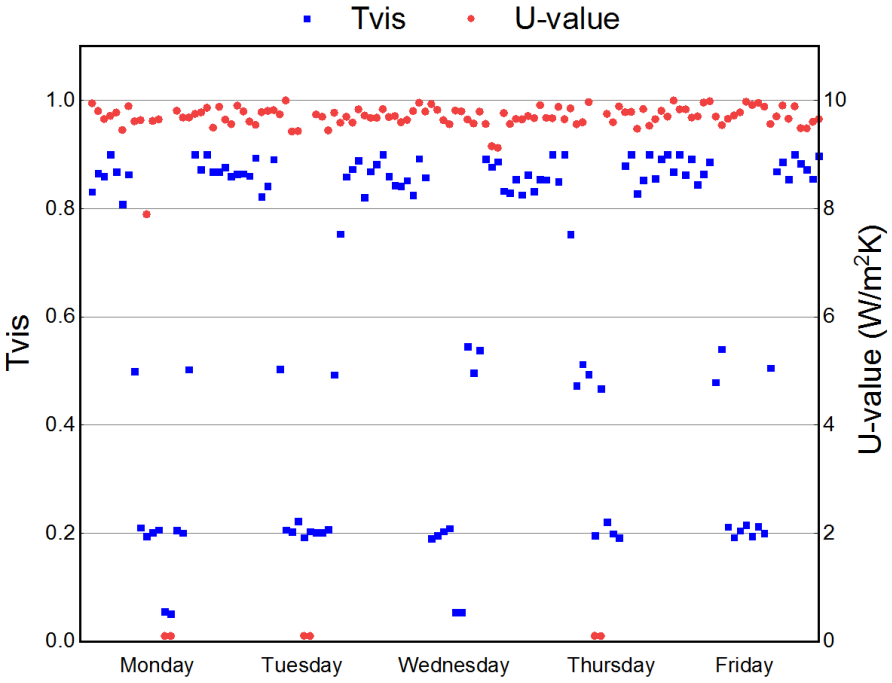

(a)

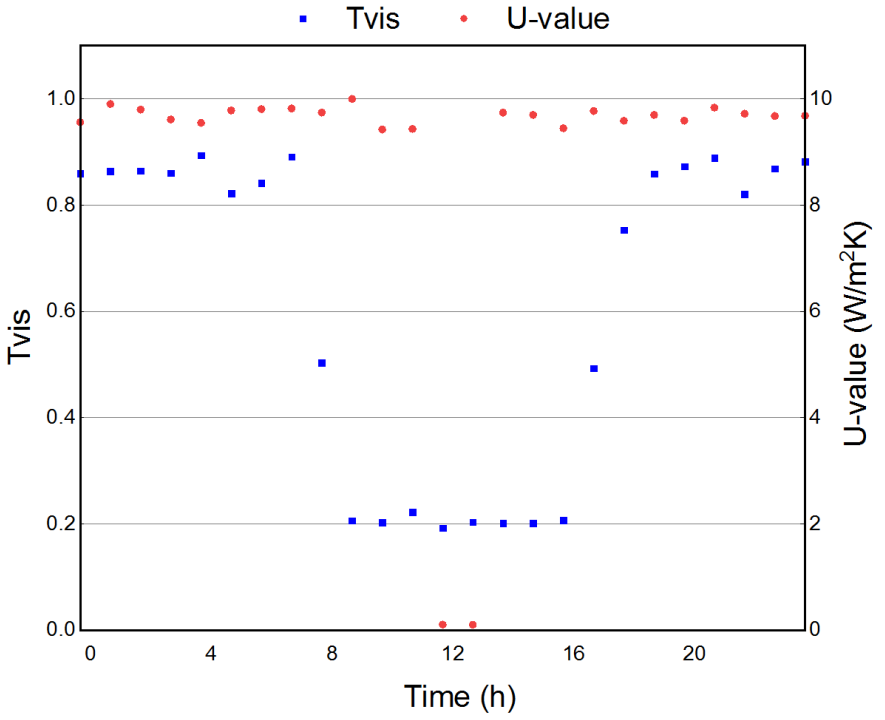

(b)

Figure 3-10. Optimized properties of the adaptive façade for case study 1:(a) summer week; (b) Tuesday in the summer week

In winter, the opposite trend of U-value is revealed when the thermal transmittance U-value is kept at a minimum most of the time and is adjusted to the maximum value at midday, as shown in Figure 11a and 11b. This can be explained by the fact that the Melbourne climate in winter is colder than the temperature setpoints for heating, as depicted in Figure 9a, so the high insulation of the adaptive façade system should be maintained to avoid heat leaking to the external environment. The high U-values are only needed at midday during the winter week when the temperature increases. For the visual performance, it is noticed that the period with high values of Tvis in the winter week (Figure 3-11a) is longer than that of the summer week (Figure 3-10a). That can be attributed to the fact that the direct normal radiation during winter is lower than that during summer for most of the time (Figure 3-9b). Therefore, the high Tvis values are required to allow more sunlight penetration, and thereby maintain visual comfort. On Wednesday in the winter week, high Tvis values during the entire day are required as the direct normal radiation is low on this day, as shown in Figure 3-9b.

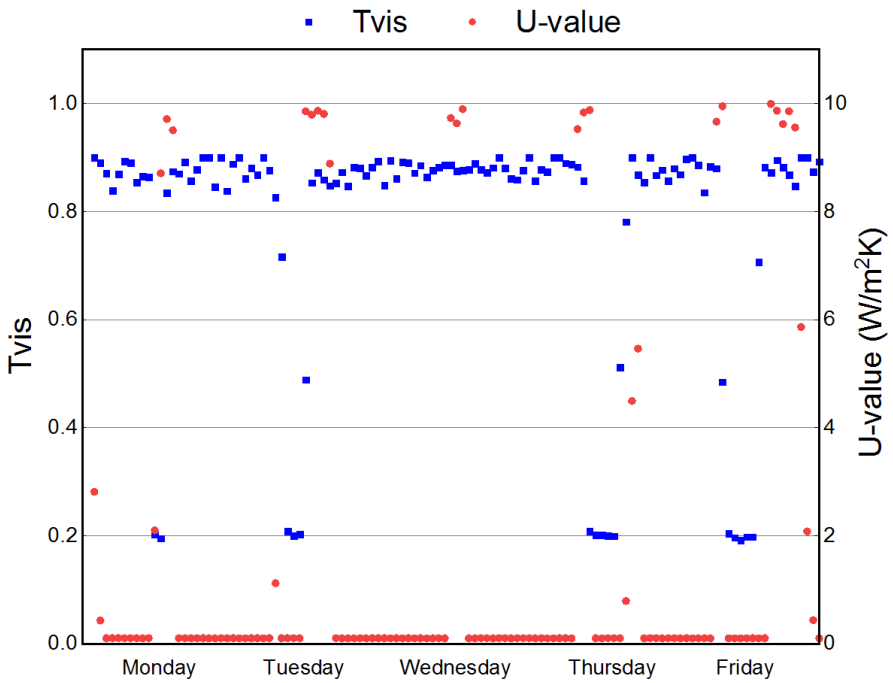

(a)

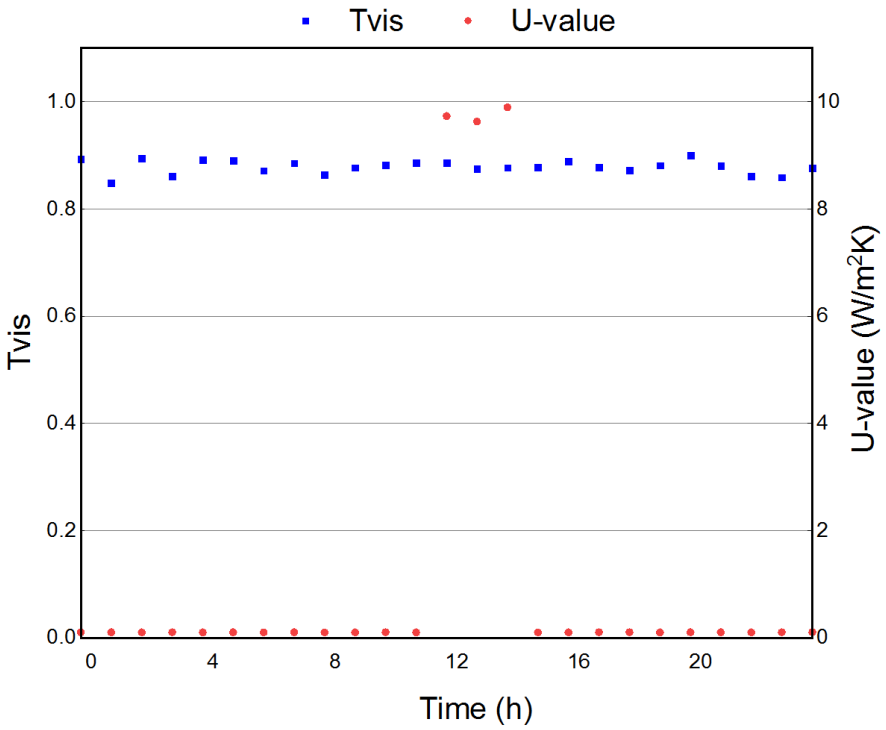

(b)

Figure 3-11. Optimized properties of the adaptive façade for case study 1: (a) winter week; (b) Wednesday during the winter week.

3.8 Conclusions

The adaptive façade is considered as a potential solution to enhance the energy efficiency of buildings. We proposed a computational optimisation approach, which uses a combination of building energy modelling software (EnergyPlus), the metaheuristic optimisation algorithm (MFA) and Eppy toolkit to design and assess the viability of adaptive façades systems. Two case studies were conducted to validate the capability of the proposed approach, which was used to obtain the optimal property sequence of the adaptive façade system, including the thermal transmittance U-value and visual transmittance Tvis, to minimize the total energy consumption in each case study.

In case study 1, a typical single-zone office was tested, and we found that the adaptive façade system can save the total energy consumption by 18.8% - 29.0% in the summer week and 14.9% - 22.7% in the winter week, compared to the benchmark static façade systems. For case study 2, the proposed approach can help to save between 14.2% - 22.3% of the total energy consumption compared to the benchmark façade systems. We also analysed the optimal, time-varying U-value and Tvis of the adaptive façade system, which are reasonably responsive to dynamic climatic conditions. These results confirm the capability and effectiveness of the proposed approach in supporting the design of adaptive façades and prove the capacity of the adaptive façade system in reducing the energy consumption of buildings. The proposed computational optimisation approach and the results of this research can be used to guide future research and development processes. This work can be easily extended to different material properties or dynamic shading devices to facilitate the exploration of next-generation adaptive façade systems.

Acknowledgments

The first author would like to thank the University of Melbourne for offering the Melbourne Research Scholarship. This work was mainly supported by the CRC-P for Advanced Manufacturing of High Performance Building Envelope project, funded by the CRC-P program of the Department of Industry, Innovation and Science, Australia, and the Asia Pacific Research Network for Resilient and Affordable Housing (APRAH) grant, funded by the Australian Academy of Science, Australia. This work was also supported by the ARC Training Centre for Advanced Manufacturing of Prefabricated Housing (CAMP.H) at the University of Melbourne.

References

1. Energy, I. and C. Change, *World energy outlook special report (2015)*. IEA: Paris, France, 2017: p. 37.

2. Agency, I.E., *World energy outlook special report*. 2015.

3. Administration, E.I. and G.P. Office, *International Energy Outlook 2016, with Projections to 2040*. 2016: Government Printing Office.

4. Pérez-Lombard, L., J. Ortiz, and C. Pout, *A review on buildings energy consumption information.* Energy and Buildings, 2008. 40(3): p. 394-398.

5. Lepkova, N., D. Zubka, and R.L. Jensen, *Chapter 10 - Financial Investments for Zero Energy Houses: The Case of Near-Zero Energy Buildings*, in *Global Sustainable Communities Handbook*, W.W. Clark, Editor. 2014, Butterworth-Heinemann: Boston. p. 217-253.

6. Sun, X., Z. Gou, and S.S.-Y. Lau, *Cost-effectiveness of active and passive design strategies for existing building retrofits in tropical climate: Case study of a zero energy building.* Journal of Cleaner Production, 2018. 183: p. 35-45.

7. Li, W., C. Koo, S.H. Cha, T. Hong, and J. Oh, *A novel real-time method for HVAC system operation to improve indoor environmental quality in meeting rooms.* Building and Environment, 2018. 144: p. 365-385.

8. Jung, W. and F. Jazizadeh, *Human-in-the-loop HVAC operations: A quantitative review on occupancy, comfort, and energy-efficiency dimensions.* Applied Energy, 2019. 239: p. 1471-1508.

9. Andjelkovic, A., T. Cvjetković, D. Đaković, and I. Stojanović, *Development of simple calculation model for energy performance of double skin façades.* Thermal Science, 2012. 16.

10. Gao, Y., et al., *A photovoltaic window with sun-tracking shading elements towards maximum power generation and non-glare daylighting.* Applied Energy, 2018. 228: p. 1454-1472.

11. Rodrigues, E., M.S. Fernandes, A.R. Gaspar, Á. Gomes, and J.J. Costa, *Thermal transmittance effect on energy consumption of Mediterranean buildings with different thermal mass.* Applied Energy, 2019. 252: p. 113437.

12. Loonen, R., *Approaches for computational performance optimization of innovative adaptive façade concepts*, in *Department of the Built Environment*. 2018, Eindhoven University of Technology: Netherlands.

13. Al-Obaidi, K.M., M. Ismail, and A.M. Abdul Rahman, *Passive cooling techniques through reflective and radiative roofs in tropical houses in Southeast Asia: A literature review*. Frontiers of Architectural Research, 2014. 3(3): p. 283-297.

14. Lee, C.-s., *Simulation-based performance assessment of climate adaptive greenhouse shells*. 2017, PhD Thesis, TU Eindhoven.

15. Crawley, D.B., L.K. Lawrie, C.O. Pedersen, and F.C. Winkelmann, *Energy plus: energy simulation program.* Ashrae Journal, 2000. 42(4): p. 49-56.

16. Wisconsin, T.U.o. *A TRaNsient SYstems Simulation Program*. Available from: http://sel.me.wisc.edu/trnsys/.

17. Strathclyde, D.o.M.E.U.o. *ESP-r*. Available from: http://www.esru.strath.ac.uk/Programs/ESP-r.htm.

18. Hirsch, J.J. *eQUEST the QUick Energy Simulation Tool*. Available from: http://www.doe2.com/equest/.

19. Crawley, D.B., J.W. Hand, M. Kummert, and B.T. Griffith, *Contrasting the capabilities of building energy performance simulation programs.* Building and Environment, 2008. 43(4): p. 661-673.

20. Chong, A., W. Xu, S. Chao, and N.-T. Ngo, *Continuous-time Bayesian calibration of energy models using BIM and energy data.* Energy and Buildings, 2019. 194: p. 177-190.

21. Kamal, R., F. Moloney, C. Wickramaratne, A. Narasimhan, and D.Y. Goswami, *Strategic control and cost optimization of thermal energy storage in buildings using EnergyPlus.* Applied Energy, 2019. 246: p. 77-90.

22. Iken, O., S.e.-D. Fertahi, M. Dlimi, R. Agounoun, I. Kadiri, and K. Sbai, *Thermal and energy performance investigation of a smart double skin facade integrating vanadium dioxide through CFD simulations.* Energy Conversion and Management, 2019. 195: p. 650-671.

23. Liu, M., K.B. Wittchen, and P.K. Heiselberg, *Control strategies for intelligent glazed façade and their influence on energy and comfort performance of office buildings in Denmark.* Applied Energy, 2015. 145: p. 43-51.

24. Johnsen, K. and F.V. Winther, *Dynamic Facades, the Smart Way of Meeting the Energy Requirements.* Energy Procedia, 2015. 78: p. 1568-1573.

25. Taveres-Cachat, E., S. Grynning, J. Thomsen, and S. Selkowitz, *Responsive building envelope concepts in zero emission neighborhoods and smart cities - A roadmap to implementation.* Building and Environment, 2019. 149: p. 446-457.

26. Taveres-Cachat, E., S. Grynning, O. Almas, and F. Goia, *Advanced transparent facades: market available products and associated challenges in building performance simulation.* Energy Procedia, 2017. 132: p. 496-501.

27. Hosseini, S.M., M. Mohammadi, and O. Guerra-Santin, *Interactive kinetic façade: Improving visual comfort based on dynamic daylight and occupant's positions by 2D and 3D shape changes.* Building and Environment, 2019. 165: p. 106396.

28. Ahmed, M., A. Abdel-Rahman, M. Bady, and E.K. Mahrous, *The thermal performance of residential building integrated with adaptive kinetic shading system.* International Energy Journal, 2016. 16: p. 97-106.

29. Mahmoud, A.H.A. and Y. Elghazi, *Parametric-based designs for kinetic facades to optimize daylight performance: Comparing rotation and translation kinetic motion for hexagonal facade patterns.* Solar Energy, 2016. 126: p. 111-127.

30. Wu, L.Y.L., Q. Zhao, H. Huang, and R.J. Lim, *Sol-gel based photochromic coating for solar responsive smart window.* Surface and Coatings Technology, 2017. 320: p. 601-607.

31. Zhang, Y., et al., *Perovskite thermochromic smart window: Advanced optical properties and low transition temperature.* Applied Energy, 2019. 254: p. 113690.

32. Liang, R., Y. Sun, M. Aburas, R. Wilson, and Y. Wu, *Evaluation of the thermal and optical performance of thermochromic windows for office buildings in China.* Energy and Buildings, 2018. 176: p. 216-231.

33. Lee, E.S., C. Gehbauer, B.E. Coffey, A. McNeil, M. Stadler, and C. Marnay, *Integrated control of dynamic facades and distributed energy resources for energy cost minimization in commercial buildings.* Solar Energy, 2015. 122: p. 1384-1397.

34. Ajaji, Y. and P. André. *Support for energy and comfort management in an office building using smart electrochromic glazing: dynamic simulations*. in *Proceedings of BS2015: 14th conference of IBPSA*. 2016. BS publications.

35. Hoon Lee, J., J. Jeong, and Y. Tae Chae, *Optimal control parameter for electrochromic glazing operation in commercial buildings under different climatic conditions.* Applied Energy, 2020. 260: p. 114338.

36. Ngo, N.-T., *Early predicting cooling loads for energy-efficient design in office buildings by machine learning*. Energy and Buildings, 2019. 182: p. 264-273.

37. Lee, S.W. and J.S. Park, *Evaluating thermal performance of double-skin facade using response factor*. Energy and Buildings, 2019: p. 109657.

38. Loonen, R.C.G.M., *Shaping the next generation of adaptive facade concepts with the use of simulations*, in *Facade2014 - Conference on Building Envelopes, 28 November 2014, Lucerne, Switzerland*, A. Luible and U. Zihlmann, Editors. 2014, s.n. p. 84 - 95.

39. Inc, A. 2019; Available from: https://www.autodesk.com.au/products/revit/overview.

40. Santosh Philip, Tuan Tran, Eric Allen Youngson, and J. Bull. *Eppy*. 2013; Available from: https://eppy.readthedocs.io/en/latest/index.html.

41. Bui, D.-K., T. Nguyen, J.-S. Chou, H. Nguyen-Xuan, and T.D. Ngo, *A modified firefly algorithm-artificial neural network expert system for predicting compressive and tensile strength of high-performance concrete.* Construction and Building Materials, 2018. 180: p. 320-333.

42. Chou, J.-S. and N.-T. Ngo, *Modified firefly algorithm for multidimensional optimization in structural design problems.* Structural and Multidisciplinary Optimization, 2017. 55(6): p. 2013-2028.

43. Yang, X.-S., *Firefly algorithm, stochastic test functions and design optimisation.* International Journal of Bio-Inspired Computation, 2010. 2(2): p. 78-84.

44. Piccolo, A. and F. Simone, *Effect of switchable glazing on discomfort glare from windows.* Building and Environment, 2009. 44(6): p. 1171-1180.

45. (DOE), U.S.D.o.E. *Commercial Reference Buildings*. Available from: https://www.energy.gov/.

Chapter 4
The computational design of biomimetic adaptive façade for energy efficiency building

[IN PROGRESS[2]]

4.1 Abstract

Chapter 3 has demonstrated the capacity of the adaptive façade (AF) system in reducing the energy consumption of buildings. This chapter further extends the study in chapter 3 by transferring the biological features found in chameleons into designing façade systems. By combining the bioinspiration and advanced electrochromic (EC) glazing systems, this chapter proposes the concept and design of biomimetic adaptive façade (BAF) to enhance the energy efficiency of buildings. A comprehensive analysis is conducted to identify the similarities between the mechanism of EC glazing and chameleon's skin, thereby providing the bioinspiration features for the proposed BAF system. In addition, the computational optimisation approach, which was presented in the previous chapter, is extended with a decision-making assistance tool, to design and assess the viability of BAF systems. A medium office building is used as a case study to validate the capability of the proposed approach for two weather conditions in Melbourne, Australia and Texas, United State. The results show that the proposed façade system can reduce energy consumption by 9.2% - 27.3% and 14.6% - 19.6% for Melbourne and Texas, respectively, compared to the benchmarking facade systems. The results confirm the potential of BAF in improving the energy efficiency of buildings.

[2]Bui, D.-K., T.N. Nguyen, A. Ghazlan, and T.D. Ngo, *Enhancing building energy efficiency by adaptive façade: A computational optimization approach*. Ready to submit in Applied Energy (in-progress).

4.2 Introduction

Buildings, in general, account for approximately 40% of the global energy consumption [1]. The energy used by the buildings keeps growing by around 2% per year from 2012 to 2040 [2]. A large proportion of the energy consumption in a building is used for the operational stage during its life cycle [3, 4], which is mainly used to maintain the thermal and visual comfort of occupants in the building i.e. for lighting, heating, and cooling. The thermal comfort condition is defined as the condition that building occupants satisfy with the thermal environment (i.e. a person is not feeling too hot or too cold) [5], while the visual comfort includes a variety of aspects such as views of outside space, luminosity, light quality and absence of glare. Both thermal and visual comforts are affected by façade system (e.g. glazing systems) because it is a mediator between inside and outside environment. Hence, the façade system plays an essential role in the total energy consumption in buildings. As a result, the façade system is very important to achieve the efficient use of energy in a building, which strongly affects its ability to achieve the green building certificates in the Green Building Rating system [6] as well as the Near-Zero Energy Buildings (NZEB) target [7].

The development of new façade systems for enhancing building energy efficiency can be categorized into two main strategies. The first strategy focus on developing better shading devices, which can reduce heat gain from sunlight but still ensure the views connected to nature and light quality of occupant [8-10]. In cooling seasons, some shading devices are designed to function as reflectors, which can bounce natural light into building interiors [11]. The second approach target on designing new material with high thermal resistance for façade systems [8, 12]. The high thermal resistance property of façade can help the building be more insular with the environment; however, in winter, the high thermal resistance also restricts a building to absorb solar energy from sunlight, thereby increasing heating energy [13]. It should be noticed

that the two strategies both aim to reduce energy for lighting, heating and cooling of buildings by controlling the thermal and visual exchange between building and environment.

Notably, many approaches from both strategies for energy-efficient façade system are inspired by nature [14-16], which has evolved over many years to develop a unique strategy to adapt to living environments. These approaches, called biomimicry façade design, look at the material, dimension, operation of façade system from a biomimetic point of view. The terminology of ”biomimicry” was introduced in [17], where the concept of resembling ecosystems was proposed by balancing nature and mankind. Many living organisms look for the physiologically tolerable conditions, called homeostasis in biology, which is analogous to the attempt to maintain a comfortable environment for occupants in building with respect to the variation of the external environment conditions. Living organisms have many strategies, which have been developed through many years of evolution, to adapt to dynamically environmental conditions. The adaptation may take place throughout the second (e.g., Mimosa pudica quickly respond to touch), the day (e.g., sunflowers follow the solar), the seasons (e.g., the seals have different blubber distribution in each season), or the evolution (e.g., the skin colour of a human) [18]. Especially, adaptation, which is one of the most crucial features, helps living organisms able to survive in harsh environmental conditions. The adaptation feature of living organisms can provide engineers and architects great inspiration to improve the performance of façade. In fact, one of the most significant challenges to design an effective façade system is the variations of climatic conditions (e.g., daylighting, heat gain from sunlight, natural ventilation). Many studies concluded that the energy efficiency of façade systems is very sensitive to outside environment conditions [19, 20].

This study aims to develop the design concept and solution for a BAF system, which is inspired by the adaptation mechanisms of chameleons. Enabling by the state-of-the-art electrochromic (EC) glass technology, the adaptation mechanisms of chameleons can be

applied to the design of a biomimetic, EC glazing system by changing its colour to control the solar heat and sunlight exchange between internal building space and external environments.

4.3 Literature Review

Biomimicry approaches in designing glazing systems can be classified into two groups: (1) form and (2) function [21]. The first group is to mimic the morphological appearance, visual shape of the organism or biological system in nature. For instance, Sheikh and Asghar, inspired from the shape of Oxalis oregana leaf, proposed a two-axes, foldable shading device which can be folded along both horizontal and vertical axes as shown on Figure 4-1 [14]. The device can enable shading under several angles of sunlight, thereby reducing the sun-glare and overheating in the building during the hot season. They also validated the performance of the biomimicry shading device by applying to a 20-story commercial building in Lahore, Pakistan. The results showed that the proposed device can reduce the energy load in the building by 32% and still keep a haft of floor plan under the natural light level of 500 – 750 lux [14]. In another study, Han *et al.* proposed a bio-inspired building envelope after investigating the particular retro-reflective property of flower petals [22]. Many application inspired by Strelitzia reginae flower, spruce cones are presented [16].

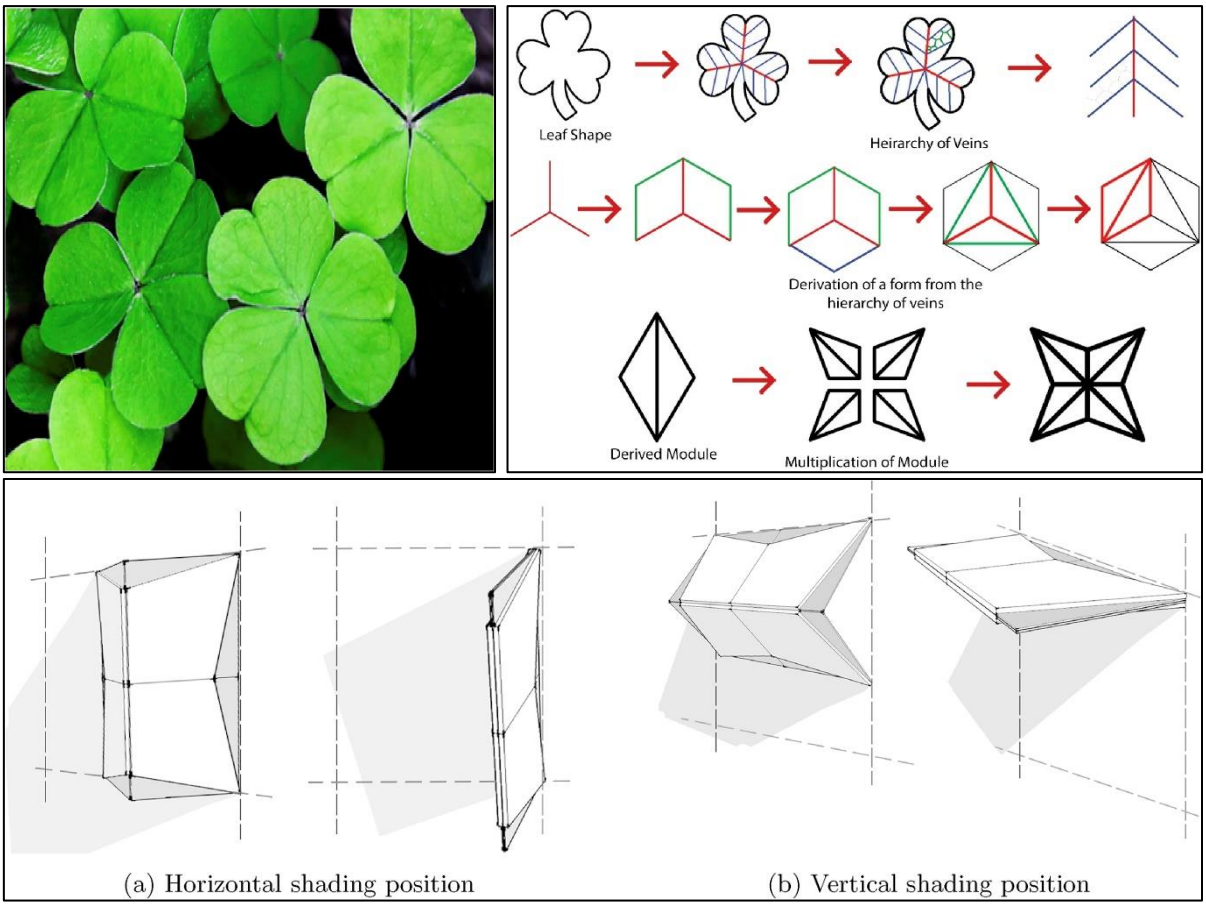

Figure 4-1. A two-axes, foldable shading device is inspired from the shape of Oxalis oregana leaf [14]

On the other hand, the second group is to copy the underlying biological mechanism. This group focus on what the façade does rather than how its look and they can directly or indirectly inspire from nature [23-27]. The direct approach directly mimics the functional fundamentals of organism or biological system into same-role elements of façade system, while the indirect approach needs to add more steps into the transformation. For example, Webb *et al.* investigated the heat transfer of animal fur and then transferred that distinctive performance characteristic to building façades [23]. The results from this study showed that the fur-lined façade could reduce the heat gains and heat losses by 50% during summer and winter, respectively, when comparing with a conventional lightweight façade. In another study,

Taghizade and Taraz focused on the effect of the pattern of bird feathers on the energy consumption of the bird. They then proposed a design of a mobile surface inspired by bird feathers to reduce energy consumption and increase the shade for buildings [24]. These studies all focus on developing a kinetic façade, which can move and change the position, but the study on adaptive thermal material is limited. In addition, most of all published studies on BAF remain at a conceptual stage of development, and there are under ten percentage of studied that having energy analysis [15].

The electrochromic (EC) window technology is one of the most significant developments in glazing systems and can enable the adaptation of bioinspiration in façade design. An EC window can change its thermal and visual properties by adjusting the applied small voltage to reflect or absorb solar energy. However, the effective design and operation of EC system energy efficiency is still unresolved because of the complex nonlinear relationship between the status of EC windows and the energy consumption in a building [28-30]. Mäkitalo validated the performance of EC windows in an office building in Stockholm, Sweden [28]. He reported that EC windows could save more energy than regular windows with blinds do. Nevertheless, this research only focuses on the thermal performance of the building, and there is a lack of visual comfort analysis. In another study, Dussault and Gosselin performed a sensitivity analysis of the design parameter of an office building, which has EC windows, on energy performance [29]. The study showed that the EC windows have a significant effect on the total energy consumption of the building. In addition to this,building location, window to wall ratio and façade orientation have more impacts on the energy performance of building compared to other design parameters such as internal gains, thermal mass, and airtightness rating [29]. Similarly, in the study conducted by Lee *et al.* [30], an optimisation process is proposed to find the control variable that has the biggest effect on the performance of the EC window. The study used a medium-sized commercial building as a case study and simulated with different weather

conditions of several cities in the United States. The results of this study demonstrated that outdoor air temperature is the most efficient parameter in improving the performance of the EC window. However, these studies did not go through details of the control strategy of EC windows yet, so optimising operation of EC windows is still challenging.

In this study, the biological and adaptive mechanisms of chameleon skin are analysed to identify the transferrable features of bioinspiration. Then, the design concept of BAF system based on the chameleon's skin is proposed. An in-house computational optimisation approach, which is built upon building energy modelling (BEM), optimisation techniques and a decision-making tool is used to explore the potential performance of the BAF system design for reducing the energy consumption of buildings. EnergyPlus, a BEM software, is used to evaluate the energy consumption of buildings with the variation of climatic conditions, and a computational approach is proposed to optimise the operation of the biomimicry adaptive façade. The data exchange between EnergyPlus and the computational approach is handled by Eppy, a Python toolkit. This study demonstrates that the BAF system can significantly improve the building energy efficiency.

4.4 Methodology

This section provides a background of biomimicry approach to façade design. The design of BAF then is presented along with the control mechanism of the proposed BAF.

4.4.1 Biomimicry inspiration and mechanisms

The natural inspiration and mechanisms of chameleons are presented in this section. Chameleons have 202 species described as of 2015, and these species come in a variety of colours [31]. The ability of chameleon to change its skin colour has been recognized as the most famous and intriguing feature in natural systems. However, it is a common misunderstanding that chameleons only change their skin colour for camouflaging purposes.

In fact, Walton and Bennett [32] found that chameleons primarily change their colour to regulate their body temperature [32]. Changing skin colour helps chameleons maintain pleasant body temperature as they cannot generate their own body heat. Therefore, chameleons must use solar radiation as a source for heat gain, and their skin colour affects the absorptance and reflectance to the visible wavelengths of solar radiation. Chameleons change their skin to a dark (bright) colour to absorb more (less) radiation, respectively. Rapid heating is notably important for chameleons which begin morning activity at low temperature. On the contrary, increasing reflectance can help chameleons reduce body temperature during midday when the level of solar radiation is high.

The intriguing feature of chameleons is attributed to the microstructure of their skin, which is a multilayer structure, as shown in Figure 4-2. The first layer of the skin is the transparent layer which enables the penetration of sunlight. Underneath this layer, there are four layers, namely xanthophores, erythrophores, iridophores and melanophores [33]. These layers contain specialized cells, called chromatophores, which are filled with sacs of different pigments. Xanthophores, erythrophores and iridophores layer contain yellow, red and blue pigments, respectively. The melanophores layer fills brown melanin, which also exists in human skin. In the normal condition, chameleons keep these pigments locking inside the tiny sacs in the cells. When chameleon needs to change body temperate, its nervous system will control the specific chromatophores in the xanthophores, erythrophores and iridophores layers to expand or narrow, thereby changing the colour of the cells. For example, in Figure 4-2a, the chameleon has a yellow colour when chromatophores in the xanthophores layer expand and chromatophores in other layers narrow. Then, the chameleon changes colour to blue by simultaneously expanding chromatophores in iridophores layers and narrowing chromatophores in the xanthophores layer, as shown in Figure 4-2b. Chameleons can create a variety of colour patterns by choosing the combination of different chromatophores in all the

skin layers [33]. This process enables the adaptation of chameleon by actively control the absorption and reflection of solar radiation.

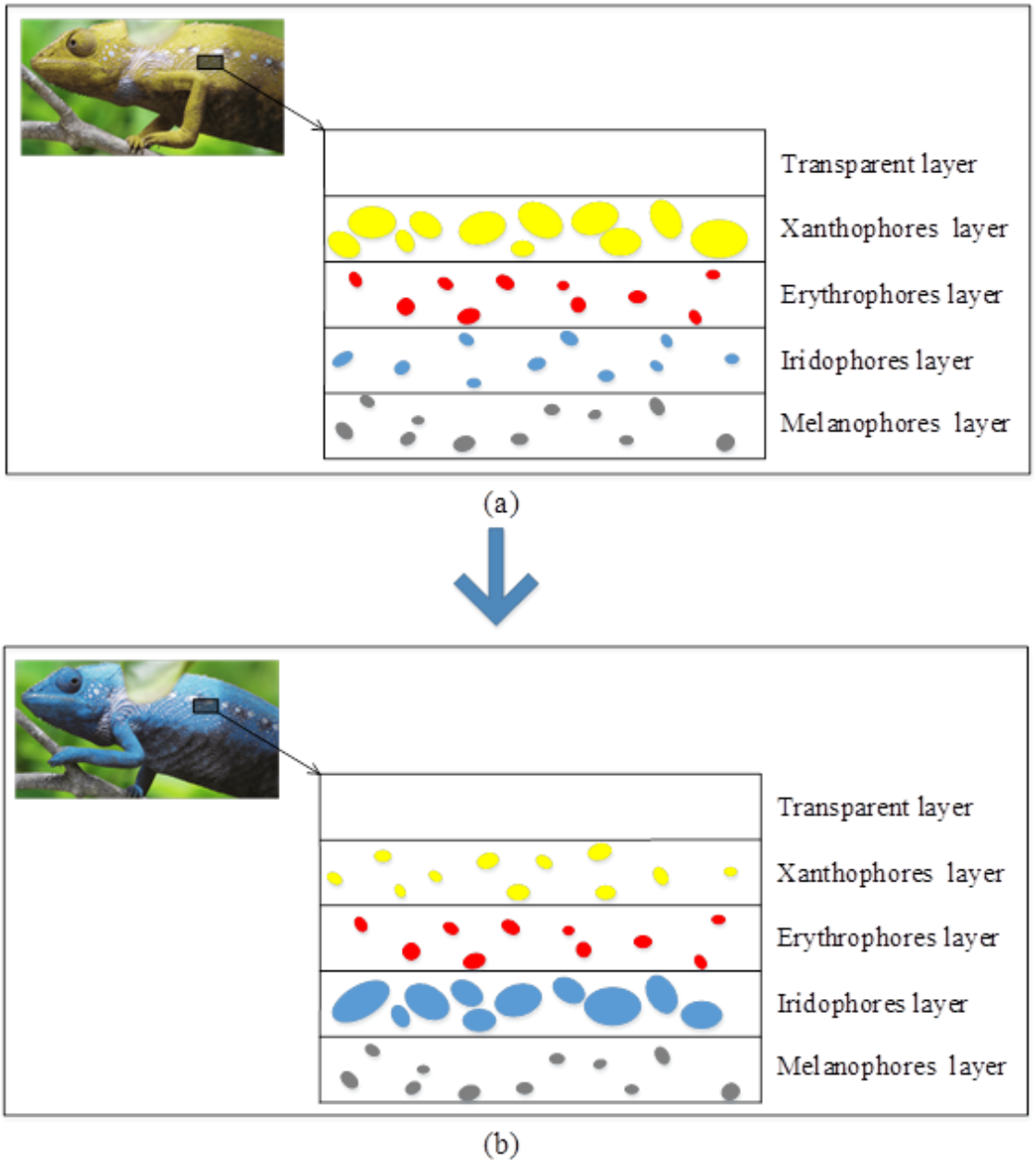

Figure 4-2. Chameleon has several skin layers which contain chromatophores

4.4.2 The biomimetic, electrochromic glazing system

The ability of chameleons to change their skin colour is an inspiration for many engineering fields such as material science and chemistry. In this study, it is found that the

mechanism of chameleons' skin is closely analogous to the essential requirement of façade system design for building energy efficiency. In the same manner with chameleon's skin, the façade system of buildings can be designed to proactively response to climatic conditions to regulate indoor thermal and visual conditions with minimal energy consumption. Inspired by the adaptive mechanisms of chameleon's skin, this study proposes the BAF system based on EC glazing material, as shown in Figure 4-3. The EC behaviour of materials, which was first introduced by Platt [34], is the phenomenon that a material can change its optical properties by applying a small external voltage or electrical current. Many technologies and materials based on this phenomenon are currently under speedy development. In particular, the application of EC glass in the building industry has emerged as a promising solution for both the efficient use of energy and indoor comfort in a building.

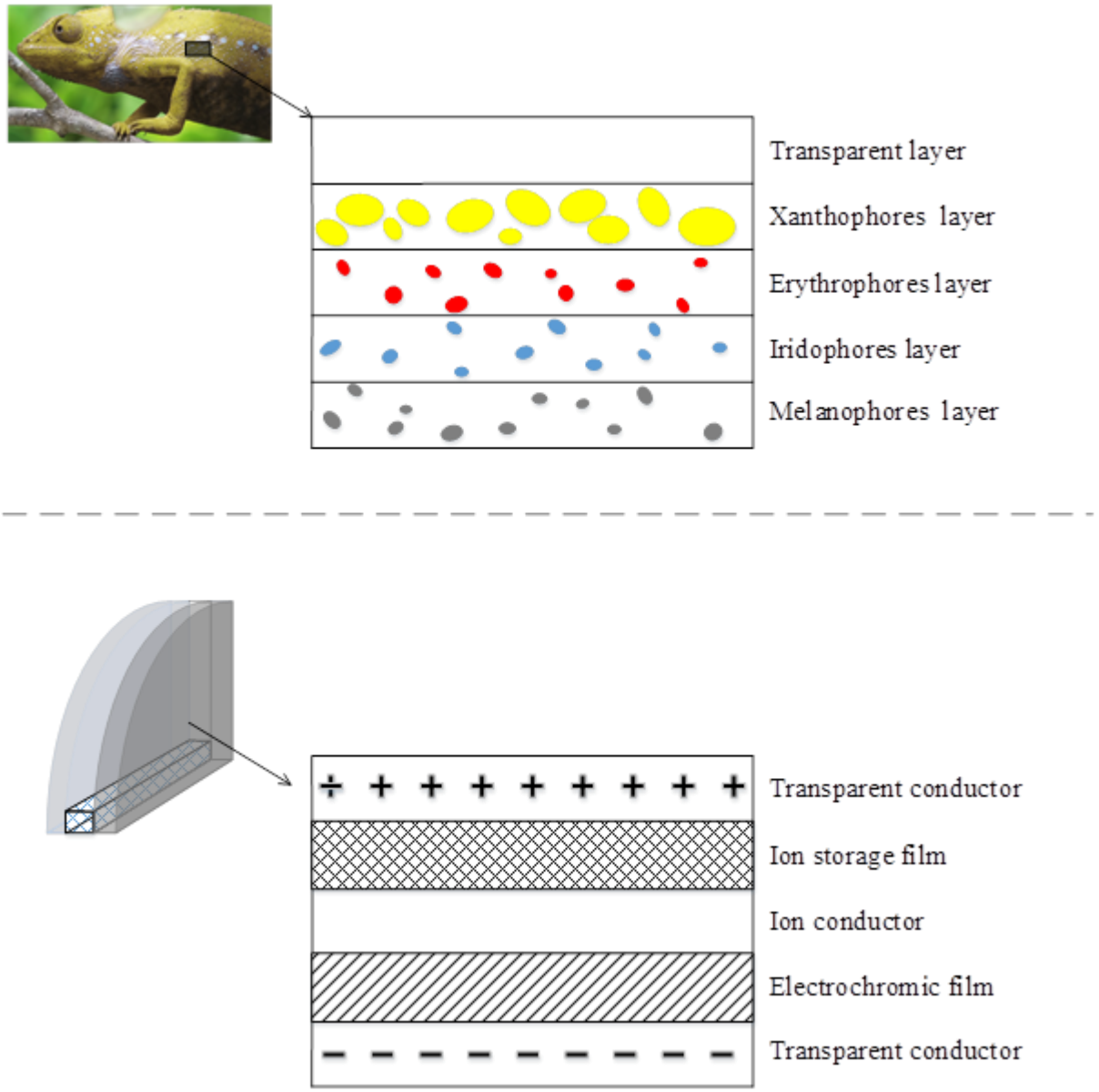

Figure 4-3. Mechanism of chameleons' skin is closely analogous to the EC glazing system.

Inspired by the extraordinary feature of chameleons and the advanced development of EC glass, the biomimetic adaptive glazing system is proposed and designed in this study. The system contains an EC coating layer, two glass layers and an argon-filled layer as shown in Figure 4-4. The EC coating layer, which is located on the inside surface of the exterior glass panel, represents the role of the pigment layer in chameleons' skin to provide the adaptive

ability of the proposed biomimetic, EC glazing system. The EC coating layer can change its colour from tint to dark to control the solar heat gain and transparent properties of the system.

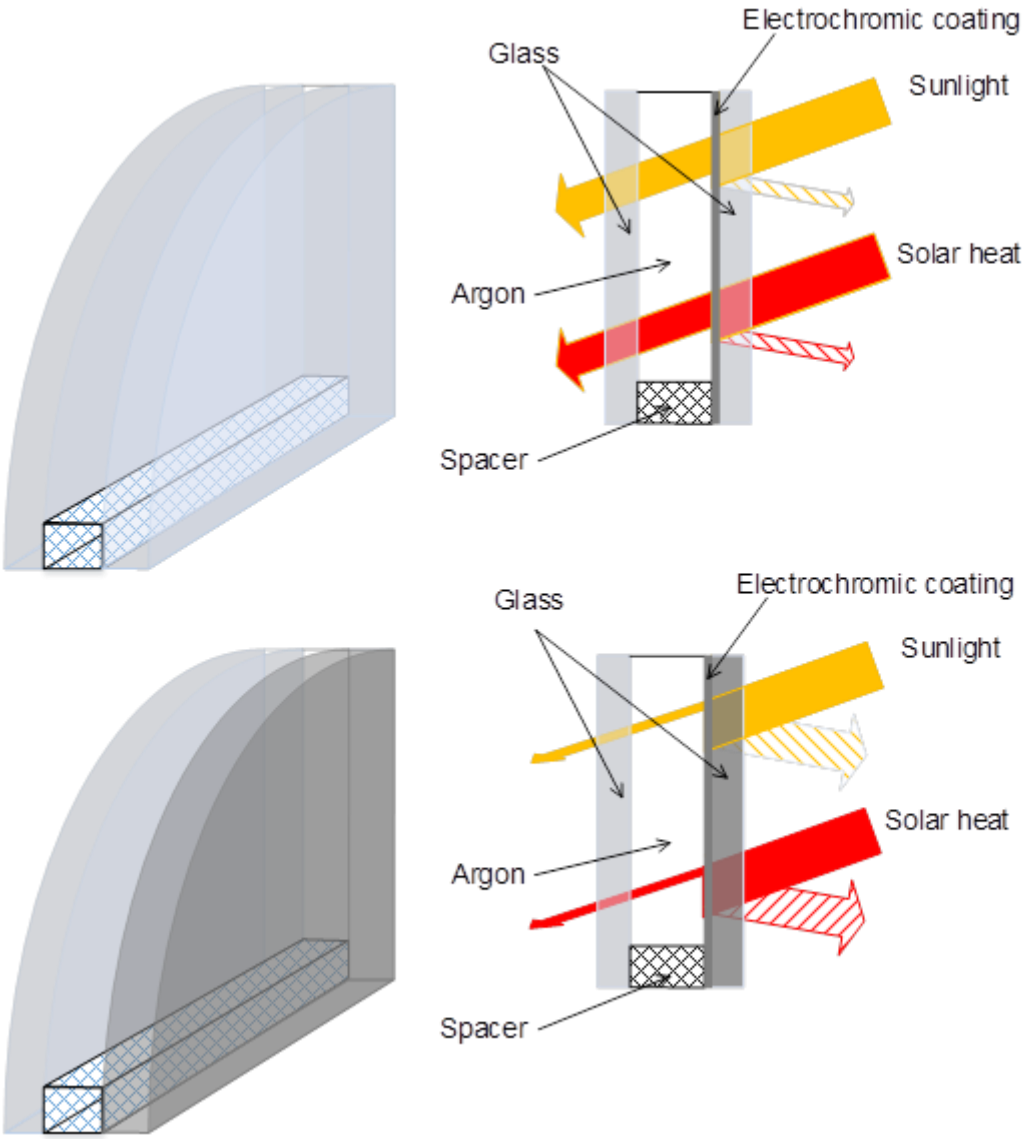

Figure 4-4. EC window in clear and tinted states.

The EC coating layer is a multilayer structure, which is similar to the skin of chameleons, as shown in Figure 4-5. Two sides of the coating layer are the anode and cathode, transparent conductor. Next to the anode layer, there is an ion storage film, which is used to store ionic species such as hydrogen ions (H^+) or lithium ions (Li^+) [35]. These ions are usually used because they are small and therefore, can easily move under the electric field. At the middle of

the coating layer, there is an ion conductor layer made by a solid-state electrolyte. The solid-state electrolyte is used to separate ion storage film and EC film because it is good for ion conductor and electron insulator. The last layer is an EC film which can conduct both electrons and ions. This layer is made by Tungsten oxide in most of the recent EC materials [36].

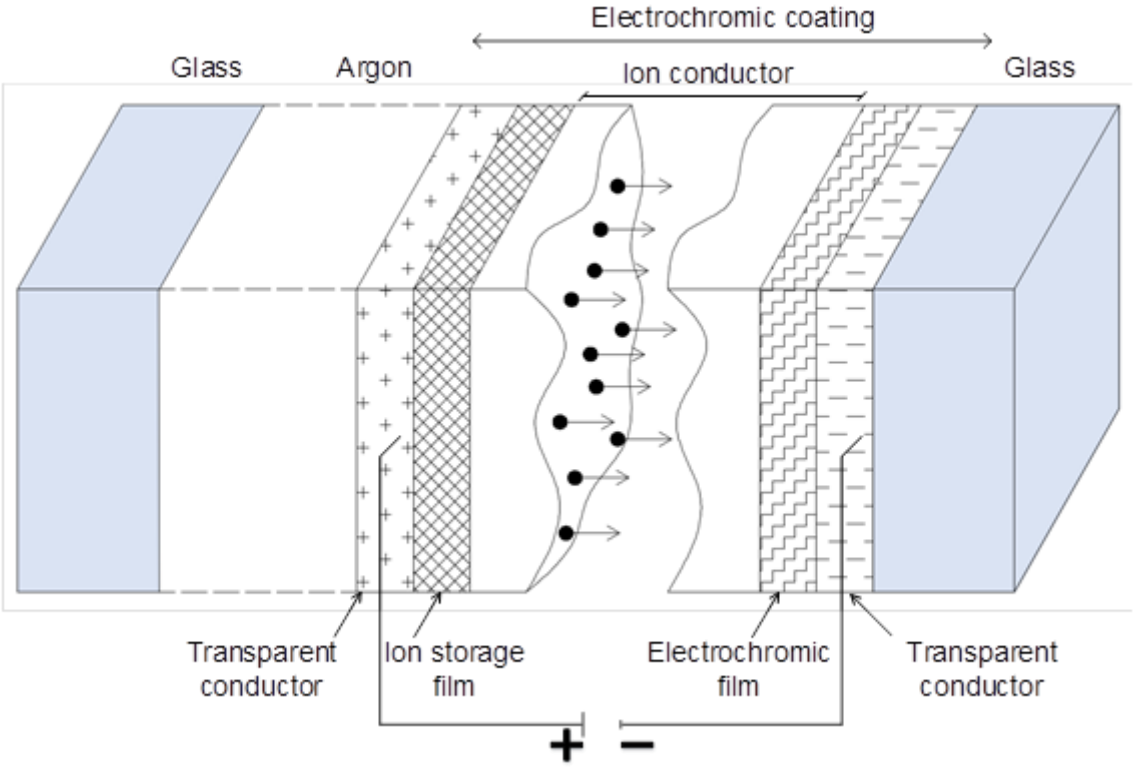

Figure 4-5. EC coating has five layers, including two transparent conductors, one ion storage film, one ion conductor and one EC film.

When applying a small voltage between the two transparent conductors, the EC coating darkens because the ions in the ion storage film move to the EC film. Electrons from the transparent conductor then insert into the EC film to balance the charge of these ions. Reversing the voltage polarity will help the coating return to a clear state as the ions return to their original layer. For an EC film made by Tungsten trioxide (WO_3), the insertion of ions (H^+) and electron (e^-) will alter the colour of the film. the simplified electrochemical reaction as below can be used to explain the change of colour:

$$\left[WO_3 + H^+ + e^- \right]_{\text{bleached}} \leftrightarrow \left[HWO_3 \right]_{\text{colored}} \quad (4.1)$$

Similarly, ion storage film contains Nickel (Ni) oxide, and its colour will change when removing ions (H+) and electron (e-) as follows:

$$\left[Ni(OH)_2 \right]_{\text{bleached}} \leftrightarrow \left[NiOOH + H^+ + e^- \right]_{\text{colored}} \quad (4.2)$$

Generally, transferring ions and electron from ion storage film to EC film causes both films to turn dark and to return the charge makes both films get back their transparency. Moreover, the optical absorption of Tungsten oxide and Nickel oxide are complementary, so they can help EC glass obtain too many shades of colour. This process enables the variation of optical properties (e.g. solar heat gain coefficient and visual transmittance) of EC glass. The operation of the proposed glazing system is energy efficiency because it only requires a small voltage, which uses less than 5V, for changing the optical properties of EC glass [37].

4.4.3 Design methodology for the biomimetic, electrochromic glazing system

4.4.3.1 WINDOW software

WINDOW software, which was developed by Lawrence Berkeley National Laboratory [38], is used to calculate window thermal performance indices (i.e., solar heat gain coefficients (SHGC), visual transmittance (Tvis), thermal transmittance (U-value)) of the EC window in this study. WINDOW is a popular software that can assist engineers in designing and developing new window products. This software can simulate for single or multi-layer glazing and calculate U-value, Tvis and SHGC of the glazing system.

4.4.3.2 Computational approach

This section provides the detailed structure of the computational approach for designing the adaptive façade. Figure 4-6 shows the framework of the approach. In the proposed

framework, WINDOW is used to calculate SHGC, Tvis and U-value of EC windows. These values, along with occupants' behaviour and geometry of the building, and weather condition, are used as input data for the optimisation process. The optimisation process simulates all scenarios based on the input data to find the optimal design of the BAF system. Then, the optimal results, which are the best sequence of EC glazing state, are transferred to a decision-making assistance tool to decide if it is worth to keep EC glazing in the current state or switch to another state by comparing the saving energy and energy consumption for the operation of EC glazing. In the last step, the final outputs are sent back to building operation system to control the EC glazing accordingly.

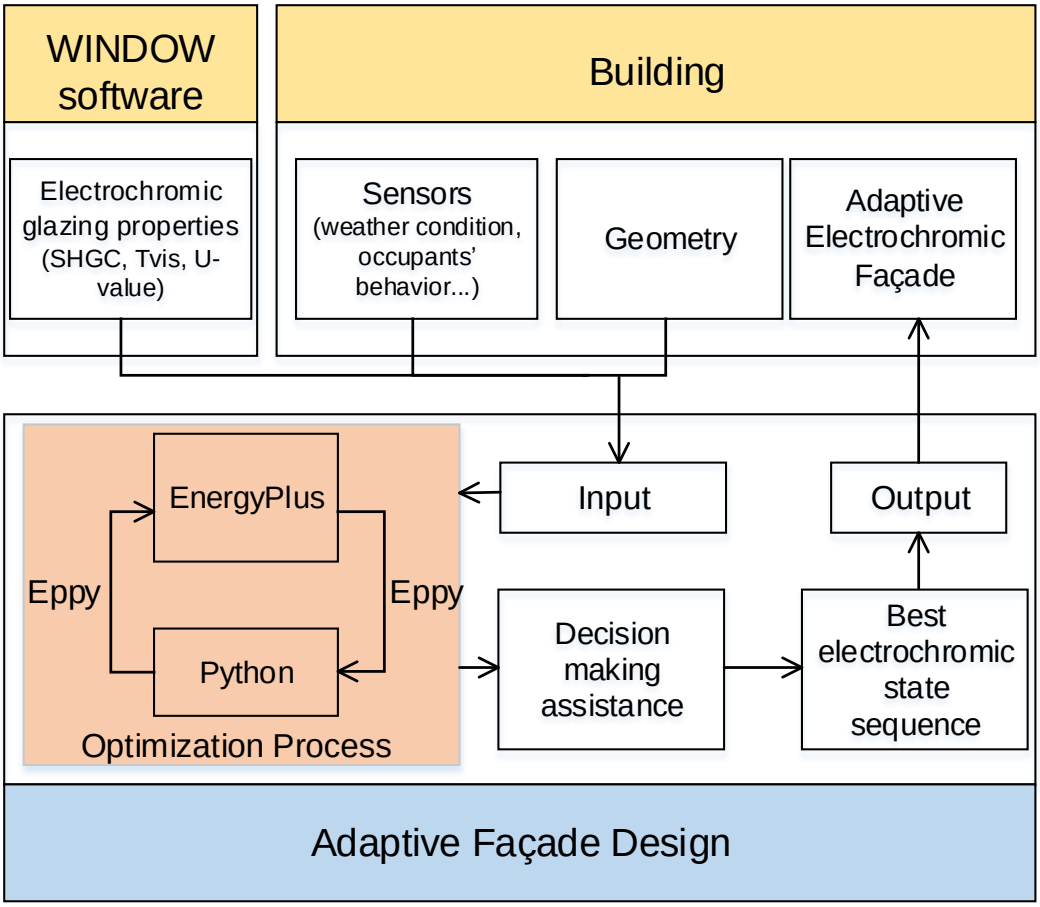

Figure 4-6. The framework of the computational optimisation approach for BAF design.

In this process, many EnergyPlus simulations are automatically performed in a Python environment with the assistance of Eppy package. Eppy, developed by Philip *et al.* [39] in Python, is an open-source package to control and manipulate EnergyPlus software in a systematic and programmatic way. The optimisation process finds the best EC state sequence to minimize energy consumption (i.e., lighting, heating and cooling) and satisfy visual comfort requirement. The design of BAF in this study can be formulated as an optimisation problem as follow:

Input: Building geometry, dynamic climatic conditions and EC glazing properties

Controlled variable: EC glazing state

Objective: minimize $E_{total} = E_{heating} + E_{cooling} + E_{lighting}$

Constraint: Glare index ≤ 22

The design of the EC glazing is subjected to building geometry, dynamic climatic conditions and EC glazing properties. Besides, the glare index is used as a constraint to keep the visual comfort for all building occupants. For an office, it will be too bright for working condition if the glare index is higher than 22 [40]. It is worth mentioning that the EC window requires energy to change its optical properties and maintain tint stages. This study takes into account this energy consumption for the operation of EC glazing by developing a decision-making assistance tool. This tool calculates the energy to maintain EC glazing at any tint state or switch to another state and the energy saved by this decision. The saving energy then is compared with the energy for the operation to have a final decision, as shown in Figure 4-7.

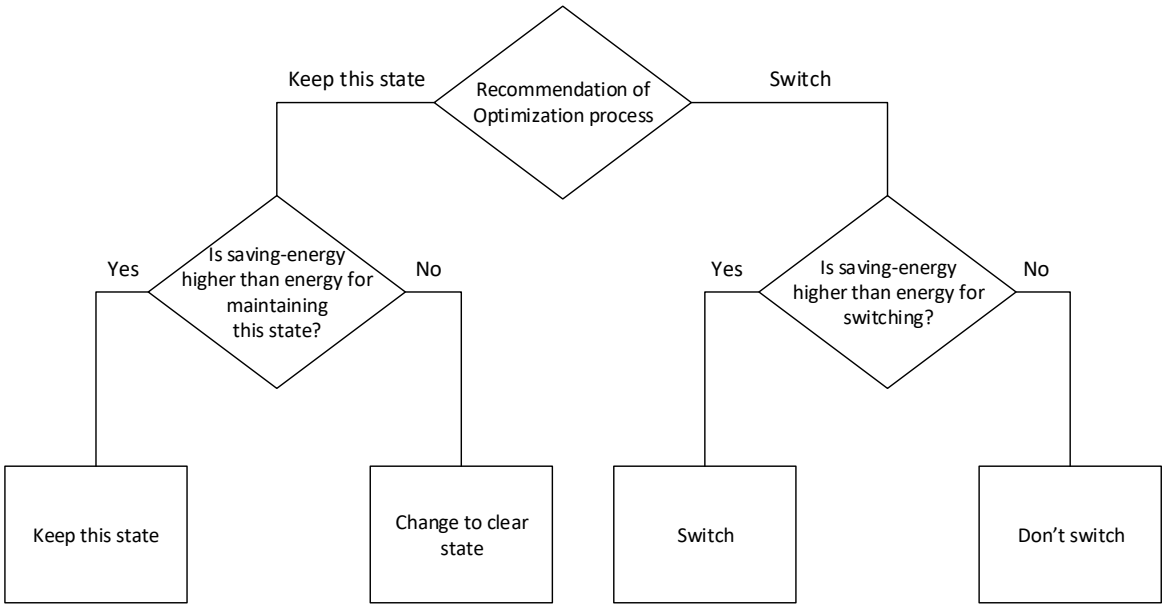

Figure 4-7. The flowchart of the decision-making assistance tool.

4.5 The energy performance of adaptive façades – case study

A case study of a medium office, which has three floors, and the total floor area is 4982 m^2, is developed in this study to demonstrate the capability of the proposed computational approach in improving the performance of EC glazing. This building, was used by the

Department of Energy as a building benchmark model [41], has a window on all four sides and the window-to-wall ratio is 60%, as shown in Figure 8. The windows of this building are assumed to use SageGlass EC glazing, and the windows on each side of the building are controlled separately. SageGlass EC glazing has a clear state, and three tint states, the thermal and visual properties of each state are calculated by WINDOW and shown in Table 4-1. In addition, this study also compares the adaptive EC glazing with a reference building with a conventional low-emittance window (U-value = 3.211 W/m^{2}K, SGHC = 0.522, Tvis = 0.728), which is static window and does not change its properties. The energy required to switch EC glazing from a clear state to tint state is 2.7 W/m^2 while the energy required to maintain the glazing to a given tint level is 1.5 W/m^2 [42]. The tinting of EC coating lags the command by around 10 min [42].

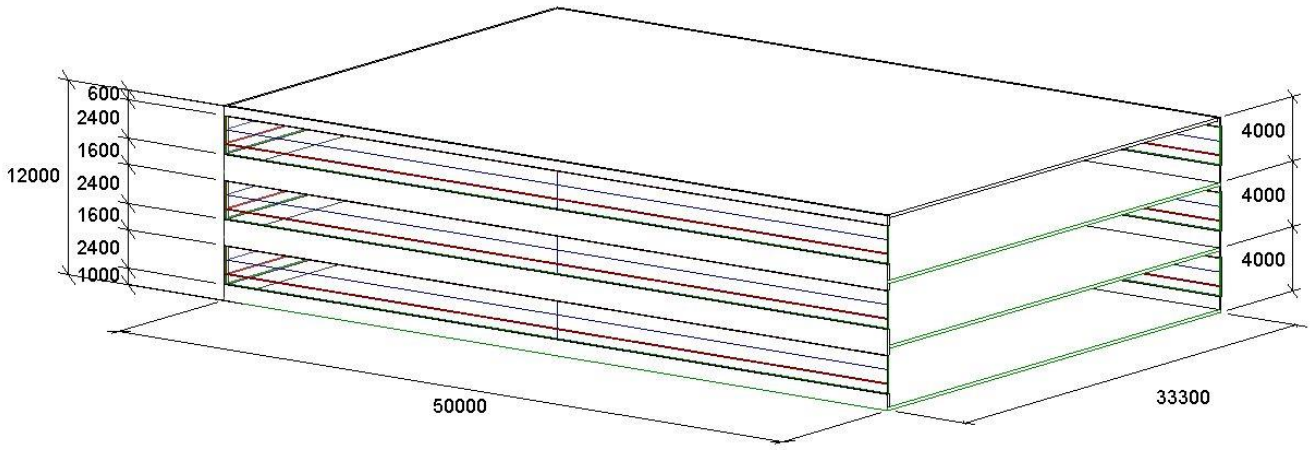

Figure 4-8. Case study: a medium office model

Table 4-1. Details thermal and visual properties of each state SageGlass EC glazing.

Window	SageGlass EC glazing				Low-E glass
	Clear	Intermediate state 1	Intermediate state 2	Fully tinted	

U-Value (W/m^2K)	3.534	3.534	3.534	3.534	3.228
SGHC	0.522	0.249	0.220	0.187	0.229
Tvis	0.728	0.203	0.119	0.014	0.189

In EnergyPlus simulations, it is assumed that people work from 8:00 to 17:00 on working days. The heat gain per floor area for lights is 12.9 (W/m2), and the lighting is scheduled to be on between working hours. The temperature setpoints of the HAVC system for heating and cooling are 18°C and 25°C, respectively, during the occupied hours. For non-working hours, these temperature setpoints are adjusted to 15°C and 28°C, respectively. Besides, a minimum workplace illuminance of 500 lux is maintained, and an illuminance sensor is placed at the centre of the room at the work plan level. Two locations, which are Melbourne, Australia and Texas, United State, of the office building, are investigated in this study and a typical meteorological year of each city is used for energy simulation. The study calculates annual energy consumption, including heating, cooling, and lighting of the office building, and the time step for the simulation is 1-hour.

4.6 Numerical results and Discussion

The performances of the BAF design are analysed and compared with the five reference benchmarks to show its potential to improve building energy efficiency. A comparison of the energy and visual performance for a whole year is shown in Table 4-2 for the two locations. The energy performance is the energy using for lighting, heating, and cooling while the visual performance is the percentage of time that the glare index does not exceed 22 during working hours. In other words, the visual performance of 100% meets the visual comfort requirements and vice versa. In Figure 4-9, the first four columns represent the performance of four static states of Sageglass glazing, while the last two column shows the energy consumption of the Low-E glazing and the adaptive case, respectively.

Table 4-2. Detailed energy and visual performance of the case study for BAF and reference benchmarks.

	Unit	Sageglass EC glazing				Low-e glazing	Adaptive EC glazing
		Clear	Tint 1	Tint 2	Tint 3		
Case 1 - Melbourne							
Lighting	10^8 kJ	1.58	2.51	2.84	3.26	2.57	2.22
Heating	10^8 kJ	2.66	2.83	2.85	2.86	2.80	2.47
Cooling	10^8 kJ	5.06	4.75	4.73	4.72	4.70	4.26
Operation	10^8 kJ	0.00	0.57	0.57	0.57	0.00	0.28
Energy consumption	10^8 kJ	9.30	10.66	10.99	11.41	10.07	9.22
Save	%	-	-	19.1	23.7	9.2	-
Visual performance	%	65	97	100	100	100	100
Case 2 - Texas							
Lighting	10^8 kJ	1.28	2.20	2.64	3.24	2.28	2.06
Heating	10^8 kJ	2.67	2.89	2.92	2.96	2.86	2.54
Cooling	10^8 kJ	10.04	9.02	8.99	9.00	8.91	8.25
Operation	10^8 kJ	0.00	0.57	0.57	0.57	0.00	0.34
Energy consumption	10^8 kJ	13.99	14.68	15.12	15.77	14.05	13.19
Save	%	-	-	14.6	19.6	-	-
Visual performance	%	56	86	99	100	89	100

*Energy save = (energy of the reference benchmark – energy of the adaptive façade)/ energy of the adaptive façade

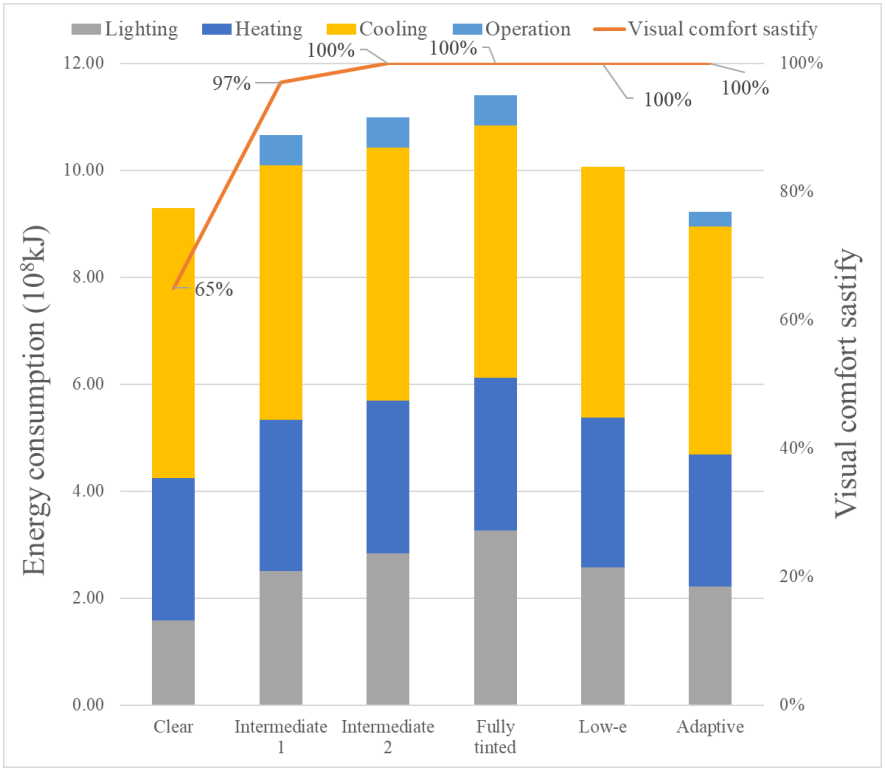

(a)

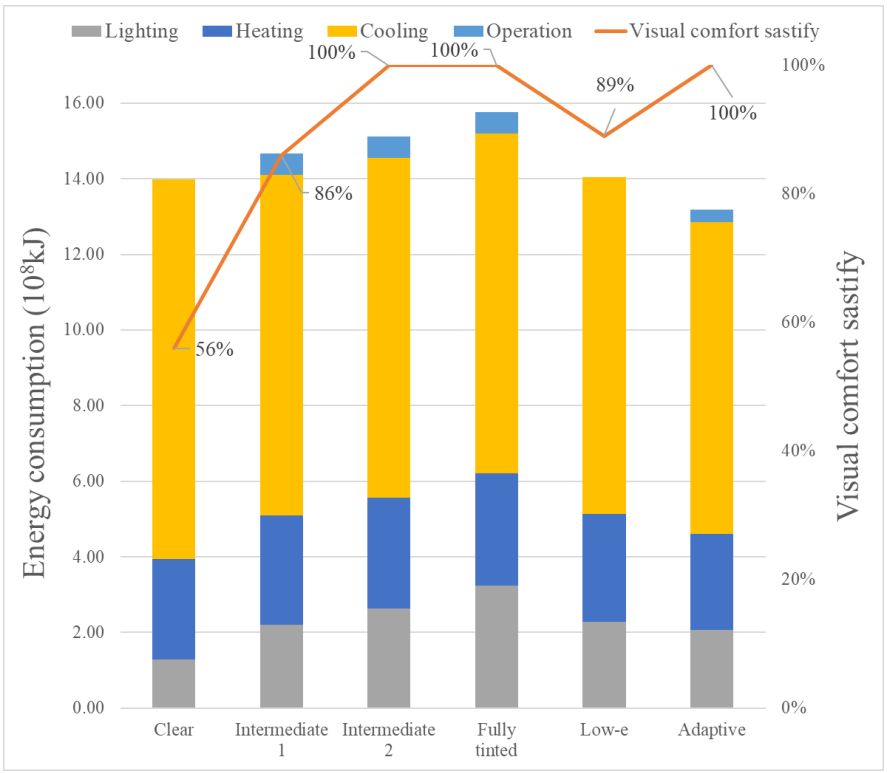

(b)

Figure 4-9. Comparison of results for (a) Melbourne and (b) Texas.

For the case study in Melbourne, the building with the adaptive EC glazing has consumed the smallest total energy (9.22E+8 kJ) for lighting, heating, cooling, and operation and satisfies the visual comfort with a visual performance of 100%. The buildings with static clear and Tint 1 Sageglass window do not satisfy the visual comfort requirements as the visual performances are 65% and 97%, respectively, as shown in Table 4-2. This means that the lighting condition of these cases is too bright and does not satisfy the comfortable working environment of building occupants. The results also indicate that the lighting and heating energy increase but the cooling load decrease when changing the state of Sageglass window from clear to fully tinted. This can be attributed to the fact that the clear state, which has the largest SHGC and T-vis, allows more light and heat from the sun go through the window, thereby reducing a noticeable amount of lighting and heating energy to maintain a comfortable interior condition for visual and thermal condition, respectively. On the other hand, the building with a clear state consumes more energy for cooling than other cases, especially in summer, because of receiving more light and heat from the outside environment.

It also should be noticed that the buildings, which have static Sageglass window at intermediate state 1, intermediate state 2 and fully tinted, have spent an amount of energy for keeping the window at that state. It is called operation energy and is calculated based on the area of EC glazing. On the contrary, the buildings with Sageglass clear state and Low-E glazing do not consume energy for operation. The computational optimisation approach found the optimal state for adaptive EC glazing at each side of the building to minimize the total of energy consumption but still satisfy the visual performance requirement.

The same tendency is noticed for the building in Texas when the building, which has adaptive EC glazing, consumed a minimum amount of energy for lighting, heating, cooling and operation among these models, with a total energy consumption of 13.19E+8 kJ. Three buildings with the adaptive EC glazing, the static intermediate state 2 Sageglass and the static

fully tinted Sageglass satisfy the visual comfort with visual performance is 100%. While the buildings with the static clear Sageglass, the static intermediate state 1 Sageglass and Low-E glazing do not pass the visual condition, as they have visual performances of 56%, 86% and 89%, respectively, as shown in Table 4-2. Compared to the static intermediate state 2 Sageglass and the static fully tinted Sageglass, the adaptive EC glazing can help to save 14.6% - 19.6% of the total energy consumption.

The durability of EC glazing is also investigated in this study. It is reported that the Sageglass EC glazing products can have a maximum of 100000 cycles over 30 years or 3333 cycles per year [43]. Table 4-3 shows the number of times that the glazing switches to another state in both case studies. The south-facing window in Texas case has the highest cycles with 2127 cycles over a year, which is smaller than the recommendations from the manufacturer. Therefore, the results from this study satisfy the durability condition of the Sageglass EC glazing products.

Table 4-3. Switching time of each side of the building

Orientation / Location	South	East	North	West
Melbourne	1603	1165	523	1125
Texas	2127	1215	1436	1136

4.7 Conclusions

In this study, the design concept and solution of BAF, which is inspired by the chameleon, is proposed and analysed to demonstrate its potential for improving the energy efficiency of buildings. This study provides a comprehensive analysis of the similarities between the mechanism of chameleon's skin and EC glazing. In addition, a computational

optimisation approach, which combines building energy modelling software (EnergyPlus), Eppy toolkit, and the decision-making assistance tool, is used to design and assess the viability of BAF systems.

Two locations, which are Melbourne, Australia and Texas, United States, were used for simulation to validate the capability of the proposed approach in optimising the total energy consumption. For each location, a computational optimisation approach obtains the optimal property sequence of the BAF that achieves the minimal energy consumption while satisfying the visual and thermal comfort for building occupants. For the office building in Melbourne, the BAF system can save the total energy consumption by 9.2% - 27.3% compared to the static Sageglass windows and Low-E window. For the case in Texas, the BAF can save between 14.6% - 19.6% of the total energy consumption compared to the reference windows. These results confirm both the potential of BAF in improving the energy efficiency and the capability of the proposed computational optimisation approach in supporting the design of BAF. The results of this research can be used as a guide to discover future research and development processes of BAF.

Acknowledgments

The first author would like to thank the University of Melbourne for offering the Melbourne Research Scholarship. This work was mainly supported by the CRC-P for Advanced Manufacturing of High Performance Building Envelope project, funded by the CRC-P program of the Department of Industry, Innovation and Science, Australia, and the Asia Pacific Research Network for Resilient and Affordable Housing (APRAH) grant, funded by the Australian Academy of Science, Australia. This work was also supported by the ARC Training Centre for Advanced Manufacturing of Prefabricated Housing (CAMP.H) at the University of Melbourne.

References

1. IEA, *World Energy Outlook 2015*. 2015.

2. Administration, U.S.E.I., *INTERNATIONAL ENERGY OUTLOOK 2016*. 2016.

3. Pérez-Lombard, L., J. Ortiz, and C. Pout, *A review on buildings energy consumption information.* Energy and Buildings, 2008. 40(3): p. 394-398.

4. Aye, L., T. Ngo, R.H. Crawford, R. Gammampila, and P. Mendis, *Life cycle greenhouse gas emissions and energy analysis of prefabricated reusable building modules.* Energy and Buildings, 2012. 47: p. 159-168.

5. Standardization, I.O.f., *ISO 7730 2005-11-15 Ergonomics of the Thermal Environment: Analytical Determination and Interpretation of Thermal Comfort Using Calculation of the PMV and PPD Indices and Local Thermal Comfort Criteria*. 2005: ISO.

6. Australia, G.B.C.o. *Green Star is an internationally-recognised sustainability rating system*. 2020; Available from: https://new.gbca.org.au/green-star/rating-system/.

7. Lepkova, N., D. Zubka, and R.L. Jensen, *Chapter 10 - Financial Investments for Zero Energy Houses: The Case of Near-Zero Energy Buildings*, in *Global Sustainable Communities Handbook*, W.W. Clark, Editor. 2014, Butterworth-Heinemann: Boston. p. 217-253.

8. Chua, K.J. and S.K. Chou, *Evaluating the performance of shading devices and glazing types to promote energy efficiency of residential buildings.* Building Simulation, 2010. 3(3): p. 181-194.

9. Taveres-Cachat, E., G. Lobaccaro, F. Goia, and G. Chaudhary, *A methodology to improve the performance of PV integrated shading devices using multi-objective optimization.* Applied Energy, 2019. 247: p. 731-744.

10. Chi, F.a., R. Wang, G. Li, L. Xu, Y. Wang, and C. Peng, *Integration of sun-tracking shading panels into window system towards maximum energy saving and non-glare daylighting.* Applied Energy, 2020. 260: p. 114304.

11. Luo, S., H. Li, Y. Mao, and C. Yang, *Experimental research on a novel sun shading & solar energy collecting coupling device for inpatient building in hot summer and cold winter climate zone in China.* Applied Thermal Engineering, 2018. 142: p. 89-99.

12. Bahaj, A.S., P.A.B. James, and M.F. Jentsch, *Potential of emerging glazing technologies for highly glazed buildings in hot arid climates.* Energy and Buildings, 2008. 40(5): p. 720-731.

13. Poirazis, H., Å. Blomsterberg, and M. Wall, *Energy simulations for glazed office buildings in Sweden.* Energy and Buildings, 2008. 40(7): p. 1161-1170.

14. Sheikh, W.T. and Q. Asghar, *Adaptive biomimetic facades: Enhancing energy efficiency of highly glazed buildings.* Frontiers of Architectural Research, 2019. 8(3): p. 319-331.

15. Kuru, A., P. Oldfield, S. Bonser, and F. Fiorito, *Biomimetic adaptive building skins: Energy and environmental regulation in buildings.* Energy and Buildings, 2019. 205: p. 109544.

16. López, M., R. Rubio, S. Martín, and C. Ben, *How plants inspire façades. From plants to architecture: Biomimetic principles for the development of adaptive architectural envelopes.* Renewable and Sustainable Energy Reviews, 2017. 67: p. 692-703.

17. Frosch, R.A. and N.E. Gallopoulos, *Strategies for manufacturing.* Scientific American, 1989. 261(3): p. 144-153.

18. Badarnah, L., *Towards the LIVING envelope: biomimetics for building envelope adaptation*. 2020.

19. Al-Obaidi, K.M., M. Ismail, and A.M. Abdul Rahman, *Passive cooling techniques through reflective and radiative roofs in tropical houses in Southeast Asia: A literature review*. Frontiers of Architectural Research, 2014. 3(3): p. 283-297.

20. La Roche, P. and U. Berardi, *Comfort and energy savings with active green roofs.* Energy and Buildings, 2014. 82: p. 492-504.

21. Zari, M.P., *Biomimetic design for climate change adaptation and mitigation.* Architectural Science Review, 2010. 53(2): p. 172-183.

22. Han, Y., J.E. Taylor, and A.L. Pisello, *Toward mitigating urban heat island effects: Investigating the thermal-energy impact of bio-inspired retro-reflective building envelopes in dense urban settings.* Energy and Buildings, 2015. 102: p. 380-389.

23. Webb, M., E. Hertzsch, and R. Green. *Modelling and optimisation of a biomimetic façade based on animal fur*. in *Proceedings of building simulation*. 2011.

24. Taghizade, K. and M.J.A.J.M.E.T. Taraz, *Designing a mobile facade using bionic approach.* 2013. 1(2): p. 22-29.

25. Fernández, M.L., R. Rubio, and S.M. González. *Architectural envelopes that interact with their environment*. in *2013 International Conference on New Concepts in Smart Cities: Fostering Public and Private Alliances (SmartMILE)*. 2013. IEEE.

26. Yowell, J. and N. Oklahoma, *Biomimetic building skin: A phenomenological approach using tree bark as model*. 2011, Citeseer.

27. Stegmaier, T., M. Linke, H.J.P.T.o.t.R.S.A.M. Planck, Physical, and E. Sciences, *Bionics in textiles: flexible and translucent thermal insulations for solar thermal applications.* 2009. 367(1894): p. 1749-1758.

28. Mäkitalo, J., *Simulating control strategies of electrochromic windows: Impacts on indoor climate and energy use in an office building*. 2013.

29. Dussault, J.-M. and L. Gosselin, *Office buildings with electrochromic windows: A sensitivity analysis of design parameters on energy performance, and thermal and visual comfort.* Energy and Buildings, 2017. 153: p. 50-62.

30. Hoon Lee, J., J. Jeong, and Y. Tae Chae, *Optimal control parameter for electrochromic glazing operation in commercial buildings under different climatic conditions.* Applied Energy, 2020. 260: p. 114338.

31. Glaw, F., *Taxonomic checklist of chameleons (Squamata: Chamaeleonidae).* Vertebrate Zoology, 2015. 65(2): p. 167-246.

32. Walton, B.M. and A.F. Bennett, *Temperature-Dependent Color Change in Kenyan Chameleons.* Physiological Zoology, 1993. 66(2): p. 270-287.

33. Teyssier, J., S.V. Saenko, D. van der Marel, and M.C. Milinkovitch, *Photonic crystals cause active colour change in chameleons.* Nature Communications, 2015. 6(1): p. 6368.

34. Platt, J.R., *Electroehromism, a possible change of color producible in dyes by an electric field.* The Journal of Chemical Physics, 1961. 34(3): p. 862-863.

35. Granqvist, C.G., *20 - Electrochromic glazing for energy efficient buildings*, in *Nanotechnology in Eco-efficient Construction (Second Edition)*, F. Pacheco-Torgal, et al., Editors. 2019, Woodhead Publishing. p. 467-501.

36. Thummavichai, K., Y. Xia, and Y. Zhu, *Recent progress in chromogenic research of tungsten oxides towards energy-related applications.* Progress in Materials Science, 2017. 88: p. 281-324.

37. Sbar, N.L., L. Podbelski, H.M. Yang, and B. Pease, *Electrochromic dynamic windows for office buildings.* International Journal of Sustainable Built Environment, 2012. 1(1): p. 125-139.

38. LBNL, B.L. *WINDOW*. Available from: https://windows.lbl.gov/software/window.

39. Santosh Philip, Tuan Tran, Eric Allen Youngson, and J. Bull. *Eppy*. 2013; Available from: https://eppy.readthedocs.io/en/latest/index.html.

40. Piccolo, A. and F. Simone, *Effect of switchable glazing on discomfort glare from windows.* Building and Environment, 2009. 44(6): p. 1171-1180.

41. (DOE), U.S.D.o.E. *Commercial Reference Buildings*. Available from: https://www.energy.gov/.

42. Lee, E.S., C. Gehbauer, B.E. Coffey, A. McNeil, M. Stadler, and C. Marnay, *Integrated control of dynamic facades and distributed energy resources for energy cost minimization in commercial buildings.* Solar Energy, 2015. 122: p. 1384-1397.

43. Tällberg, R., B.P. Jelle, R. Loonen, T. Gao, and M. Hamdy, *Comparison of the energy saving potential of adaptive and controllable smart windows: A state-of-the-art review and simulation studies of thermochromic, photochromic and electrochromic technologies.* Solar Energy Materials and Solar Cells, 2019. 200: p. 109828.

Chapter 5
A data-driven approach for predicting energy consumption in building

[PUBLISHED JOURNAL[3]]

5.1 Introduction to the paper

Chapter 3 and chapter 4 have showed that the proposed computational optimisation approach can support the design and operation process of biomimetic adaptive façade (BAF). However, the building energy simulation software in the proposed approach has some limitations such as time consuming and requiring expertise experience. Therefore, this chapter proposes a data-driven approach to complement the building energy simulation software in the computational optimisation approach. The data-driven approach can learn from the provided energy data and try to understand the relationship among all variables in the data. Therefore, it can improve existing limitations on modelling building energy consumption. This chapter is a published article in *Energy journal (Journal Impart Factor: 5.537, Rank 8/408 in Civil Engineering)*, titled "An artificial neural network (ANN) expert system enhanced with the electromagnetism-based firefly algorithm (EFA) for predicting the energy consumption in buildings". This chapter presents the third research objective of this thesis, which is the development and

[3] Bui, D.-K., T.N. Nguyen, T.D. Ngo, and H. Nguyen-Xuan, An artificial neural network (ANN) expert system enhanced with the electromagnetism-based firefly algorithm (EFA) for predicting the energy consumption in buildings. Energy, 2020. 190: p. 116370.

evaluation of a data-driven approach for prediction of energy consumption in building. The highlights of this study are:

- A new hybrid machine learning model is proposed to predict the energy consumption in the building.
- The hybrid model is based on artificial neural network and Electromagnetism-based Firefly Algorithm.
- Two datasets are used to validate the capability of the proposed model.
- The proposed approach can provide an effective alternative tool for making fast and accurate predictions of energy consumption in the building.

The key findings of this study are:

- This chapter has successfully integrated an in-house optimisation algorithm, namely Electromagnetism-based Firefly Algorithm, with a machine learning algorithm, called artificial neural network, into a hybrid model.
- The proposed model can improve the accuracy in predicting the energy consumption of buildings by 16.18% - 98.50% compared to other machine learning models.
- The proposed model can provide a sensitivity analysis to identify the inputs, which have a critical impact on the output of each dataset. This result can help designers to quickly validate their design of a façade system and improve its energy performance by focusing on these essential inputs.
- The proposed approach can be used as a useful tool for quickly and accurately solving many problems in engineering, including energy-efficient buildings, construction material strength, and structural strength.

During the course of this PhD research, another application of the proposed data-driven approach is also conducted for predicting the properties of concrete material. This work was

published in *Construction and Building Material* journal, titled "A modified firefly algorithm-artificial neural network expert system for predicting compressive and tensile strength of high-performance concrete" and is presented in Appendix A.

5.2 Abstract

In this study, a new hybrid model, namely the Electromagnetism-based Firefly Algorithm - Artificial Neural Network (EFA-ANN), is proposed to forecast the energy consumption in buildings. The model is applied to evaluate the heating load (HL) and cooling load (CL) using two given datasets. Each dataset was obtained by monitoring the effect of the façade system and dimensions of the building, respectively, on energy consumption. The performance of EFA-ANN is validated by comparing the obtained results with other methods. It is shown that EFA-ANN provides a faster and more accurate prediction of HL and CL. A sensitivity analysis is conducted to identify the impact of each input on the energy performance of the building. From the results of this study, it is evident that EFA-ANN can assist civil engineers and construction managers in the early designs of energy-efficient buildings.

5.3 Introduction

There are three major economic sectors in the world, including transportation, industry, and building [1]. A substantial share of global energy is consumed by buildings, which is expected to increase to 32.4% by 2040 [2]. In participating nations of the Organization for Economic Cooperation and Development (OECD), including Australia, New Zealand, United Kingdom and the United States, energy consumption in buildings has grown by 1.5% per year from 2012 to 2040. In non-OECD nations, being mostly developing countries, the growth rate is 2.1% per year in the same period [3]. Therefore, the development of energy efficient building systems is essential and consequently, many efforts have been devoted to this area [4, 5].

In the majority of cases, heating and cooling energy demands mostly account for building energy consumption [6]. Therefore, the early prediction and reduction of heating and cooling loads plays a vital role in designing an energy-efficient building. This provides designers with access to various building designs or Heating Ventilation and Air Conditioning (HAVC) system control options to find the optimal solution for reducing energy consumption in buildings. For instance, Zemella et al. optimized the design of façades of energy-efficient buildings by making early predictions of energy consumption due to heating, cooling, and lighting [7]. Also, Magnier and Haghighat applied a method to predict the energy consumption due to heating, cooling, and fan systems, and optimized the building design based on these predictions [8]. In another study, Ferreira et al. proposed a model-based predictive control methodology to control the HAVC system in a building and reported savings of around 50% in energy consumption [9]. Ghahramani et al. provided a systematic approach to optimize the setpoint and deadband parameter of the HVAC system by pre-calculating the energy consumption of HVAC [10]. Therefore, the early prediction of heating and cooling loads is critical to reducing the total energy consumption of a building.

However, many aspects, including temperature, sunlight equipment, occupant behavior, wall materials, glazing area, surface, height and volume of the building, have interactions between the overall energy requirements of the building [11-13]. For instance, Ihara *et al.* concluded that all façade properties including solar reflectance, U-value, solar heat gain coefficient (SHGC) have different effects on the energy efficiency of buildings. They suggested that the reduction of SHGC is the most effective method for reducing energy consumption [14]. In contrast, Liu et al. showed that reducing SHGC does not improve the energy efficiency of a building without an appropriate U-value [15]. Many other factors affect the total energy consumption in a building, including weather conditions, building dimensions, and the

behaviour of occupants. Therefore, it is quite challenging to calculate energy consumption given that all the above parameters and their interactions should be considered.

There are three main categories in building energy assessment, including engineering calculations, numerical simulations, and machine learning. The first approach focuses on using physical laws to calculate the energy consumption of an entire building. This approach is only suitable for preliminary analysis as it is mathematically intensive. In this research, the numerical simulation approach was used to simulate the energy performance of a building and overcome the limitations of engineering calculations. Several building energy simulation programs, including EnergyPlus, DOE-2, Window, Autodesk Ecotect, TRNSYS, and eQUEST, were used to simulate and predict energy consumption of a building. However, this method employs physics-based simulations, which are often time-consuming and resource-intensive, and the complexity and demand increase with the size and complexity of the project [16]. Also, the optimisation process must be manual based on user experience [17]. In many cases, energy models cannot reflect the actual performance of a building in reality as they lack the required details and need to make simplifications [18]. Thus, the conventional procedures are often unsatisfactory for designing a façade because they are mainly based on a particular design condition and the experience of experts. Accordingly, a significant development of an advanced approach is required.

To this effect, machine learning (ML), was proposed to design energy-efficient building services. This method applies a learning process to infer a relationship between the building data and energy consumption of buildings. In recent years, several advantages of ML have been demonstrated over conventional approaches [19, 20]. Consequently, many ML techniques have been applied to solve energy problems [21-23]. Robinson et al. successfully applied various ML techniques to predict the energy consumption of a commercial building based on various building features [21]. Ahmad et al. proposed four ML approaches to forecast short, medium

and long-term energy consumption in a building [22]. In another study, Chou and Tran used a hybrid ML model to estimate the energy consumption of residential householders with high accuracy [23]. ML can also be used to support several adaptive systems in a building [24, 25]. For example, Ghahramani et al. developed a novel adaptive hybrid metaheuristic algorithm based on ML and other smart components to optimize the energy of an HVAC system [24]. Moon et al. proposed an ML model for controlling the temperature of an adaptive double skin envelope [25].

Recently, among many ML techniques, an artificial neural network (ANN) has been widely used in optimizing the design of an energy-efficient building. Jin et al. used an ANN-based thermal control logic model to optimize the initial conditions and heating system operations in a building [26]. In another study, Wang et al. forecasted the dynamic building cooling load by combining ANN and an ensemble model [27]. Chung et al. proposed an ANN model to design a comfortable indoor thermal environment in an energy-efficient manner [28].

Notwithstanding many advantages, the ANN model depends on several initial parameters, including weights and biases [29]. Therefore, many studies were carried out to improve the performance of ANN by combining it with optimisation algorithms. For example, Yam and Chow optimized the initial weights of ANN by using linear algebraic methods [30]. Liu et al. enhanced the generalizations and accuracies of ANN by using an ensemble method [31]. Also, Chang et al. [32] and Lee et al. [33] proposed a genetic algorithm and a harmony search algorithm, respectively, to optimize the initial weights of the ANN model.

Among many optimisation algorithms, our approach is to propose an Electromagnetism-based Firefly Algorithm (EFA), which is found to be an efficient optimisation tool that can solve complicated problems. For instance, Shammari et al. combined the firefly algorithm (FA) and support vector machine model to predict the heating load of a heating system [34]. Coelho

and Mariani proposed FA and a Gaussian distribution function to optimize the loading of a chiller for energy conservation [35]. Chu and Chang used the Electromagnetism Algorithm (EA) to solve the resource allocation problem in stochastic networks [36]. However, both FA and EA still show several disadvantages, including premature convergence and divergence [37-39], which will be discussed in the following section. Therefore, in this study, we propose a new approach based on a hybrid model of FA and EA, called EFA, which aims to enhance the capability of ANN for predicting the energy consumption of a building.

Section 2 and 3 describe the theory behind of EFA and ANN, respectively. Details of the proposed EFA-ANN are provided in Section 4. Section 5 introduces the two datasets used to train EFA-ANN. The proposed method is validated in Section 6. Concluding remarks and recommendations for future research are provided in Section 7.

5.4 Electromagnetism-based Firefly Algorithm – Artificial Neural Network Model

5.4.1 An electromagnetism-based firefly algorithm

The Electromagnetism-based Firefly Algorithm (EFA) is a new hybrid optimisation algorithm that incorporates the advantages of the firefly algorithm (FA) and Electromagnetism Algorithm (EA). Firstly, FA, which was proposed by Yang [37], is a swarm intelligence method and is based on the flashing patterns and behavior of tropical fireflies. In FA, the brightness of a firefly is determined by an objective function. A firefly will tend to move closer to the brighter firefly and is not affected by a darker one. On the other hand, the EA was introduced by Birbil and Fang [39]. It imitates the attraction-repulsion mechanism to solve global optimisation problems. In EA, all points converge to the highly attractive valleys and move further away from steeper hills. This idea is the same as the attraction-repulsion mechanism described by the theory of electromagnetism. However, better points are easily

distracted if there are many worse points in the population. Also, EA is not effective in a local search because it randomly moves all points without any advanced technique.

In EFA, all fireflies are assumed to be magnetized, and the charge of a firefly depends on its objective value. Therefore, fireflies will move close to attractive fireflies and move away from the repulsive ones. Thus, all fireflies can contribute to the search process and improve the performance of EFA. Based on their charges, all fireflies are ranked in each iteration, and a firefly only has attraction and repulsion by an attractive or repulsive neighboring firefly, respectively. In this way, fireflies are not distracted by many forces as in EA. Consequently, EFA can quickly find promising areas in the exploration phase and then perform local searches in these areas to find the optimal solution in the exploitation phase. Local searches in EFA are performed using Lévy flight inspired by FA.

5.4.1.1 Initialization

Firstly, EFA is initialized in the same manner as FA, when the coordinates of the initial population of fireflies are uniformly distributed between the corresponding lower and upper bounds as follows

$$x^o = lb_k + rand\,(0,1)(ub_k - lb_k) \tag{5.1}$$

where lb_k, ub_k are the lower and upper boundaries of the k^{th} coordinate, respectively; $rand\,(0,1)$ is a random number following a normal distribution within [0,1]. This study uses a logistic map to improve the performance of EFA. The logistic map generates the initial coordinates of fireflies using Eq. (5.2). It can provide an initial diverse population and also reduce the probability of premature occurrence [40]:

$$x_o^{\bar{t}+1} = a x_o^{\bar{t}} \left(1 - x_o^{\bar{t}}\right) \tag{5.2}$$

where $x_o^{\bar{t}}$ is a chaotic number at $\bar{t}$ iteration of the initialization process; a is fixed at 4 [41].

5.4.1.2 Local search

EFA inherits the exploitation capacity of FA and EA for searching conducting a local search in the vicinity of each coordinate. In other words, the local search of EFA follows Eq. (5.3) and the improvement of each firefly is sought by coordinate. In this way, the probability of finding a better point is increased.

$$x_i^{t+1} = x_i^t + \alpha^t \varepsilon L(s) \tag{5.3}$$

where ε is a vector of random numbers and is defined by Eq. (5.4) as follows:

$$\varepsilon = rand - 1/2 \tag{5.4}$$

where *rand* is a random number generated by a uniform distribution in [0, 1].

In addition, α^t is a trade-off constant at *t* iteration [37] and is calculated as follows:

$$\alpha^t = \alpha_0 \theta^t \tag{5.5}$$

where α_0 and α^t are the initial trade-off coefficient and the trade-off coefficient at the t^{th} iteration, respectively; and θ is the adaptive parameter ($0 < \theta < 1$) [37].

Finally, $L(s)$ is the Lévy distribution, which can be defined as follows:

$$L(s) \sim s = \frac{u}{|v|^{1/\tau}} \tag{5.6}$$

where *s* is a power-law distribution, τ is an index, and *v* and *u* are calculated to follow a normal distribution as follows:

$$v \sim N\left(0, \sigma_v^2\right) \tag{5.7}$$

$$u \sim N\left(0, \sigma_u^2\right) \tag{5.8}$$

where:

$$\sigma_v = 1 \tag{5.9}$$

$$\sigma_u = \left\{ \frac{\Gamma(1+\tau)\sin(\pi\tau/2)}{\Gamma\left[(1+\tau)/2\right]\tau 2^{(\tau-1)/2}} \right\}^{1/\tau} \tag{5.10}$$

where $\Gamma(z)$ is the Gamma function, which is determined by:

$$\Gamma(z) = \int_0^\infty t^{z-1} e^{-t} dt \tag{5.11}$$

5.4.1.3 **Movement**

EFA benefits from the advantages of both EA and FA. Firstly, EFA has inspired the concept of attraction and repulsion forces from EA. However, EFA ranks all fireflies based on their objective function values and a firefly *i* is only affected by the attraction (F_g) and repulsion force (F_r) from the next better $(i-1)$ and worse firefly $(i+1)$. In contrast, all fireflies in the population are considered in EA. In this way, EFA can mitigate the interference from many fireflies and quickly find the optimal solution. The movement of a magnetic firefly is written as:

$$x_i^{t+1} = x_i^t + \left(x_{i-1}^t - x_i^t\right)\frac{F_g}{\left\|F_g\right\|}(1-\alpha) + \left(x_{i+1}^t - x_i^t\right)\frac{F_r}{\left\|F_r\right\|}\alpha + \alpha\varepsilon L(s) \tag{5.12}$$

where F_g and F_r are attraction and repulsion forces, which are defined by Eq. (13) and Eq. (14), respectively:

$$F_g = |x_{i-1} - x_i| \frac{q_{i-1}q_i}{\left\|x_{i-1} - x_i\right\|^2} \tag{5.13}$$

$$F_r = | x_i - x_{i+1} | \frac{q_i q_{i+1}}{\left\| x_i - x_{i+1} \right\|^2} \tag{5.14}$$

where q_i is the charge of the point i, which is defined as follows:

$$q_i = \exp\left(- \frac{f\left(x^i\right) - f\left(x^{best}\right)}{\sum_{k=1}^{n} \left(f\left(x^i\right) - f\left(x^{best}\right) \right)} \right) \tag{5.15}$$

where $f(x)$ is the objective function. A firefly with better objective values has a higher charge. The objective function used in EFA-ANN model will be discussed in more detail in Section 2.3.

EFA uses the weights 1-α and α to modify the effects of the attraction (F_g) and repulsion (F_r) forces during the optimisation process. As alpha decreases from 1 to 0 during the optimisation process in the early stages, the fireflies are significantly influenced by F_r to explore the promising area. In the final stages, the effect of F_g and F_r is increased and decreased, respectively, to help the fireflies exploit the optimal solution in the best promising area. Therefore, these improvements help EFA find a better solution as opposed to the separate applications of EA and FA. The efficiency of EFA will be validated in the following sections.

In each iteration, EFA chooses the best firefly based on the value of the objective function. The best firefly then performs a local search around its place by Levy flight while the rest of the population searches for other areas. At the end of the iteration, the best firefly is chosen, and the process continues until the termination criteria are reached. The termination criteria helps to reduce the computing time without affecting the solution quality. The objective function and termination criteria in this study will be discussed in Section 5.1.3.3. Figure 5-1

summarizes the pseudo-code of EFA, while Figure 5-2 illustrates a flowchart of the search process of EFA.

Start EFA

Eq. (5.1) \\ Generate initial population of fireflies by logistic map

Define objective function *f(x)* for all fireflies

Rank the fireflies based on objective function and find the current best

while (*t* <*MaxGeneration*)

for *i* = 1: *n* \\ *n* is number of fireflies

if $i \neq 1$ \\ the current best firefly is not attracted by others

Eq. (5.12) \\Move firefly *i* in *d*-dimension (Exploration phase)

end if

Eq. (5.3) \\Local search (Exploitation phase)

Evaluate new solutions and update the coordinate and the objective function

end for *i*

t = t +1

end while

Post process results and visualization

End EFA

Figure 5-1. Pseudocode for EFA.

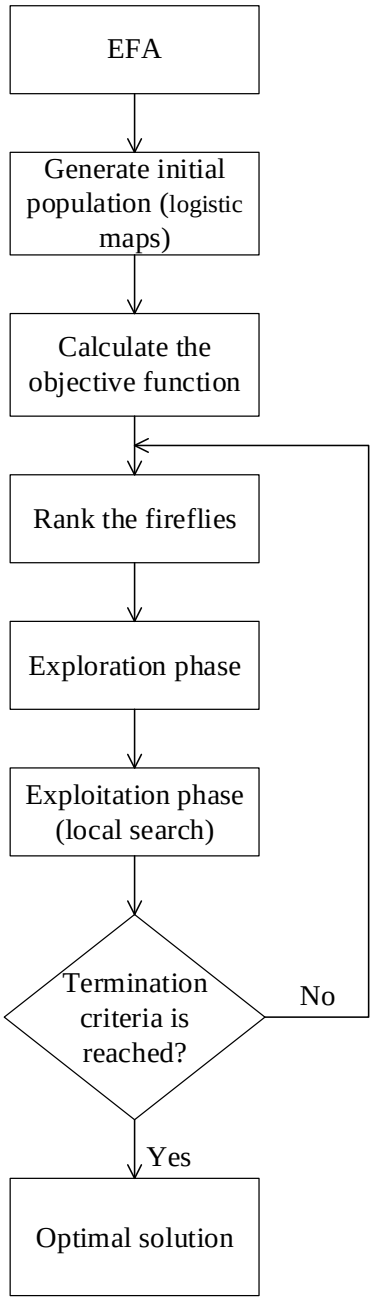

Figure 5-2. The flowchart of EFA

5.4.2 Artificial Neural Network

Technical details of ANN can be found in a previous study by [42, 43]. This study outlines the main concepts of the ANN model. Figure 5-3 illustrates the layout of an ANN model with a set of artificial neurons. Each neuron in a layer sends a signal to another neuron in the next layer by a connection, which is assigned a weight, and the weight represents the strength of the signal [44, 45].

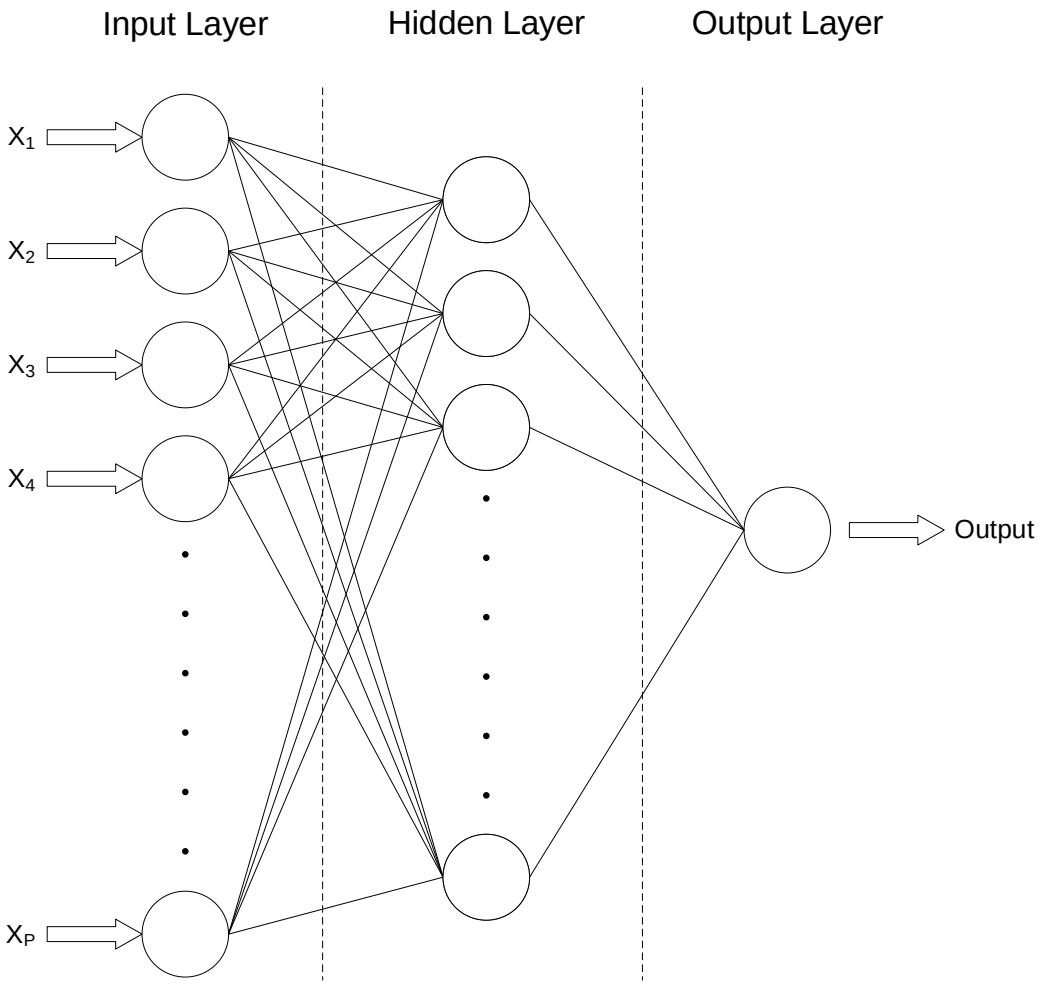

Figure 5-3. The layout of an ANN model.

In the hidden layer, the signals from the input layer are calculated by a linear function (see Eq. 5.16) and a transfer function (see Eq. 5.17) to generate the output signal of a hidden node [46] as depicted in Figure 5-4.

$$net_i = \sum_{p=1}^{P} w_{i,p} I_p + b_i \tag{5.16}$$

where net_i is the value of the i^{th} net; w_{ip} and b_i are the weight of the p^{th} input to the i^{th} hidden node and the bias parameter of the i^{th} hidden node, respectively; I_p is the value of the p^{th} input node.

The transfer function is defined as:

$$y_i = f\left(net_i\right) = \frac{1}{1 + exp\left(-net_i\right)} \tag{5.17}$$

where the transfer function in this study is a sigmoid function and y_i is the output signal of the i^{th} hidden node.

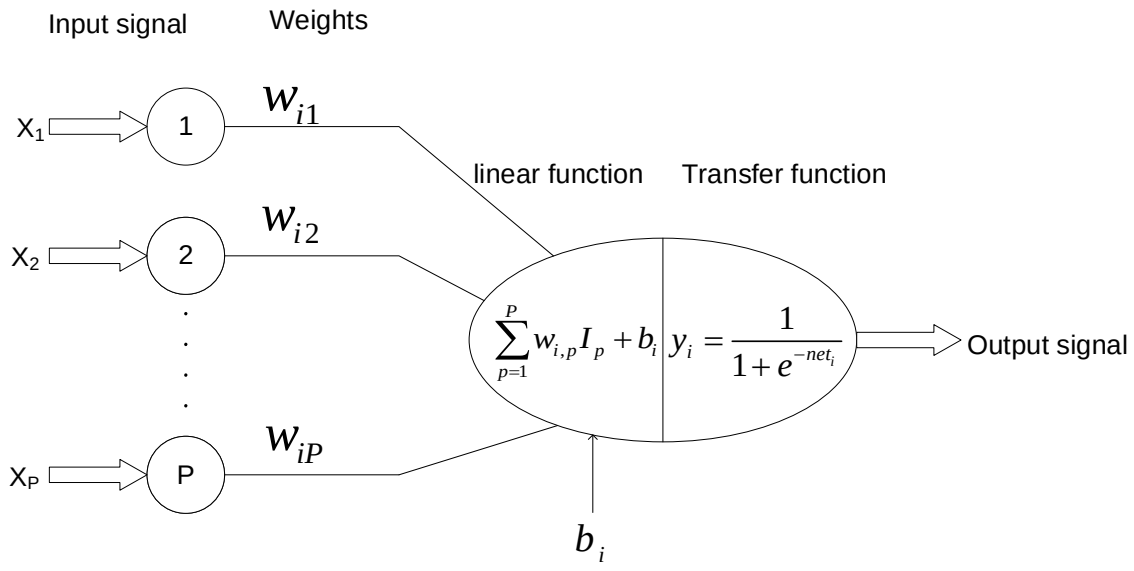

Figure 5-4. The structure of a neuron in an ANN model.

During the learning process, ANN uses the Mean Square Error (MSE), to evaluate the performance of the model as follows:

$$MSE = \frac{1}{NN_{out}} \sum_{n=1}^{N} \sum_{o=1}^{N_{out}} \left(e_{n,o}\right)^2 \tag{5.18}$$

where N and N_{out} are the number of instances and the number of outputs, respectively; $e_{n,o} = \bar{y}_{n,o} - y_{n,o}$ is the training error at the o^{th} output with n^{th} instance; y is the actual output and is the predicted output by ANN.

The Levenberg–Marquardt algorithm [47, 48] is used to update the weights and biases to minimize the MSE. The calculation of the Levenberg–Marquardt algorithm is presented as:

$$w^{k+1} = w^k - \left(J^{k^T} J^k + \mu \bar{I} \right)^{-1} J^{k^T} e^k \tag{5.19}$$

where w^k is the weight and bias matrix at the k^{th} iteration; $\bar{I}$ is the identity matrix; is the combination coefficient (; and J is the Jacobian matrix [49]:

$$J = \begin{array}{c} \begin{array}{cccccc} \overbrace{\quad\quad}^{\text{Node 1}} & & & \overbrace{\quad\quad}^{\text{Node } i} & & \\ \end{array} \\ \begin{bmatrix} \frac{\partial e_{1,1}}{\partial w_{1,1}} & \frac{\partial e_{1,1}}{\partial w_{1,2}} & \cdots & \frac{\partial e_{1,1}}{\partial w_{i,1}} & \frac{\partial e_{1,1}}{\partial w_{i,2}} & \cdots \\ \frac{\partial e_{1,2}}{\partial w_{1,1}} & \frac{\partial e_{1,2}}{\partial w_{1,2}} & \cdots & \frac{\partial e_{1,2}}{\partial w_{i,1}} & \frac{\partial e_{1,2}}{\partial w_{i,2}} & \cdots \\ \cdots & \cdots & \cdots & \cdots & \cdots & \cdots \\ \frac{\partial e_{1,N_{out}}}{\partial w_{1,1}} & \frac{\partial e_{1,N_{out}}}{\partial w_{1,2}} & \cdots & \frac{\partial e_{1,N_{out}}}{\partial w_{i,1}} & \frac{\partial e_{1,N_{out}}}{\partial w_{i,2}} & \cdots \\ \cdots & \cdots & \cdots & \cdots & \cdots & \cdots \\ \frac{\partial e_{n,1}}{\partial w_{1,1}} & \frac{\partial e_{n,1}}{\partial w_{1,2}} & \cdots & \frac{\partial e_{n,1}}{\partial w_{i,1}} & \frac{\partial e_{n,1}}{\partial w_{i,1}} & \cdots \\ \cdots & \cdots & \cdots & \cdots & \cdots & \cdots \\ \frac{\partial e_{n,o}}{\partial w_{1,1}} & \frac{\partial e_{n,o}}{\partial w_{1,2}} & \cdots & \frac{\partial e_{n,o}}{\partial w_{i,1}} & \frac{\partial e_{n,o}}{\partial w_{i,1}} & \cdots \\ \cdots & \cdots & \cdots & \cdots & \cdots & \cdots \\ \frac{\partial e_{N,1}}{\partial w_{1,1}} & \frac{\partial e_{N,1}}{\partial w_{1,2}} & \cdots & \frac{\partial e_{N,1}}{\partial w_{i,1}} & \frac{\partial e_{N,1}}{\partial w_{i,2}} & \cdots \\ \frac{\partial e_{N,2}}{\partial w_{1,1}} & \frac{\partial e_{N,2}}{\partial w_{1,2}} & \cdots & \frac{\partial e_{N,2}}{\partial w_{i,1}} & \frac{\partial e_{N,2}}{\partial w_{i,2}} & \cdots \\ \cdots & \cdots & \cdots & \cdots & \cdots & \cdots \\ \frac{\partial e_{N,N_{out}}}{\partial w_{1,1}} & \frac{\partial e_{N,N_{out}}}{\partial w_{1,2}} & \cdots & \frac{\partial e_{N,N_{out}}}{\partial w_{i,1}} & \frac{\partial e_{N,N_{out}}}{\partial w_{i,1}} & \cdots \end{bmatrix} \end{array} \begin{array}{l} o = 1 \\ o = 2 \\ \cdots \\ o = N_{out} \\ \cdots \\ o = 1 \\ \cdots \\ o = \text{o} \\ \cdots \\ o = 1 \\ o = 2 \\ \cdots \\ o = N_{out} \end{array} \begin{array}{l} \\ \\ \\ \\ \\ \\ \\ \\ \\ \\ \\ \\ \\ \\ \end{array} \begin{array}{l} \\ \\ \\ n = 1 \\ \\ \\ \\ n = n \\ \\ \\ \\ n = N \end{array} \tag{5.20}$$

where the error vector e at each neuron is written as [46]:

$$e = \begin{bmatrix} e_{1,1} \\ e_{1,2} \\ \cdots \\ e_{1,N_{out}} \\ \cdots \\ e_{N,1} \\ e_{N,2} \\ \cdots \\ e_{N,N_{out}} \end{bmatrix} \tag{5.21}$$

5.4.3 EFA-ANN implementation

A flowchart of EFA-ANN is shown in Figure 3-5. Firstly, historical data is divided into learning and test data following k-fold cross-validation. The learning data is then divided into training and validation data with a ratio of 90% and 10%, respectively. The training data are trained by the Levenberg–Marquardt algorithm, while the validation data are used to validate the trained ANN. After finding an optimal ANN model, the test data is used to evaluate its performance. The EFA-ANN will be validated in Section 5.6.

This study also applied initial weights and biases in the range of [-0.5,0.5] at the beginning of the training process. Chang *et al.*[32] showed that this is the optimal range for finding initial weights and biases of ANN. Figure 5-5 shows that the weights and biases are first updated inside the ANN. EFA automatically memorizes and optimizes these parameters to minimize prediction errors. As a result, the computing time can be significantly reduced. The Root Mean Square Error (RMSE) is used to calculate the objective function of EFA-ANN as follows:

$$f = RMSE_{Validation-data} \tag{5.22}$$

It is essential to clarify that RMSE is the objective function of EFA-ANN while the Mean Square Error (MSE) mentioned in Section 5.1.3.2 is the error function inside the ANN model. Also, the maximum generation is used as the termination criterion in this study.

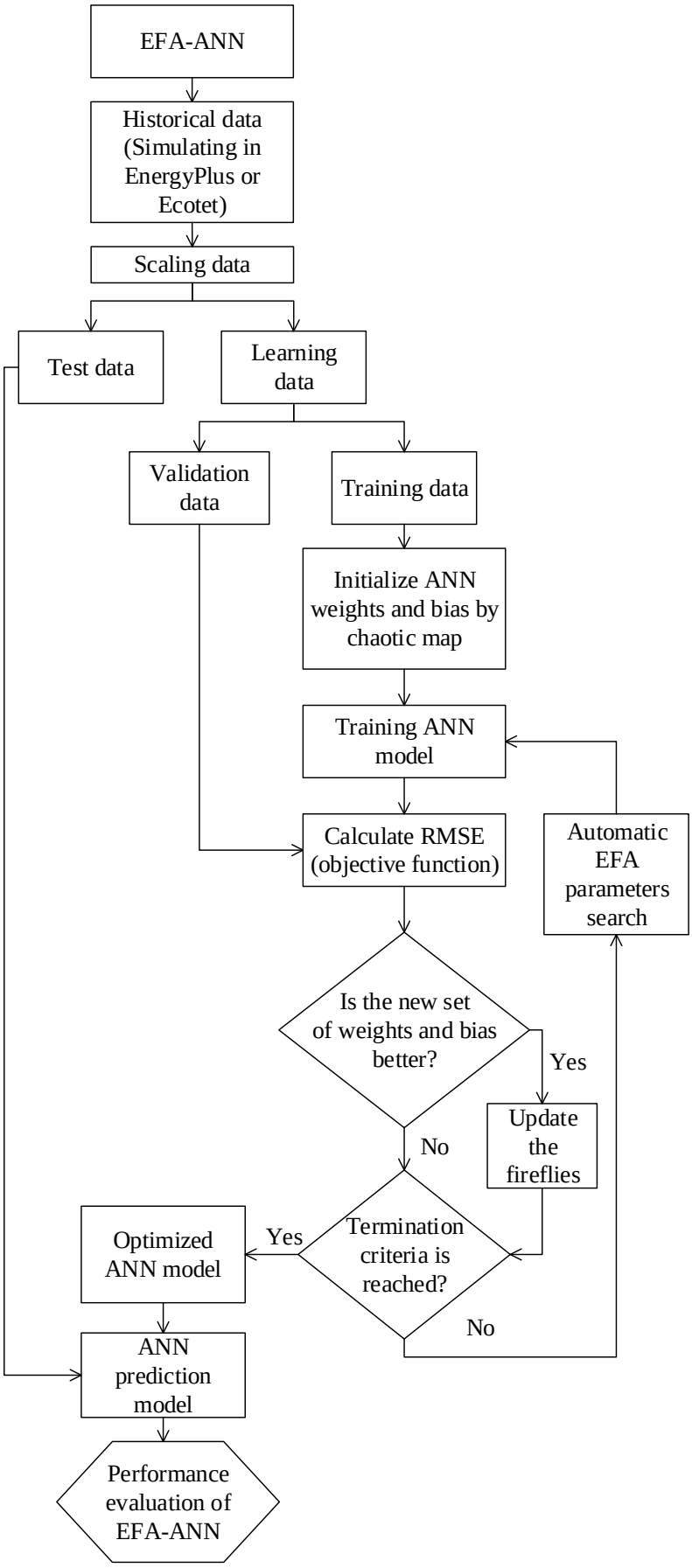
EFA-ANN
Historical data (Simulating in EnergyPlus or Ecotet)
Scaling data
Test data
Learning data
Validation data
Training data
Initialize ANN weights and bias by chaotic map
Training ANN model
Calculate RMSE (objective function)
Automatic EFA parameters search
Is the new set of weights and bias better?
Yes
No
Update the fireflies
Termination criteria is reached?
Yes
No
Optimized ANN model
ANN prediction model
Performance evaluation of EFA-ANN

Figure 5-5. A flowchart of the EFA-ANN model.

5.5 Model performance evaluation methods

Five performance measures were used to evaluate the performance of the proposed model. These include the linear correlation coefficient (R), determination coefficient (R^2), root mean square error (RMSE), mean absolute error (MAE) and mean absolute percentage error (MAPE). Details of these performance measures can be found in the literature [42, 50, 51] and are calculated as follows:

$$R = \frac{NN_{out}\sum_{n=1}^{N}\sum_{o=1}^{N_{out}} y_{n,o}.\bar{y}_{n,o} - \left(\sum_{n=1}^{N}\sum_{o=1}^{N_{out}} y_{n,o}\right)\left(\sum_{n=1}^{N}\sum_{o=1}^{N_{out}} \bar{y}_{n,o}\right)}{\sqrt{NN_{out}\left(\sum_{n=1}^{N}\sum_{o=1}^{N_{out}} y_{n,o}^2\right) - \left(\sum_{n=1}^{N}\sum_{o=1}^{N_{out}} y_{n,o}\right)^2}\sqrt{NN_{out}\left(\sum_{n=1}^{N}\sum_{o=1}^{N_{out}} \bar{y}_{n,o}^2\right) - \left(\sum_{n=1}^{N}\sum_{o=1}^{N_{out}} \bar{y}_{n,o}\right)^2}} \quad (5.23)$$

$$R^2 = RR \quad (5.24)$$

$$RMSE = \sqrt{\frac{1}{NN_{out}}\sum_{n=1}^{N}\sum_{o=1}^{N_{out}}\left(\bar{y}_{n,o} - y_{n,o}\right)^2} \quad (5.25)$$

$$MAE = \frac{1}{NN_{out}}\sum_{n=1}^{N}\sum_{o=1}^{N_{out}}\left|y_{n,o} - \bar{y}_{n,o}\right| \quad (5.26)$$

$$MAPE = \frac{1}{NN_{out}}\sum_{n=1}^{N}\sum_{o=1}^{N_{out}}\left|\frac{y_{n,o} - \bar{y}_{n,o}}{y_{n,o}}\right| \quad (5.27)$$

5.6 Data collection

5.6.1 Dataset 1

Dataset 1 was generated by modeling a typical single-family house with a lightweight wood-frame structure in Istanbul, Turkey [52]. In this case study, the effect of the façade system on the total heating and cooling energy were investigated by changing its properties. Fig. 5-6

shows the details of the façade system including glass wool insulation (layer iii), two layers of oriented strand board (OSB) applied as sheathing (layer ii and v), two layers of gypsum board (layer i and iv) and a layer of cement-bonded particleboard used as the exterior finishing of the wall.

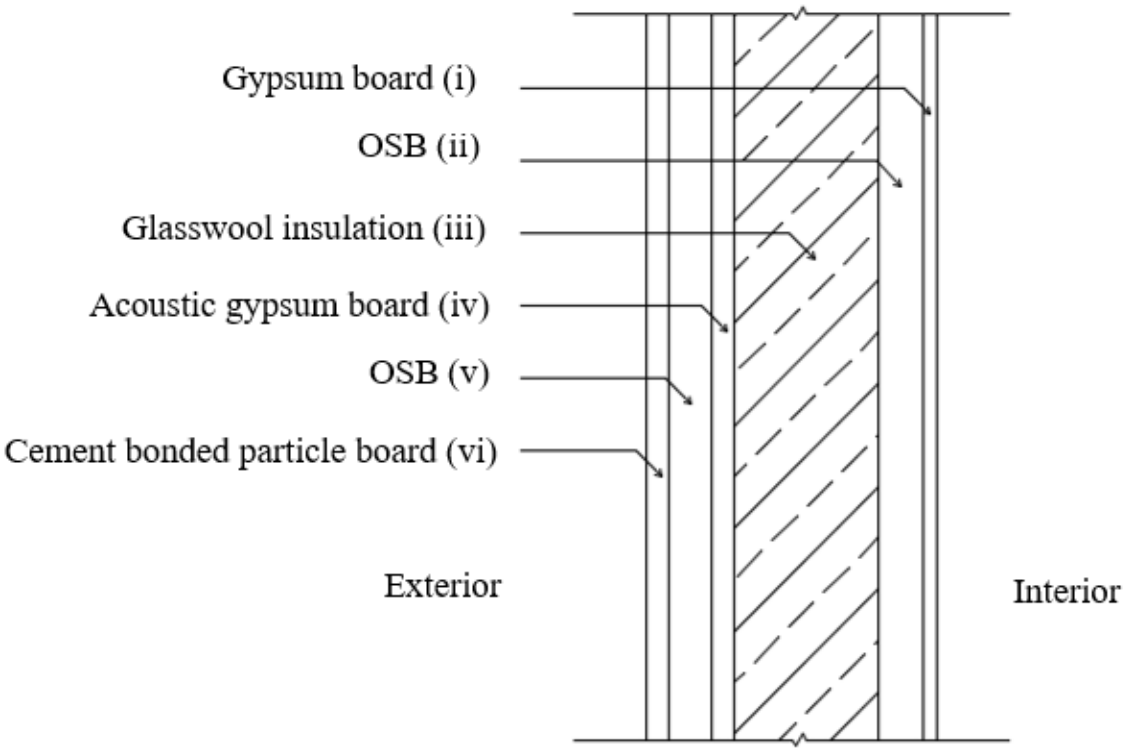

Figure 5-6. The details of the façade system in dataset 1.

The façade system was modeled using different properties for the insulation layer, namely thickness and thermal conductivity (K-value), which are listed in Table 1. Five types of façades with different layer thicknesses were also investigated. The thickness of layer i, ii, iv, v and vi of type 1 are 1.5 cm, 2.5 cm, 2 cm, 2.5 cm and 1.5 cm, respectively. The details of all five types are listed in Table 5-1. A total of 180 simulations were carried out to evaluate how the thermal conductivity and thickness of the façade affect the total heating and cooling energy in the building.

Table 5-1. Statistical parameters for dataset 1.

Parameter	Unit	Values	Variable
Insulation K-value (iii)	W/m-K	0.03, 0.04, 0.05, 0.08	Input
Insulation thickness (iii)	cm	4, 6, 8, 10, 12, 14, 16, 18, 20	
Façade type	N/A	1 [i, ii, iv, v, vi: 1.5, 2.5, 2, 2.5, 1.5 (cm)]	
		2 [i, ii, iv, v, vi: 2, 2, 2.5, 2, 1.5 (cm)]	
		3 [i, ii, iv, v, vi: 1, 3, 1.5, 3, 1.5 (cm)]	
		4 [i, ii, iv, v, vi: 2.5, 1.5, 3, 1.5, 1.5 (cm)]	
		5 [i, ii, iv, v, vi: 1, 3.5, 1.9, 1, 1.5 (cm)]	
Total heating and cooling energy	kWh	Min: 6094.24; Max: 11095.06	Output

After determining the simulated cases, the building models were drawn in Sketchup, and the thermal properties of the wall components, including window location, direction and orientation, were then inputted into EnergyPlus to simulate the energy consumption of the building. As the primary purpose of the simulation is to validate the effect of the façade system on the total heating and cooling energy in the building, the variables of these simulations are restricted to the type of façade material. Other factors of the building were maintained constant, and the properties used in the simulation are listed in Table 5-2.

Table 5-2. Design information in EnergyPlus simulation.

	Unit	Value
Building type	-	Residential building
Building location	-	Istanbul, Turkey
Floor area		
First story	m^2	81.7
Second story	m^2	48.4
Run period	year	1
Electric equipment	W/m^2	10
Lighting	W/m^2	12
Thermostat		
Heating setpoint (constant)	°C	21
Cooling setpoint (constant)	°C	26

5.6.2 Dataset 2

Dataset 2 consisted of 768 entries that were generated from twelve building types using Ecotect simulation software [53]. These twelve building types were represented by 18 simple cubes (3.5m x 3.5m x 3.5m) and the shape of each type is shown in Fig.7. Therefore, the buildings have the same volume but different surface areas and dimensions. These buildings were each simulated as a residential building in Athens, Greece. This dataset is used to investigate the effect of dimension on the cooling load (CL) in a building. Hence, the same material properties of the façade system were used for all twelve buildings, including U-value of the wall (1.78 W/m^2K), window (2.26 W/m^2K) floors (0.86 W/m^2K) and roofs (0.50 W/m^2K). The lighting level and latent heat were set to 300 lux and 2 W/m^2, respectively. The cooling load of the residential building was simulated by using eight features including the relative compactness (RC), surface area, wall area, roof area, overall height, orientation, glazing area and glazing distribution.

Each input parameter represents a property of the building. For instance, the *RC* indicator [54] represents the type of building, and the *RC*-value of each building is shown in Fig. 5-7. The *RC* is calculated by Eq. (5.27) as follows:

$$RC = 6V^{2/3}A^{-1} \tag{5.28}$$

where *V* and A are the volume and surface area of the building, respectively.

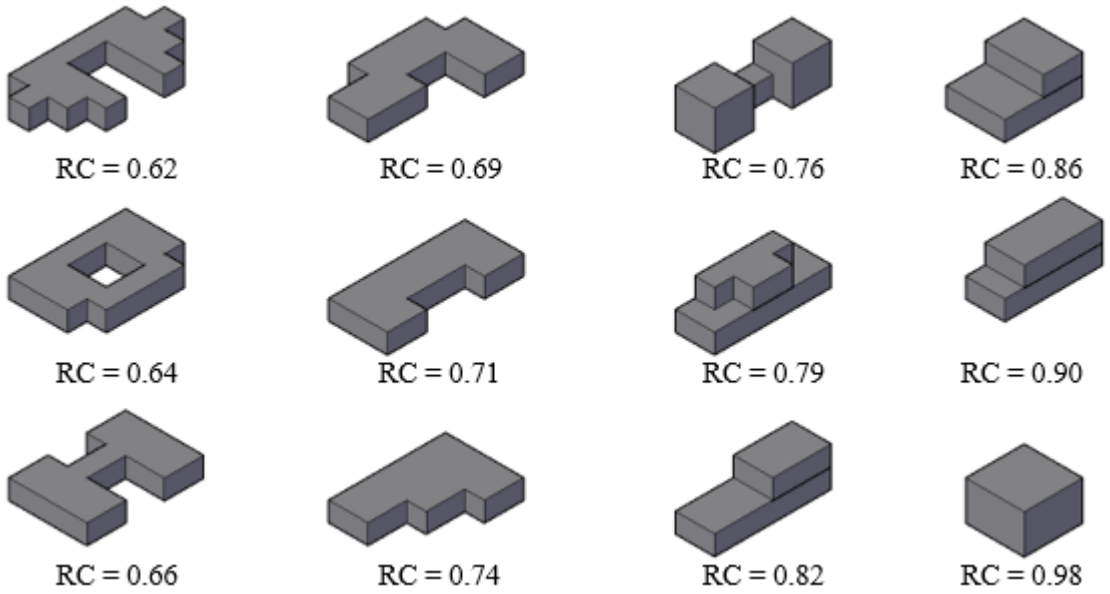

Figure 5-7. Shapes of the buildings in dataset 2.

The experiments simulated the building using two configurations, namely with and without glazing. In a glazing system, three glazing-to-floor area ratios were used, including 10%, 25%, and 40%. Five glazing distributions are considered including: (1) 25% glazing for each faces; (2) 55% for the north side and 15% for the other faces; (3) 55% for the east face and 15% for the remaining faces; (4) 55% for the south face and 15% for the other faces; and (5) 55% for the west face and 15% for the other faces [53]. Finally, all building shapes were rotated to four orientations, namely north, south, east and west. Overall, 768 building configurations were simulated, and the details of the input and output parameters are provided

in Table 4. By applying this process, all input values are discretized and calculated from the twelve building types. The number of possible values of each input are also listed in Table 5-3.

Table 5-3. Descriptions of dataset 2.

Parameter	Unit	No. of possible	Min.	Max.	Variable
Relative compactness	N/A	12	0.62	0.98	Input
Surface area	m^2	12	514.50	808.50	
Wall area	m^2	7	245.00	416.50	
Roof area	m^2	4	110.25	220.50	
Overall height	m	2	3.50	7.00	
Orientation	N/A	4	-	-	
Glazing area	%	4	0.00	40.00	
Glazing distribution	N/A	6	0.00	5.00	
Cooling load (CL)	kW	768	10.90	48.03	Output

5.7 Performance Evaluation and Discussion

5.7.1 Data Pre-processing and Model Application

This study used the K-fold cross-validation method to alleviate problems with over-fitting data [55]. The historical data was divided into 10 folds, which is the optimal number determined by other researchers [56]. Also, the K-fold cross-validation method can help to provide equal weightings to the results to obtain a fair comparison. The models that were used to assess the performance of our proposed model also utilized the K-fold cross-validation method [50, 53, 57].

In this method, each dataset is randomly divided into 10 separate folds. There are 10 rounds in the entire process. In each round, nine folds are used for training the EFA-ANN and the remaining fold is used for testing in each round. Therefore, all data is guaranteed to be used

in both the learning and testing phases. Finally, the average results in ten rounds are obtained to assess the performance of the model. The flowchart for each round is shown in Figure 5-5. In addition, all parameters of EFA-ANN used in this study are listed in Table 5-4.

Table 5-4. The parameter setting in EFA-ANN.

	Parameters	Setting
EFA	Number of fireflies	15
	Number of Maximum	15
	α_o	0.9
	Adaptive inertial weight (θ)	$(10^{-2} / 0.9)^{1/MaxGeneration}$
	Percentage of training data	90%
	Percentage of validation data	10%
	Number of folds	10
	Objective function	RMSE
ANN	Transfer function	Sigmoid
	Learning algorithm	Levenberg–Marquardt
	Number of hidden layers	1
	Number of nodes	20

At the beginning of the training process, the data is normalized to avoid numerical difficulties, i.e. inputs in higher numeric ranges may dominate those in smaller numeric ranges [58]. Therefore, this study normalizes the data to the range of [-1, 1]. The normalized value (*x'*) is calculated from the original value (*x*) as follows:

$$x' = \frac{2\left(x - \min\left(x\right)\right)}{\max\left(x\right) - \min\left(x\right)} - 1 \tag{5.29}$$

5.7.2 Results and discussion

Table 5-6 lists the predictive performance measures of the proposed model for dataset 1. Several models are used for comparing the predictive accuracy of the proposed model for the

same dataset. For example, Naji *et al.* proposed an extreme learning machine (ELM) method to forecast the energy consumption in a building [52]. Their model performs quite well (*RMSE* = 74.02 (kWh), R = 0.999 and R^2 = 0.997). Their comparison showed that ELM was superior to genetic programming (GP) and ANN' models, which were run in their study, in terms of accuracy and computing time.

Table 5-5. Performance measures and improvement rates of the EFA-ANN model for dataset 1.

Method	Performance measure					CT	Improvement rates by EFA-ANN				
	R	R^2	*RMSE*	*MAE*	*MAPE*		*R*	R^2	*RMSE*	*MAE*	*MAPE*
	(-)	(-)	(kWh)	(kWh)	(%)	(s)	(%)	(%)	(%)	(%)	(%)
Dataset 1											
ELM [52]	0.999	0.997	74.02	-	-	330	0.15**	0.30**	93.28*	-	-
ANN' [52]	0.971	0.943	331.57	-	-	424	2.97*	6.02*	98.50*	-	-
GP [52]	0.977	0.954	314.35	-	-	436	2.38*	4.81*	98.42*	-	-
ANN	0.999	0.998	39.69	28.29	0.05	66	0.15**	0.20**	87.47*	88.76*	18.84*
EFA-ANN	1.000	1.000	4.97	3.18	0.04	66	-		-	-	-

Note: CT is computing time which is calculated based on 1 running time.
*, ** indicates significance levels higher than (1%, 5%), respectively.

However, Table 5-5 indicates that the performance of EFA-ANN is superior to ELM and other methods. Moreover, EFA-ANN produces the smallest error rate (RMSE), and it is 93.28% - 98.50% better than those reported by other studies. Notably, in terms of computational cost, EFA-ANN is 5 times faster than ELM and 7 times faster than ANN' and GP. Moreover, this research also compares the performance of EFA-ANN with the ANN model to confirm that there is a prominent improvement over the combined EFA-ANN model. The

ANN model, in this case, is configured with the same setting as the ANN in the EFA-ANN model. The computing time of ANN is modified to be consistent with that of EFA-ANN for a fair comparison. The comparative results show that the error rates of EFA-ANN are 18.84% - 87.47% better than those of ANN. The results indicate that EFA-ANN can provide an alternative approach for predicting the energy consumption in a building.

The predicted results from EFA-ANN and other methods for dataset 2 are listed in Table 7. The proposed approach is shown to be superior to other methods available in the literature. For example, EFA-ANN obtains the lowest RMSE (0.51 kW) compared to other models: iteratively reweighted least squares (IRLS) (3.39 kW) [53], random forests (RF) (2.57 kW) [53], ensemble model (1.57 kW), smart artificial firefly colony algorithm-based support vector regression (SAFCA-SVR) (0.68 kWh) [57] and ANN model. Similarly, Table 7 shows that EFA-ANN has the lowest MAE and MAPE, which is equal to 0.38 (kW) and 1.71 (%), respectively. Also, the R and R^2 of EFA-ANN are equal to SAFCA-SVR, which is better than the ensemble model. With these results, EFA-ANN has improved the error rate from 16.18% to 84.84% when compared with other models. Additionally, the proposed model is around 5 times faster than the SAFCA-SVR model in predicting CL of this dataset (47 minutes compared to 240 minutes). Table 5-6 shows that the error rates of EFA-ANN are 31.87% - 53.27% better than ANN. Details of the comparison between ANN and EFA-ANN will be discussed hereafter.

Table 5-6. Performance measures and improvement rates of the EFA-ANN model for dataset 2.

Method	Performance measure					CT	Improvement rates by EFA-ANN				
	R	R^2	*RMSE*	*MAE*	*MAPE*		*R*	R^2	*RMSE*	*MAE*	*MAPE*
	(-)	(-)	(kW)	(kW)	(%)	(s)	(%)	(%)	(%)	(%)	(%)
Dataset 2											

IRLS [53]	N/A	N/A	3.39	2.21	9.41	N/A	-	-	84.84*	83.02*	81.83*
RF [53]	N/A	N/A	2.57	1.42	4.62	N/A	-	-	80.00*	73.58*	62.99*
Ensemble model [50]	0.99	0.97	1.57	0.97	3.46	N/A	1.27**	2.55**	67.18*	61.44*	50.51*
SAFCA-SVR [57]	1.00	0.99	0.68	0.47	2.04	1440	-	0.30	24.41**	20.17**	16.18***
ANN	1.00	0.99	1.10	0.56	2.51	280	-	0.59	53.27**	33.00**	31.87**
EFA-ANN	1.00	1.00	0.51	0.38	1.71	280	-	-	-	-	-

Note: CT is computing time which is calculated based on 1 running time.;

*, ** indicates significance levels higher than (1%, 5%), respectively;

This study compares the EFA-ANN model with the single ANN model to investigate the effects of EFA on the RMSE value and computing time. In order to make a fair comparison, the parameters in the single ANN model were set to be identical with the ANN model in EFA-ANN. Only the number of iterations of the single ANN model, in this case, was increased to extend the computing time (to be consistent with EFA-ANN). Both single ANN and EFA-ANN were run on the same computer. Figure 5-8 shows that the single ANN is stuck at the local optima after around 20 and 50 seconds for Dataset 1 (a) and Dataset 2 (b), respectively. In contrast, EFA-ANN approaches a better result because EFA helps ANN find better weights and bias values. This comparison confirms that EFA is effective in optimizing the weights and biases of ANN.

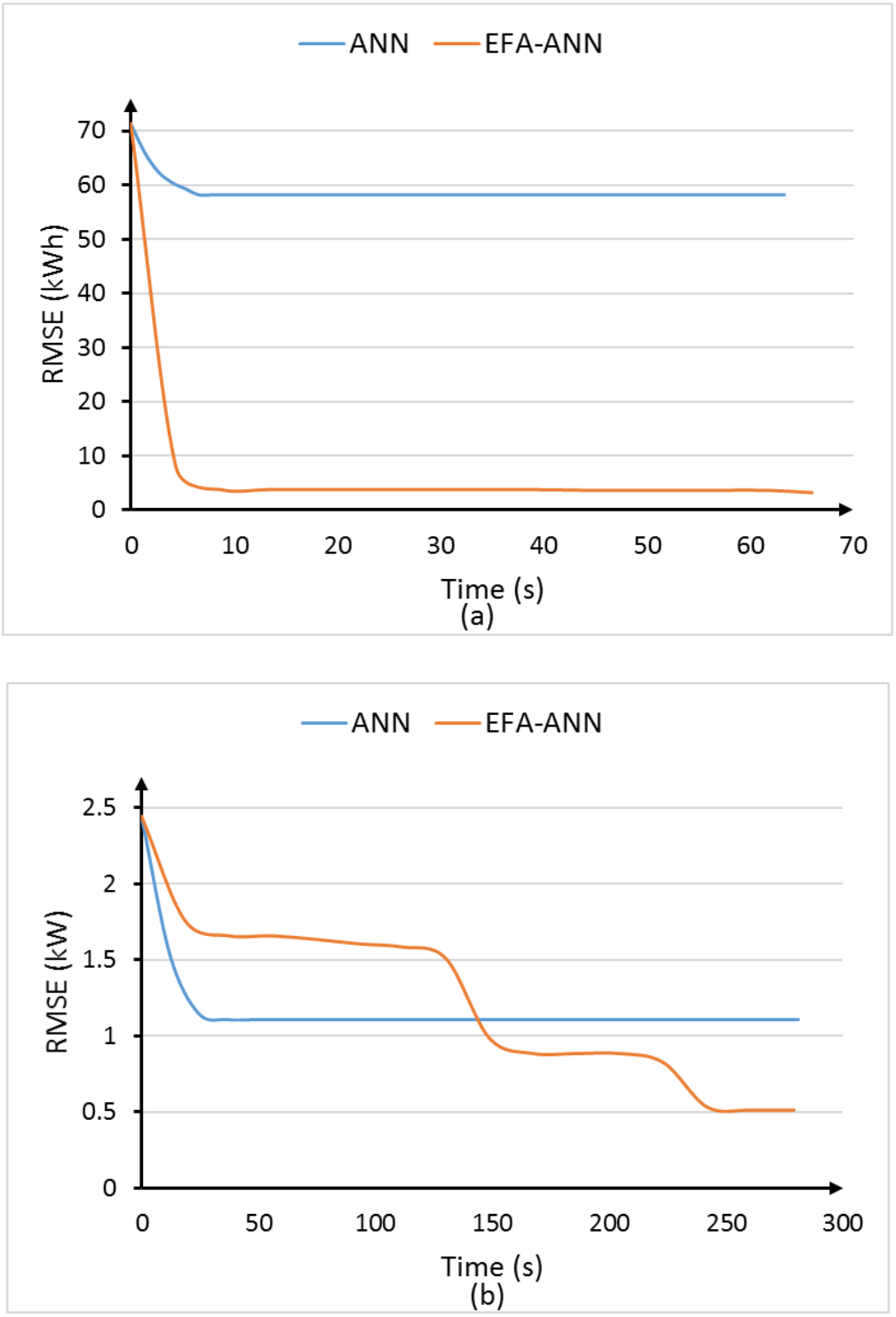

Figure 5-8. Convergence results of ANN and EFA-ANN for (a) Dataset 1 and (b) Dataset 2

The statistical relationship between the predicted outputs obtained by EFA-ANN and the actual outputs of the two datasets is shown in Figure 5-9. The *R*-values for the two datasets are almost equal to 1, which indicates that the predicted values from EFA-ANN have a strong correlation with the actual values. Notably, the MAPE in dataset 1 is equal to 0.04%, which indicates that the predicted values are approximately equal to the actual values. In other words, the proposed model can forecast the exact energy consumption for dataset 1. Meanwhile, the MAPE for dataset 2 is higher than that for dataset 1 but remains negligible (1.71%). The results of EFA-ANN are slightly different from the actual values, but these results are predicted with better accuracy than the aforementioned methods. Therefore, the proposed EFA-ANN is an efficient model for predicting the energy consumption (including HL and CL) of a building.

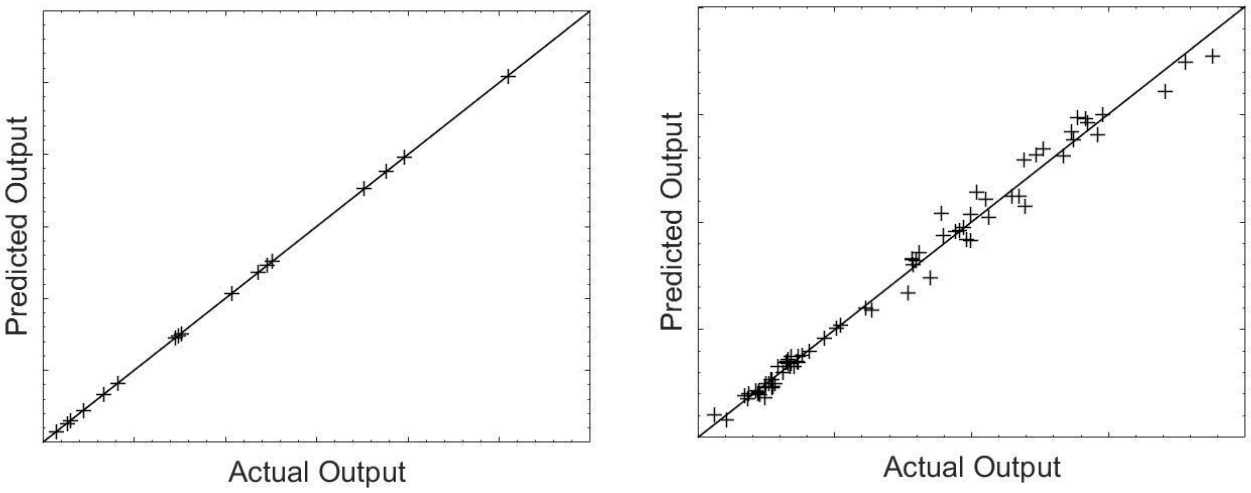

(a) (b)

Figure 5-9. The correlation between the actual and the predicted outputs for dataset 1 (a) and dataset 2 (b).

5.7.3 Sensitivity Analysis

A sensitivity analysis is performed to quantify the effects of different inputs on the predicted energy consumption. Among the different approaches, this study used the method proposed by Garson [59] because it is suitable for discrete input data such as wall type, relative compactness, orientation, and glazing distribution. This method is also suitable for the ANN model as the sensitivity analysis deconstructs the weights of the connections between neurons to quantify the influence of the various inputs. The influence of a specified input on the output can be determined by assessing all the connecting weights between the nodes of interest. Therefore, all connecting weights between a specific input and output are identified, and the importance of all the inputs is calculated (as a percentage) by the following equation:

$$Q_p = \sum_{i=1} \left(\frac{w_{ip}}{\sum_{p=1} w_{ip}} \times \frac{w_{oi}}{\sum_{i=1} w_{oi}} \right) \tag{5.30}$$

Where Q_p is the impact of the input p^{th} on the output in percentage; w_{ip} is the weight of the p^{th} input to the i^{th} hidden node; w_{oi} is the weight of the i^{th} hidden node to the output.

The results from the sensitivity analysis on datasets 1 and 2 are shown in Figure 5-10. For dataset 1, the insulation thickness has the highest impact on the total heating and cooling load (43.8%), followed by the façade type and K-value of the insulation (34.1% and 22.1%, respectively). This result is reasonable because the insulation thickness has a prominent effect on the energy consumption in a building, which was shown in previous studies [60, 61]. Meanwhile, the glazing area (29.4%) and the relative compactness (27.5%) are the most critical parameters that affect the total cooling load in dataset 2. This result is expected because the solar heat gain will increase with a larger glazing area, which thereby affects the cooling load in the building. Also, several studies confirmed that an increasing window-to-wall ratio causes

an increase in the cooling load [62, 63].In contrast, the orientation of the façade and the roof area have the least impact with just under 5%. The results of the sensitivity analysis can help a designer to quickly identify which input should be modified to improve the energy performance of the building. For example, the insulation thickness in dataset 1 or the glazing area and relative compactness in dataset 2 should be modified before the other variables to effectively improve the energy performance of the building.

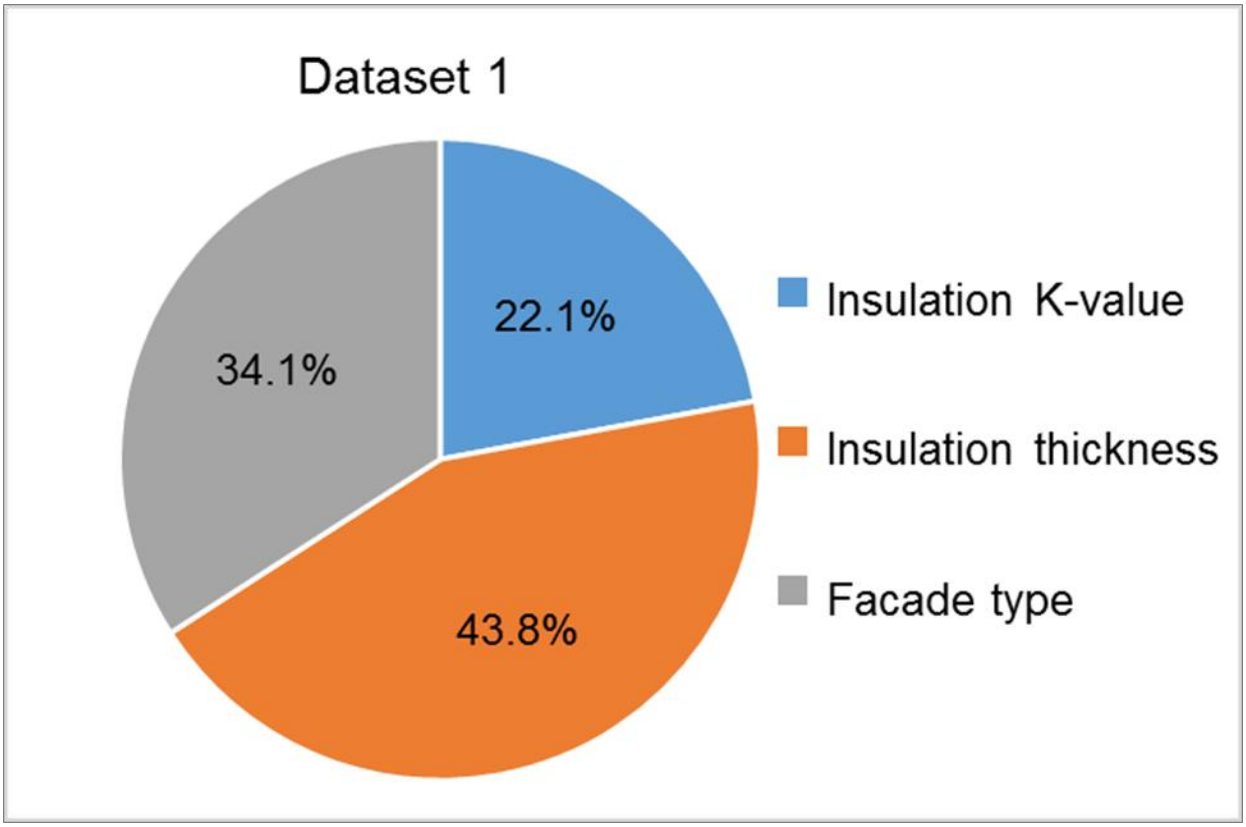

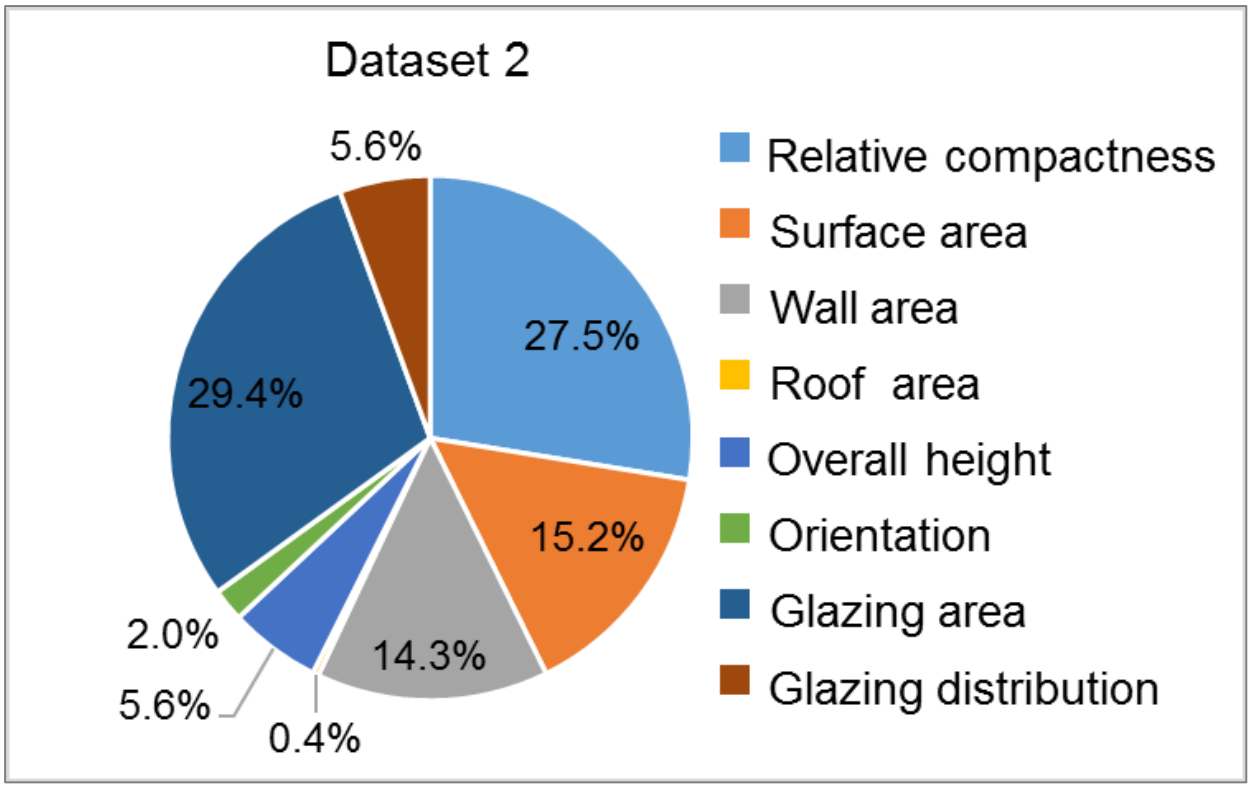

Figure 5-10. The effect of several design parameters on the energy consumption of the building.

5.8 Conclusions

A novel method was developed for predicting the energy consumption in a building. The model, namely EFA-ANN, integrates EFA into ANN to improve its performance by optimizing the set of initial parameters. The proposed approach was compared with several published models in terms of its speed and accuracy in forecasting heating and cooling energy. Two datasets with various material and isolation properties (dataset 1), and building characteristics (dataset 2) were used to validate EFA-ANN. Additionally, a 10-fold cross-validation method was applied to mitigate the over-fitting problem when comparing the performance of these models.

In dataset 1, EFA-ANN showed a 93.28% - 98.50% improvement of other methods reported in the literature. Notably, EFA-ANN is 5 times faster than the ELM method and 7

times faster than GP in terms of computing time. Similarly, EFA-ANN not only obtained the lowest RMSE, MAE and MAPE, but also the highest *R*-value compared to the other techniques for dataset 2. Also, the computing time of EFA-ANN is less 5 times than that of SAFCA-SVR. The obtained results demonstrated the strong capabilities of machine learning in predicting the energy consumption of buildings.

A sensitivity analysis was also performed to identify the input with the most critical impact on the output of each dataset. The results of the sensitivity analysis indicate that the insulation thickness and the glazing area have the most significant impact for datasets 1 and 2, respectively. This result can help designers to quickly validate their design of a building and improve its energy performance by focusing on these essential inputs.

This study showed that the proposed EFA-ANN model achieved both good results and a short computational time relative to other methods. Therefore, EFA-ANN can help energy engineers to design energy-efficient buildings whilst reducing experimental requirements and it could assist civil engineers and construction managers in the early design phase of energy-efficient buildings. Besides, the proposed approach can be used as a useful tool for quickly and accurately solving many problems in engineering, including energy-efficient buildings, construction material strength, and structure strength.

Acknowledgments

The first author would like to thank the University of Melbourne for offering the Melbourne Research Scholarship. This work was also supported by The ARC Training Centre for Advanced Manufacturing of Prefabricated Housing (CAMP.H) at the University of Melbourne.

References

1. Al-Homoud, M.S., *Computer-aided building energy analysis techniques.* Building and Environment, 2001. 36(4): p. 421-433.
2. IEA, *World Energy Outlook 2015*. 2015.
3. Administration, U.S.E.I., *INTERNATIONAL ENERGY OUTLOOK 2016*. 2016.
4. Zanchini, E. and C. Naldi, *Energy saving obtainable by applying a commercially available M-cycle evaporative cooling system to the air conditioning of an office building in North Italy.* Energy, 2019. 179: p. 975-988.
5. Ahmadi-Karvigh, S., A. Ghahramani, B. Becerik-Gerber, and L. Soibelman, *Real-time activity recognition for energy efficiency in buildings.* Applied Energy, 2018. 211: p. 146-160.
6. Pérez-Lombard, L., J. Ortiz, and C. Pout, *A review on buildings energy consumption information.* Energy and Buildings, 2008. 40(3): p. 394-398.
7. Zemella, G., D. De March, M. Borrotti, and I. Poli, *Optimised design of energy efficient building façades via Evolutionary Neural Networks.* Energy and Buildings, 2011. 43(12): p. 3297-3302.
8. Magnier, L. and F. Haghighat, *Multiobjective optimization of building design using TRNSYS simulations, genetic algorithm, and Artificial Neural Network.* Building and Environment, 2010. 45(3): p. 739-746.
9. Ferreira, P.M., A.E. Ruano, S. Silva, and E.Z.E. Conceição, *Neural networks based predictive control for thermal comfort and energy savings in public buildings.* Energy and Buildings, 2012. 55: p. 238-251.

10. Ghahramani, A., K. Zhang, K. Dutta, Z. Yang, and B. Becerik-Gerber, *Energy savings from temperature setpoints and deadband: Quantifying the influence of building and system properties on savings.* Applied Energy, 2016. 165: p. 930-942.

11. Kumar, A. and B.M. Suman, *Experimental evaluation of insulation materials for walls and roofs and their impact on indoor thermal comfort under composite climate.* Building and Environment, 2013. 59: p. 635-643.

12. Lechner, N., *Heating, cooling, lighting: Sustainable design methods for architects*. 2014: John wiley & sons.

13. Yang, Z., A. Ghahramani, and B. Becerik-Gerber, *Building occupancy diversity and HVAC (heating, ventilation, and air conditioning) system energy efficiency.* Energy, 2016. 109: p. 641-649.

14. Ihara, T., A. Gustavsen, and B.P. Jelle, *Effect of facade components on energy efficiency in office buildings.* Applied Energy, 2015. 158: p. 422-432.

15. Liu, Z., Y. Liu, B.-J. He, W. Xu, G. Jin, and X. Zhang, *Application and suitability analysis of the key technologies in nearly zero energy buildings in China.* Renewable and Sustainable Energy Reviews, 2019. 101: p. 329-345.

16. Naganathan, H., W.O. Chong, and X. Chen, *Building energy modeling (BEM) using clustering algorithms and semi-supervised machine learning approaches.* Automation in Construction, 2016. 72(Part 2): p. 187-194.

17. Hong, T., J. Kim, J. Jeong, M. Lee, and C. Ji, *Automatic calibration model of a building energy simulation using optimization algorithm.* Energy Procedia, 2017. 105(Supplement C): p. 3698-3704.

18. Ryan, E.M. and T.F. Sanquist, *Validation of building energy modeling tools under idealized and realistic conditions.* Energy and Buildings, 2012. 47(Supplement C): p. 375-382.

19. Mousavi, S.M., P. Aminian, A.H. Gandomi, A.H. Alavi, and H. Bolandi, *A new predictive model for compressive strength of HPC using gene expression programming.* Advances in Engineering Software, 2012. 45(1): p. 105-114.

20. Platon, R., V.R. Dehkordi, and J. Martel, *Hourly prediction of a building's electricity consumption using case-based reasoning, artificial neural networks and principal component analysis.* Energy and Buildings, 2015. 92: p. 10-18.

21. Robinson, C., et al., *Machine learning approaches for estimating commercial building energy consumption.* Applied Energy, 2017. 208: p. 889-904.

22. Ahmad, T., et al., *Supervised based machine learning models for short, medium and long-term energy prediction in distinct building environment.* Energy, 2018. 158: p. 17-32.

23. Chou, J.-S. and D.-S. Tran, *Forecasting energy consumption time series using machine learning techniques based on usage patterns of residential householders.* Energy, 2018. 165: p. 709-726.

24. Ghahramani, A., S.A. Karvigh, and B. Becerik-Gerber, *HVAC system energy optimization using an adaptive hybrid metaheuristic.* Energy and Buildings, 2017. 152: p. 149-161.

25. Moon, J.W., J.-H. Lee, Y. Yoon, and S. Kim, *Determining optimum control of double skin envelope for indoor thermal environment based on artificial neural network.* Energy and Buildings, 2014. 69: p. 175-183.

26. Moon, J.W., J.-H. Lee, J.D. Chang, and S. Kim, *Preliminary performance tests on artificial neural network models for opening strategies of double skin envelopes in winter*. Energy and Buildings, 2014. 75: p. 301-311.

27. Wang, L., E.W.M. Lee, and R.K.K. Yuen, *Novel dynamic forecasting model for building cooling loads combining an artificial neural network and an ensemble approach.* Applied Energy, 2018. 228: p. 1740-1753.

28. Chung, M.H., Y.K. Yang, K.H. Lee, J.H. Lee, and J.W. Moon, *Application of artificial neural networks for determining energy-efficient operating set-points of the VRF cooling system.* Building and Environment, 2017. 125: p. 77-87.

29. Kolen, J.F. and J.B. Pollack, *Back propagation is sensitive to initial conditions*, in *Proceedings of the 1990 conference on Advances in neural information processing systems 3*. 1990, Morgan Kaufmann Publishers Inc.: Denver, Colorado, USA. p. 860-867.

30. Yam, Y.F. and T.W.S. Chow, *Determining initial weights of feedforward neural networks based on least squares method.* Neural Processing Letters, 1995. 2(2): p. 13-17.

31. Liu, Q., X. Cui, Y.-C. Chou, M.F. Abbod, J. Lin, and J.-S. Shieh, *Ensemble artificial neural networks applied to predict the key risk factors of hip bone fracture for elders.* Biomedical Signal Processing and Control, 2015. 21: p. 146-156.

32. Chang, Y.-T., J. Lin, J.-S. Shieh, and M.F. Abbod, *Optimization the Initial Weights of Artificial Neural Networks via Genetic Algorithm Applied to Hip Bone Fracture Prediction.* Advances in Fuzzy Systems, 2012. 2012: p. 9.

33. Lee, A., W.Z. Geem, and K.-D. Suh, *Determination of Optimal Initial Weights of an Artificial Neural Network by Using the Harmony Search Algorithm: Application to Breakwater Armor Stones.* Applied Sciences, 2016. 6(6).

34. Al-Shammari, E.T., et al., *Prediction of heat load in district heating systems by Support Vector Machine with Firefly searching algorithm.* Energy, 2016. 95: p. 266-273.

35. Coelho, L.d.S. and V.C. Mariani, *Improved firefly algorithm approach applied to chiller loading for energy conservation.* Energy and Buildings, 2013. 59: p. 273-278.

36. Chu, W.-M. and K.-Y. Chang, *Improving electromagnetism algorithm for solving resource allocation problem in stochastic networks.* Computers & Operations Research, 2017. 86(Supplement C): p. 30-40.

37. Yang, X.-S., *Firefly algorithm, stochastic test functions and design optimisation.* International Journal of Bio-Inspired Computation, 2010. 2(2): p. 78-84.

38. Yelghi, A. and C. Köse, *A modified firefly algorithm for global minimum optimization.* Applied Soft Computing, 2018. 62: p. 29-44.

39. Birbil, Ş.İ. and S.-C. Fang, *An electromagnetism-like mechanism for global optimization.* Journal of global optimization, 2003. 25(3): p. 263-282.

40. Li, Y., S. Deng, and D. Xiao, *A novel Hash algorithm construction based on chaotic neural network.* Neural Computing and Applications, 2011. 20(1): p. 133-141.

41. Hong, W.-C., Y. Dong, L.-Y. Chen, and S.-Y. Wei, *SVR with hybrid chaotic genetic algorithms for tourism demand forecasting.* Applied Soft Computing, 2011. 11(2): p. 1881-1890.

42. Bui, D.-K., T. Nguyen, J.-S. Chou, H. Nguyen-Xuan, and T.D. Ngo, *A modified firefly algorithm-artificial neural network expert system for predicting compressive and*

tensile strength of high-performance concrete. Construction and Building Materials, 2018. 180: p. 320-333.

43. Nguyen, T., A. Kashani, T. Ngo, and S. Bordas, *Deep neural network with high‐order neuron for the prediction of foamed concrete strength.* Computer‐Aided Civil and Infrastructure Engineering, 2019. 34(4): p. 316-332.

44. Singh, T.N., S. Sinha, and V.K. Singh, *Prediction of thermal conductivity of rock through physico-mechanical properties.* Building and Environment, 2007. 42(1): p. 146-155.

45. Lee, S., J. Ha, M. Zokhirova, H. Moon, and J. Lee, *Background Information of Deep Learning for Structural Engineering.* Archives of Computational Methods in Engineering, 2017: p. 1-9.

46. Yu, H. and B. Wilamowski, *Levenberg-Marquardt Training*, in *Intelligent Systems*. 2011, CRC Press. p. 1-16.

47. Levenberg, K., *A METHOD FOR THE SOLUTION OF CERTAIN NON-LINEAR PROBLEMS IN LEAST SQUARES.* Quarterly of Applied Mathematics, 1944. 2(2): p. 164-168.

48. Marquardt, D., *An Algorithm for Least-Squares Estimation of Nonlinear Parameters.* Journal of the Society for Industrial and Applied Mathematics, 1963. 11(2): p. 431-441.

49. Wilamowski, B.M. and Y. Hao, *Neural Network Learning Without Backpropagation.* IEEE Transactions on Neural Networks, 2010. 21(11): p. 1793-1803.

50. Chou, J.-S. and D.-K. Bui, *Modeling heating and cooling loads by artificial intelligence for energy-efficient building design.* Energy and Buildings, 2014. 82: p. 437-446.

51. Chou, J.-S., W.K. Chong, and D.-K. Bui, *Nature-Inspired Metaheuristic Regression System: Programming and Implementation for Civil Engineering Applications.* Journal of Computing in Civil Engineering, 2016. 30(5).

52. Naji, S., et al., *Estimating building energy consumption using extreme learning machine method.* Energy, 2016. 97(Supplement C): p. 506-516.

53. Tsanas, A. and A. Xifara, *Accurate quantitative estimation of energy performance of residential buildings using statistical machine learning tools.* Energy and Buildings, 2012. 49: p. 560-567.

54. Mahdavi, A. and B. Gurtekin. *Shapes, Numbers, and Perception: Aspects and Dimensions of the Design Performance Space*. in *Proceedings of the 6th International Conference: Design and Decision Support Systems in Architecture, The Netherlands*. 2002.

55. Bishop, C., *Pattern Recognition and Machine Learning*. Information Science and Statistics. 2006, New York: Springer-Verlag.

56. Kohavi, R., *A Study of Cross-Validation and Bootstrap for Accuracy Estimation and Model Selection*. 1995. 1137-1143.

57. Chou, J.S. and A.D. Pham, *Smart Artificial Firefly Colony Algorithm–Based Support Vector Regression for Enhanced Forecasting in Civil Engineering.* Computer-Aided Civil and Infrastructure Engineering, 2015. 30(9): p. 715-732.

58. Lin, C.-w.H.a.C.-c.C.a.C.-j., *A practical guide to support vector classification*. 2010: Department of Computer Science, National Taiwan University,Taipei, Taiwan.

59. Garson, G.D., *Interpreting neural-network connection weights.* AI Expert, 1991. 6(4): p. 46-51.

60. Jie, P., F. Zhang, Z. Fang, H. Wang, and Y. Zhao, *Optimizing the insulation thickness of walls and roofs of existing buildings based on primary energy consumption, global cost and pollutant emissions.* Energy, 2018. 159: p. 1132-1147.

61. Olivieri, F., R.C. Grifoni, D. Redondas, J.A. Sánchez-Reséndiz, and S. Tascini, *An experimental method to quantitatively analyse the effect of thermal insulation thickness on the summer performance of a vertical green wall.* Energy and Buildings, 2017. 150: p. 132-148.

62. Marino, C., A. Nucara, and M. Pietrafesa, *Does window-to-wall ratio have a significant effect on the energy consumption of buildings? A parametric analysis in Italian climate conditions.* Journal of Building Engineering, 2017. 13: p. 169-183.

63. Alghoul, S.K., H.G. Rijabo, and M.E. Mashena, *Energy consumption in buildings: A correlation for the influence of window to wall ratio and window orientation in Tripoli, Libya.* Journal of Building Engineering, 2017. 11: p. 82-86.

Chapter 6
A computational, data-driven platform for designing biomimetic adaptive façade

6.1 Introduction

The results in chapter 5 demonstrate that the proposed data-driven approach can effectively estimate the building energy consumption. The data-driven approach can learn from the provided energy data to identify the relationship among all variables in the data. Therefore, it can be used to complement the building energy simulation software, which requires high computational time and expertise experience, in the computational optimisation approach presented in chapter 3 and 4. This chapter illustrates the capacity of proposed data-driven approach in predicting energy consumption generated by building energy simulation software (i.e., EnergyPlus) and proposes a computational, data-driven platform for designing biomimetic adaptive façade (BAF).

Designing a façades system for energy efficiency is very challenging since many aspects of the building govern the overall energy requirements of the building, including heating, cooling, and lighting [1]. For example, it was found that solar reflectance, Solar heat gain coefficient (SHGC) and U-value have different effects on the building energy efficiency in a study by Ihara *et al.* [2]. This study found that a decrease in SHGC was the most efficient way to decreasing energy consumption in buildings [2]. However, in another study, reducing SHGC only provides an improvement in building energy efficiency when it is combined with an appropriate U-value [3]. In addition, weather condition, building dimension and occupant's behaviour can strongly affect the total energy consumption in the building. Therefore, the

calculation of energy consumption needs to consider all the above parameters and their interaction.

There are several methods that can evaluate building energy consumption, and they can be classified into three main groups, including engineering calculation, computational simulation and data-driven approaches. The first approach focuses on using physical laws to calculate energy consumption in the whole building, and this approach is only suitable for preliminary analysis because the complex physical laws constraint the applications. The second approach, the computational simulation approach, is then proposed to overcome the limitations of engineering calculation. There are several building energy simulation software, including EnergyPlus, Autodesk Ecotect, TRNSYS, DOE-2, Window, and eQUEST, were used to simulate the building with façade system design and predict energy consumption. The building energy simulation software (EnergyPlus in the thesis) has been used in Chapter 3 and 4 as the backbone of the computational design platform. However, building energy simulation software still has several disadvantages such as resource-intensive exercises and time-consuming [4]. In addition, the optimisation process must be manual and uses iterative calibration until the criteria are met based on trial-and-error through the users' experience [5]. Consequently, the common procedures, which are mainly based on specific design condition and expert experience, are often unsatisfactory for designing façade.

Therefore, the data-driven approach was proposed to design energy-efficient building services. Data-driven strategies apply machine learning (ML) and statistical tools to solve problems, which are hard to handle by traditional computational techniques. The fundamental of the methods is a learning process to discover the relationship between collected building data, including structural characteristics and climate data, and energy consumption of buildings. Then, the established relationship can be used to predict the energy performance of new samples accurately and effectively. In recent years, ML is applied to enhance the

performance of façade systems. For instance, Giovanni *et al.* proposed an evolutionary neural network to design a façade module for an building [1]. In additions, Alvaro *et al.* successfully used a ML model to control active thermal energy storage and demonstrated that can the ML model could provide the energy savings, CO2 mitigation and cost reduction [6]. Abediniangerabi *et al.* proposed the association rule mining technique to study the thermal behaviour of façade systems in several scenarios [7]. The proposed data-driven technique then can be used to give recommendations in selecting energy-efficient façade systems. Martinez and Choi used several data-driven methods, including classification tree, regression and 2-sample t-test, to investigate several façade features [8].

Therefore, this chapter proposed a data-driven approach to complement the energy simulation task in the computational optimisation approach developed in chapter 3 and chapter 4. Artificial neural network (ANN), one of the most popular and effective ML model, is used in this chapter to validate the effectiveness of the proposed computational, data-driven platform. The detailed discussion on ANN was presented in chapter 5. The machine learning approach is used to predict the energy consumption in building with the training data generated by EnergyPlus software. The main difference between the platform presented in this chapter (computational, data-driven, optimisation platform) and the one used in chapter 3 and 4 (computational optimisation platform) is the data-driven engine (i.e. ANN-based prediction model). It is worth noting that the building energy simulation (EnergyPlus) need to be performed thousands of times for designing the BAF system in chapters 3 and 4, which is a significant computational bottleneck of the process. On the other hand, the process becomes less computational demand for the proposed platform in this chapter owing to the data-driven engine. After training data, the ANN model can make a prediction of energy consumption and transfer the results to the optimisation algorithm inside the optimisation process.

In this chapter, the performance of ANN model is improved by using an in-house optimisation tool, namely Electromagnetism-based Firefly Algorithm (EFA). This chapter also employs the k-fold cross-validation method to validate the proposed model. The detailed discussion on EFA-ANN and the k-fold cross-validation method was presented in chapter 5. EnergyPlus is used to generated training data for EFA-ANN, and the simulation model has considered various properties of façade along with occupants' behaviour in building and weather condition in Melbourne.

6.2 A computational, data-driven platform

This section presents the detailed structure of the computational data-driven platform for assisting the design and operation of BAF. Figure 6-1 shows a schematic of the design process, which includes four main steps for the BAF design. The first two steps have been discussed in detail in chapter 3. In this chapter, step 3 is the energy simulation by EnergyPlus to generate training data for the data-driven engine. In the last step, the EFA-ANN model is trained by the energy data from EnergyPlus. The trained EFA-ANN model is then integrated with the optimisation algorithm in the computational data-driven optimisation platform as showed in Figure 6-1.

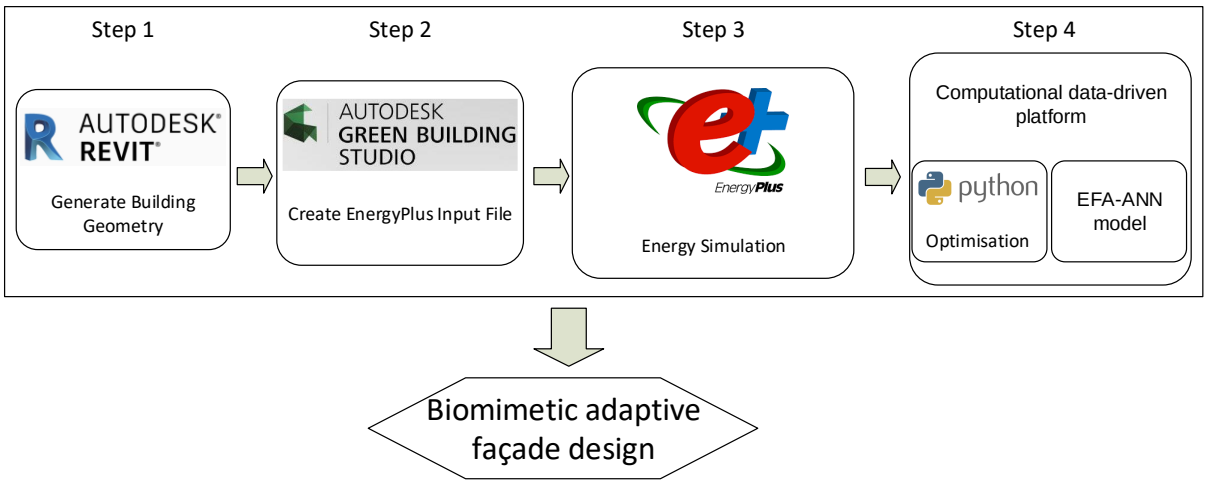

Figure 6-1. The schematic of the proposed computational data-driven platform.

The framework of the platform is shown in Figure 6-2. In the proposed platform, the building geometry, thermal and visual properties of windows and weather conditions are used as input data for the EnergyPlus model. The EnergyPlus model then will be run and provide the energy data for the EFA-ANN model. After training data, the EFA-ANN model can predict energy consumption of the given building and can be integrated with the optimisation algorithm in the optimisation process to find the optimal design and operation of BAF system. The optimal results can be used to select the best materials and operational stages for BAF systems such as electrochromic windows.

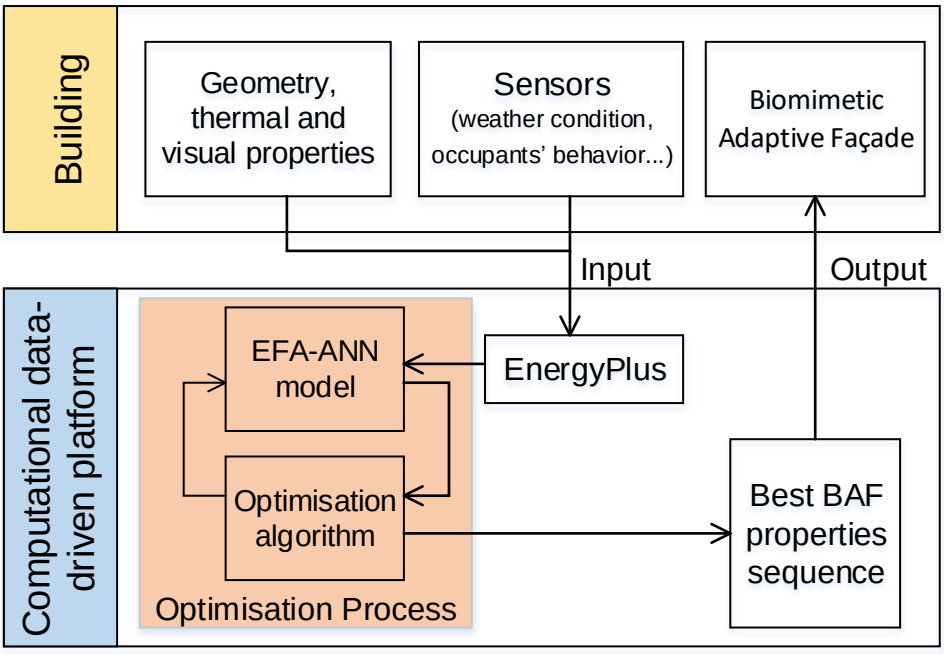

Figure 6-2. The framework of the computational, data-driven platform for designing BAF

The engine of the approach is the data-driven optimisation process, which combines the EFA-ANN model with an optimisation algorithm. The target of the optimisation process is to find the best window properties sequence to minimize energy consumption and satisfy visual comfort requirements, thereby providing a preliminary design of an BAF system. The design

of the BAF in this study can be formulated as an optimisation problem, and the details of this problem have been discussed in chapter 3.

Figure 6-3 shows the data exchanging process of EFA-ANN model and optimisation algorithm in BAF design. It is essential to notice that the training process of EFA-ANN only requires a small amount of building energy simulations, compared to the large number of simulations required in chapter 3 and 4. At the beginning of this process, the optimisation algorithm generates an initial population of properties of the façade system. EFA-ANN model then predicts the energy consumption in the building, which is sent back to the optimisation algorithm. The aim of this process is to find the optimal properties sequence that takes into account the multiple performance criteria of interest, which include minimizing the total energy consumption and satisfying the visual performance condition.

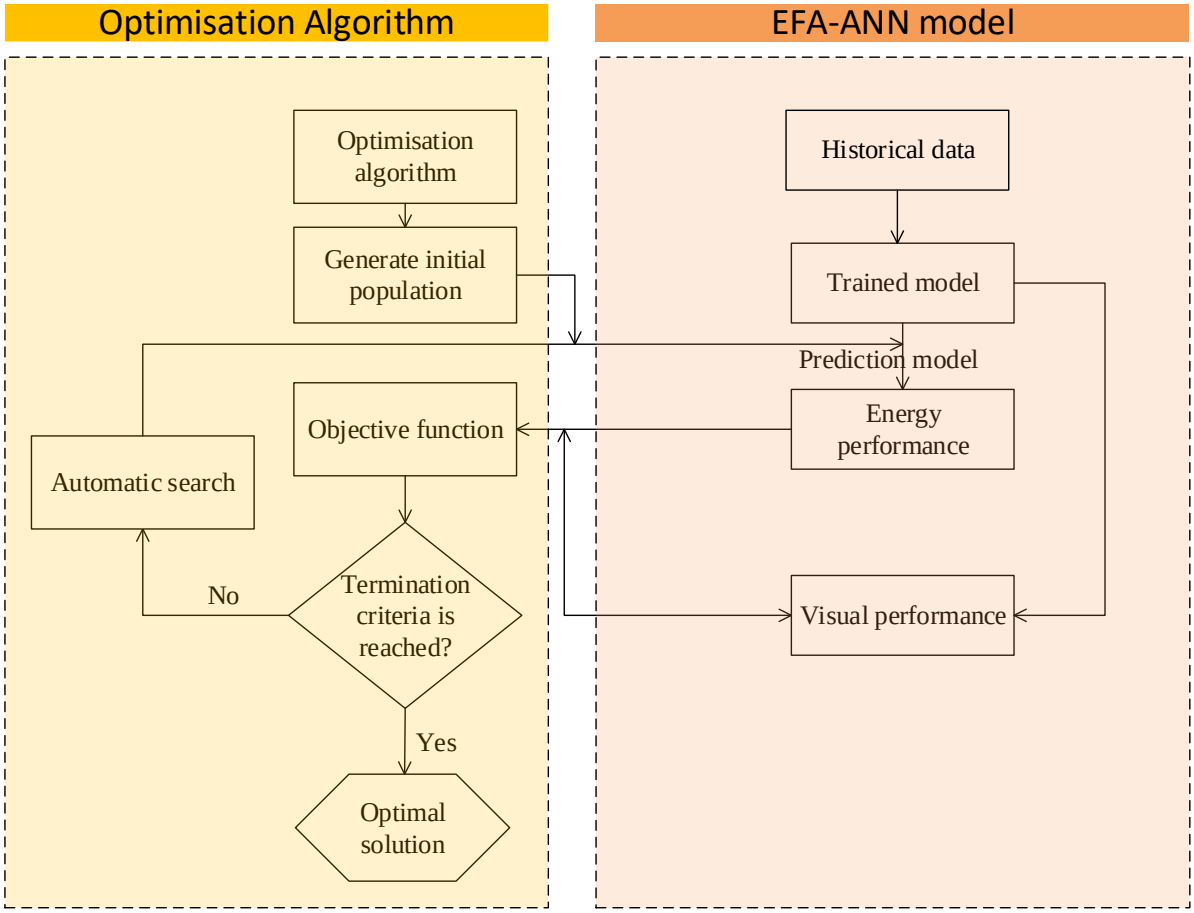

Figure 6-3. The framework of the optimisation process of the computational data-driven platform

6.3 Case study

The same office building, a building benchmark model using by the Department of Energy [9], is used in this chapter. The building has three floors, and the area of each floor is 1660 m^2. The window-to-wall ratio of the building is 60%, as shown in Figure 6-4, and the windows are simulated with a different type of glazing including four states of SageGlass electrochromic glazing and a conventional low-emittance window. Data of the energy consumption for heating, cooling, and lighting are collected in hourly during five working-day in Energyplus with five different properties of the window, so the total of data points is 600. The data has seven inputs, including three properties of window (i.e., U-value, T-vis, SHGC),

two properties of the thermostat (i.e., heating setpoint and cooling setpoint of HAVC system) that are controlled by time (i.e., working hours and non-working hours), and two variables of weather condition(i.e., temperature and direct normal radiation (DNR)). Three outputs, which are heating, cooling and lighting energy, are used for the total energy consumption. Details of all inputs and outputs are shown in Table 6-1. The temperature and direct normal radiation data in this table are from Melbourne.

Table 6-1. Details of all inputs and outputs.

Description	**Unit**	**Parameters**	**Min**	**Max**	**Variable**
U-value	$W/(m^2k)$	X1	3.23	3.53	
SHGC	-	X2	0.19	0.52	
Tvis	-	X3	0.01	0.73	
Heating setpoint	°C	X4	15.00	18.00	Input
Cooling setpoint	°C	X5	25.00	28.00	
Temperature	°C	X6	11.00	32.00	
Direct Normal Radiation (DNR)	Wh/m^2	X7	0.00	594.00	
Heating energy	kJ	Y1	1.53E+04	1.81E+04	
Cooling energy	kJ	Y2	7.75E+03	2.14E+05	Output
Lighting energy	kJ	Y3	9.26E+03	3.09E+04	

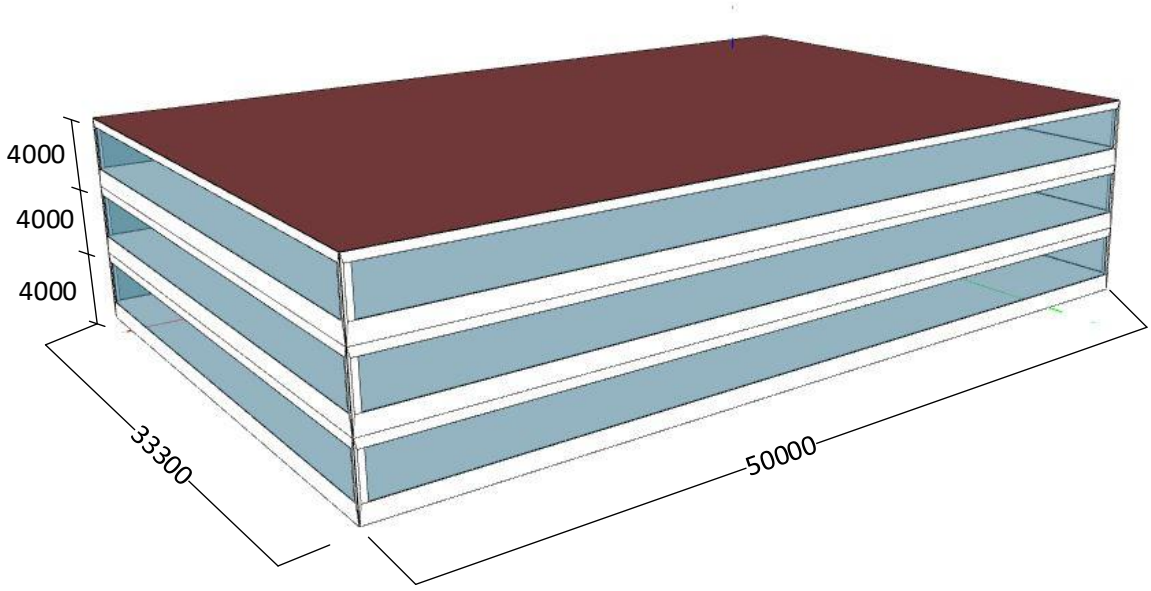

Figure 6-4. Case study: a medium office model

The working-hour is assumed from 8:00 to 17:00 on working days in EnergyPlus simulation. The heating setpoints of the HAVC system are 18 °C during the working hours and 15°C for the non-working hours. For cooling setpoints, the temperature is set to 25°C and 28°C for working hour and non-working hour, respectively. The lighting is scheduled to be on between working hours and the heat gain per floor area for lights is 12.9 (W/m2). There is an illuminance sensor placed at the centre of the room to measure the light intensity. A minimum workplace illuminance of 500 lux is maintained to help people have enough lighting condition for working. A typical meteorological year of Melbourne is used as weather condition for the energy simulation.

Four performance measures are used in this study to validate the performance of the proposed EFA-ANN model in predicting energy consumption in a building. These performance measures are linear correlation coefficient (R), mean absolute error (MAE), root mean square error (RMSE), and mean absolute percentage error (MAPE). Details of these performance measures are discussed in previous studies [10-12] and calculated as below:

$$R = \frac{N \times N_{out} \sum_{n=1}^{N} \sum_{o=1}^{N_{out}} y_{n,o} . \bar{y}_{n,o} - (\sum_{n=1}^{N} \sum_{o=1}^{N_{out}} y_{n,o})(\sum_{n=1}^{N} \sum_{o=1}^{N_{out}} \bar{y}_{n,o})}{\sqrt{N \times N_{out} (\sum_{n=1}^{N} \sum_{o=1}^{N_{out}} y_{n,o}^2) - (\sum_{n=1}^{N} \sum_{o=1}^{N_{out}} y_{n,o})^2} \sqrt{N \times N_{out} (\sum_{n=1}^{N} \sum_{o=1}^{N_{out}} \bar{y}_{n,o}^2) - (\sum_{n=1}^{N} \sum_{o=1}^{N_{out}} \bar{y}_{n,o})^2}} \quad (6.1)$$

$$MAE = \frac{1}{N \times N_{out}} \sum_{n=1}^{N} \sum_{o=1}^{N_{out}} \left| y_{n,o} - \bar{y}_{n,o} \right| \quad (6.2)$$

$$RMSE = \sqrt{\frac{1}{N \times N_{out}} \sum_{n=1}^{N} \sum_{o=1}^{N_{out}} (\bar{y}_{n,o} - y_{n,o})^2} \quad (6.3)$$

$$MAPE = \frac{1}{N \times N_{out}} \sum_{n=1}^{N} \sum_{o=1}^{N_{out}} \left| \frac{y_{n,o} - \bar{y}_{n,o}}{y_{n,o}} \right| \quad (6.4)$$

6.4 Performance evaluation and discussion

The study aims to propose the computational data-driven platform for assisting BAF design and operation. The fundamental difference of the platform, compared to the results presented in chapter 3 and 4, is the integration of data-driven engine, which is backed by the EFA-ANN prediction model. In fact, the EFA-ANN model is the backbone of the proposed platform. Therefore, in order to demonstrate the ability of the proposed platform, this section presents the validation and comparison of EFA-ANN model against direct, computationally expensive simulations using EnergyPlus.

The correlations between all variables of the dataset are calculated by Eq. (6.1) to show the effect of inputs on each target output. These correlation coefficient values are presented by a heatmap, as shown in Figure 6-5. The values range of the correlation coefficient is [-1,1]. Two variables have a high correlation when the absolute value of the correlation coefficient is near to 1. SHGC and Tvis are two inputs with high correlations with the heating energy (i.e., 0.87 for SHGC and 0.86 for Tvis). On the other hand, the temperature has the most impact on

cooling energy with a high correlation coefficient (i.e., 0.96). A high negative correlation (i.e., -0.53) is expected between DNR and lighting energy because increasing amount of DNR will lead to decrease the lighting energy. The correlation heatmap shows that it is reasonable to choose these variables as inputs because they all have correlations with the target outputs.

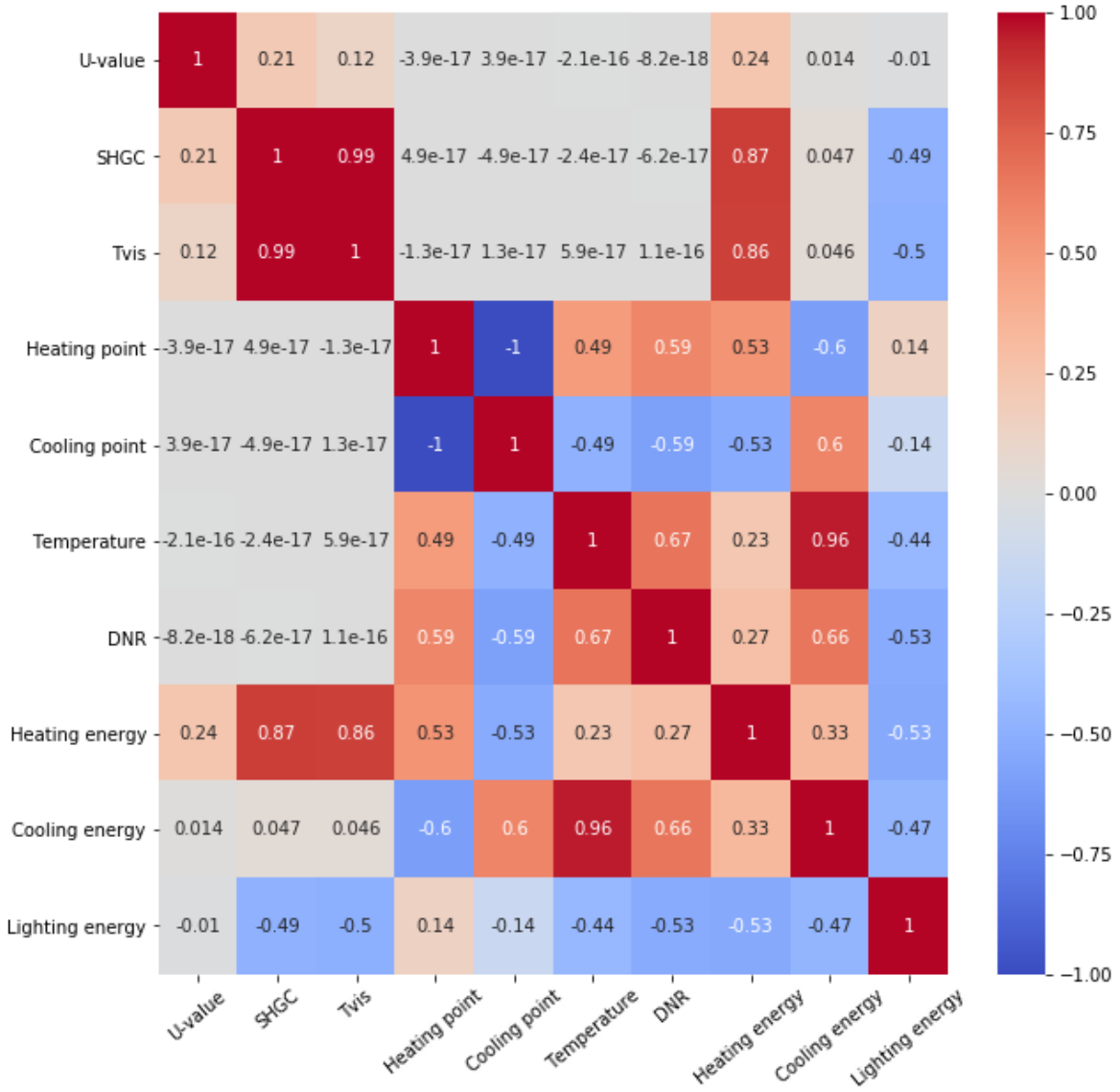

Figure 6-5. A heatmap shows correlations between inputs and target outputs

Table 6-2 shows the performance measures during the training and test phases by EFA-ANN model for heating energy data. The EFA-ANN model has an average R, RMSE, MAE,

and MAPE value of 1.000, 3.27 (kJ), 1.34 (kJ) and 0.01%, respectively, for training data. These measurement values for test data are 0.999 (R), 14.54 kJ (RMSE), 4.09 (MAE) and 0.02% (MAPE) which show the effectiveness of the proposed model. Notably, the best MAPE value obtained by EFA-ANN is 0.01% at fold 3 and fold 8 in the cross-fold validation procedure.

Table 6-2. Performance measures of heating energy obtained by EFA-ANN model.

Fold No.	Training data				Test data			
	R (-)	RMSE (kJ)	MAE (kJ)	MAPE (%)	R (-)	RMSE (kJ)	MAE (kJ)	MAPE (%)
Heating energy								
1	1.000	3.10	1.41	0.01	1.000	8.21	2.99	0.02
2	1.000	1.53	0.75	0.00	0.998	33.99	10.12	0.06
3	1.000	4.17	1.36	0.01	1.000	4.71	1.82	0.01
4	1.000	3.15	1.49	0.01	0.999	34.98	6.34	0.04
5	1.000	1.70	0.82	0.01	1.000	15.20	3.06	0.02
6	1.000	6.66	2.93	0.02	1.000	7.10	3.26	0.02
7	1.000	3.87	1.28	0.01	1.000	13.90	3.99	0.02
8	1.000	4.17	1.52	0.01	**1.000**	**1.82**	**0.98**	**0.01**
9	**1.000**	**0.79**	**0.40**	**0.00**	1.000	14.93	3.88	0.02
10	1.000	3.54	1.47	0.01	1.000	10.59	4.44	0.03
Min	1.000	0.79	0.40	0.00	0.998	1.822	0.980	0.01
Average	1.000	3.27	1.34	0.01	0.999	14.54	4.09	0.02
Max	1.000	6.66	2.93	0.02	1.000	34.98	10.12	0.06
Standard Deviation	0.00	1.67	0.68	0.00	0.00	11.39	2.57	0.02

*__Bold__ is better

The performance measures for cooling energy and lighting energy are shown in Table 6-3 and 6-4, respectively. The results demonstrate that EFA-ANN can make a reasonable prediction on cooling energy and lighting energy with the small average MAPE on the test phase (i.e., 2.43% for cooling energy and 3.40% for lighting energy). In the cross-fold

validation procedure, all folds show the excellent relationship between the actual outputs and the predicted outputs with the linear correlation coefficient (R) values are higher 0.93 in all cases.

Table 6-3. Performance measures of cooling energy obtained by EFA-ANN model.

Fold No.	Training data				Test data			
	R (-)	RMSE (kJ)	MAE (kJ)	MAPE (%)	R (-)	RMSE (kJ)	MAE (kJ)	MAPE (%)
Cooling energy								
1	0.997	1385.20	781.47	1.87	0.957	1514.70	913.94	2.05
2	0.991	1897.20	1009.50	2.24	0.972	4263.30	2092.10	3.53
3	0.995	2053.90	1017.20	2.22	0.966	2140.00	1173.50	2.51
4	0.990	1413.50	778.98	1.92	0.975	2065.40	1100.00	2.47
5	0.994	1431.50	763.00	1.92	**0.981**	**1411.10**	**826.03**	**1.67**
6	0.988	1300.20	754.69	1.80	0.983	2008.60	1184.60	2.92
7	**0.990**	**1249.00**	**693.83**	**1.67**	0.938	2027.50	1015.40	2.04
8	0.994	1230.10	752.78	1.84	0.965	2272.00	1419.80	2.68
9	0.994	1386.00	801.97	2.00	0.967	1945.20	1057.00	2.40
10	0.993	1430.60	882.92	2.12	0.976	1729.20	957.27	2.04
Min	0.988	1230.10	693.83	1.67	0.938	1411.100	826.030	1.67
Average	0.993	1477.72	823.63	1.96	0.968	2137.70	1173.96	2.43
Max	0.997	2053.90	1017.20	2.24	0.983	4263.30	2092.10	3.53
Standard Deviation	0.00	274.58	110.59	0.19	0.01	795.14	362.62	0.53

*__Bold__ is better

Table 6-4. Performance measures of lighting energy obtained by EFA-ANN model

Fold No.	Training data				Test data			
	R (-)	RMSE (kJ)	MAE (kJ)	MAPE (%)	R (-)	RMSE (kJ)	MAE (kJ)	MAPE (%)
Lighting energy								
1	0.991	816.20	419.39	1.92	0.959	811.20	529.59	2.75

2	0.995	796.94	322.02	1.41	0.957	2334.90	867.68	4.77
3	0.990	816.09	372.17	1.72	0.979	1192.10	672.62	3.04
4	0.988	519.50	319.53	1.39	0.940	1985.30	711.47	3.37
5	0.988	814.40	357.82	1.68	0.958	1137.70	635.73	3.70
6	**0.984**	**522.63**	**266.34**	**1.19**	0.991	1032.70	519.71	2.36
7	0.990	781.00	362.41	1.59	0.977	1452.60	757.90	3.10
8	0.982	831.62	395.89	1.79	**0.953**	**829.42**	**509.96**	**2.34**
9	0.980	577.72	311.47	1.53	0.981	5936.60	1256.60	5.02
10	0.990	778.81	345.10	1.59	0.982	1123.80	641.24	3.58
Min	0.980	519.50	266.34	1.19	0.940	811.200	509.960	2.34
Average	0.988	725.49	347.21	1.58	0.968	1783.63	710.25	3.40
Max	0.995	831.62	419.39	1.92	0.991	5936.60	1256.60	5.02
Standard Deviation	0.00	129.98	44.43	0.21	0.02	1539.26	222.70	0.91

*__Bold__ is better

Figure 6-6 shows the correlation between the actual output and predicted output for one case in ten-cross folds of heating, cooling, and lighting energy. The values of R heating energy are almost equal to 1, which indicates that the predicted values from EFA-ANN have a strong correlation with the actual values. Notably, the average MAPE of heating energy is equal to 0.02%, which means that the predicted heating energy is approximately equal to the actual heating energy. In other words, the proposed model can forecast the exact heating energy of the office building. Meanwhile, the average correlation coefficient of cooling energy and lighting energy are smaller than that of heating energy but remains impressive (0.968 for both cooling energy and lighting energy). Therefore, the proposed EFA-ANN is an efficient model for predicting the energy consumption including heating, cooling and lighting energy of a building.

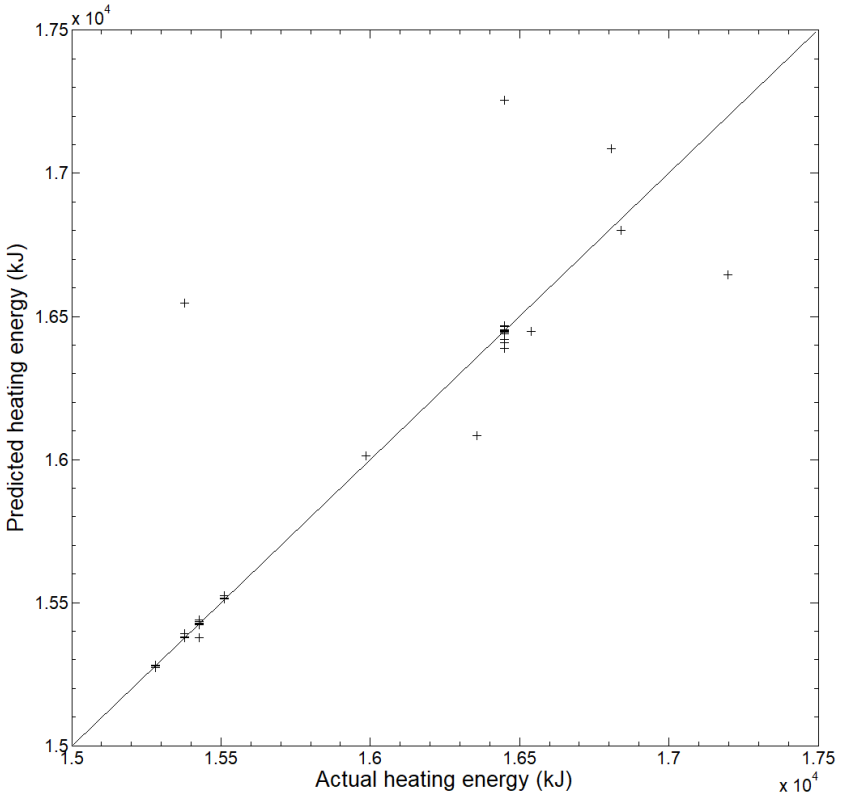
x 10^4
1.75
1.7
1.65
1.6
1.55
1.5
Predicted heating energy (kJ)
1.5
1.55
1.6
1.65
1.7
1.75
Actual heating energy (kJ)
x 10^4

(a)

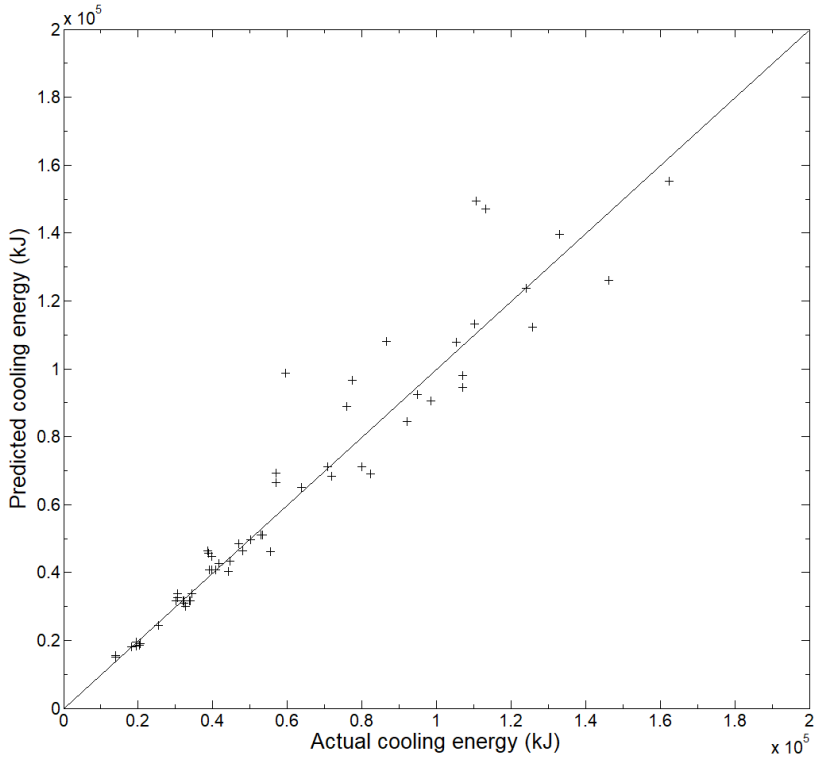
x 10^5
2
1.8
1.6
1.4
1.2
1
0.8
0.6
0.4
0.2
0
Predicted cooling energy (kJ)
0
0.2
0.4
0.6
0.8
1
1.2
1.4
1.6
1.8
2
Actual cooling energy (kJ)
x 10^5

(b)

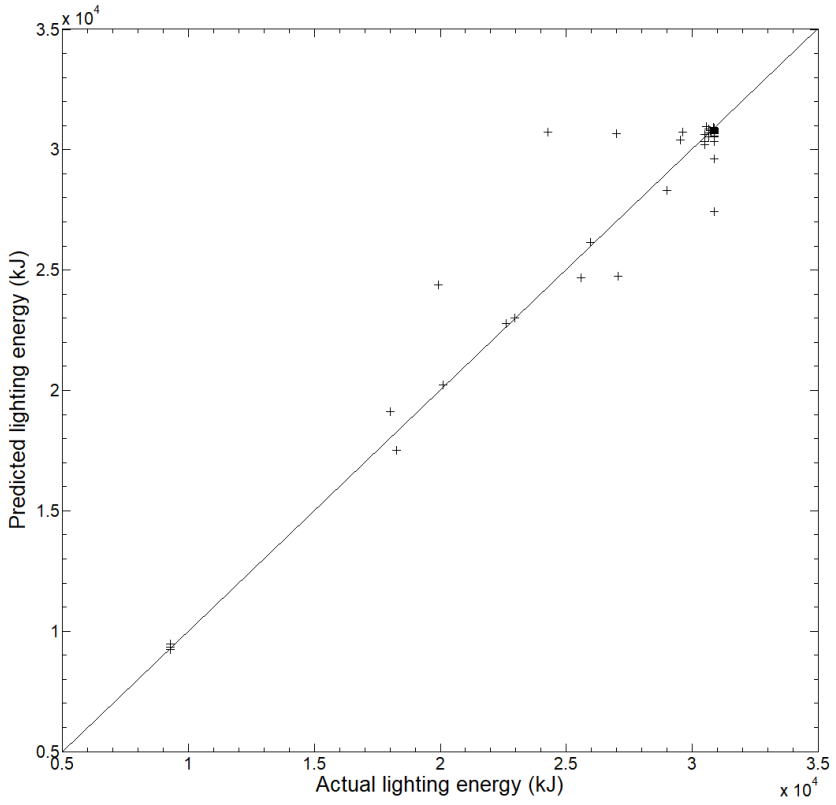

(c)

Figure 6-6. The correlation between the actual and the predicted outputs in the test phase for (a) heating energy, (b) cooling energy, (c) lighting energy.

6.5 Conclusions

This chapter proposed the computational data-driven platform for assisting the design and operation of BAF. In this platform, the data-driven engine is integrated with the computational optimisation approach presented in Chapters 3 and 4. The data-driven engine is based on the machine learning model, namely EFA-ANN. The backbone of the platform is EFA-ANN model, so this chapter validated and compared the EFA-ANN model with the computationally expensive simulations using EnergyPlus to demonstrate the ability of the proposed platform.

A dataset generated by EnergyPlus software with various thermal properties of window, occupants' behaviours, and weather conditions were used to validate EFA-ANN. Additionally, a 10-fold cross-validation method was applied to mitigate the over-fitting problem when evaluating the performance of the proposed model. The prediction results show that EFA-ANN can archive a high accuracy for predicting heating, cooling, and lighting energy. Therefore, EFA-ANN can help to complement building energy simulation in the proposed computational data-driven optimisation approach for assisting the design and operation of BAF for energy-efficient buildings.

References

1. Zemella, G., D. De March, M. Borrotti, and I. Poli, *Optimised design of energy efficient building façades via Evolutionary Neural Networks.* Energy and Buildings, 2011. 43(12): p. 3297-3302.

2. Ihara, T., A. Gustavsen, and B.P. Jelle, *Effect of facade components on energy efficiency in office buildings.* Applied Energy, 2015. 158: p. 422-432.

3. Liu, Z., Y. Liu, B.-J. He, W. Xu, G. Jin, and X. Zhang, *Application and suitability analysis of the key technologies in nearly zero energy buildings in China.* Renewable and Sustainable Energy Reviews, 2019. 101: p. 329-345.

4. Naganathan, H., W.O. Chong, and X. Chen, *Building energy modeling (BEM) using clustering algorithms and semi-supervised machine learning approaches.* Automation in Construction, 2016. 72(Part 2): p. 187-194.

5. Hong, T., J. Kim, J. Jeong, M. Lee, and C. Ji, *Automatic calibration model of a building energy simulation using optimization algorithm.* Energy Procedia, 2017. 105(Supplement C): p. 3698-3704.

6. de Gracia, A., R. Barzin, C. Fernández, M.M. Farid, and L.F. Cabeza, *Control strategies comparison of a ventilated facade with PCM – energy savings, cost reduction and CO2 mitigation.* Energy and Buildings, 2016. 130: p. 821-828.

7. Abediniangerabi, B., S.M. Shahandashti, and A. Makhmalbaf, *A data-driven framework for energy-conscious design of building facade systems.* Journal of Building Engineering, 2020. 29: p. 101172.

8. Martinez, A. and J.-H. Choi, *Exploring the potential use of building facade information to estimate energy performance.* Sustainable Cities and Society, 2017. 35: p. 511-521.

9. (DOE), U.S.D.o.E. *Commercial Reference Buildings*. Available from: https://www.energy.gov/.

10. Chou, J.-S. and D.-K. Bui, *Modeling heating and cooling loads by artificial intelligence for energy-efficient building design.* Energy and Buildings, 2014. 82: p. 437-446.

11. Chou, J.-S., W.K. Chong, and D.-K. Bui, *Nature-Inspired Metaheuristic Regression System: Programming and Implementation for Civil Engineering Applications.* Journal of Computing in Civil Engineering, 2016. 30(5).

12. Bui, D.-K., T. Nguyen, J.-S. Chou, H. Nguyen-Xuan, and T.D. Ngo, *A modified firefly algorithm-artificial neural network expert system for predicting compressive and tensile strength of high-performance concrete.* Construction and Building Materials, 2018. 180: p. 320-333.

Chapter 7
Conclusions and recommendations for future research

This thesis presents the development and evaluation of the computational data-driven platform for the design and application of biomimetic adaptive façade (BAF) systems. The developed platform will help to accelerate the use of BAF for improving building energy efficiency, thereby reducing the environmental impact of the building sector (e.g., reducing greenhouse gas emission). To develop the computational data-driven platform, the thesis presents, improves, and implements different advanced research techniques such as building energy simulation, optimisation algorithms, and data-driven methods.

For the first time, this work addresses the existing limitations on the research area of BAFs, e.g., most studies on BAFs remain at the conceptual stage of development and there is a lack of an effective platform for the design and operation of BAFs. To this end, the thesis employs multi-disciplinary approaches, namely engineered building simulation, mathematical optimisation, and data-driven analytics, to effectively analyse, understand, and design the BAF system. The developed platform was used to assist the design and operation of BAF systems to improve energy efficiency in building. The following sections present a summary of the research activities and findings in this thesis, which is followed by recommendations for future works.

7.1 Biomimetic adaptive façade

Due to the need to reduce the negative environmental impact of energy consumption in buildings, there are many efforts to improve the energy efficiency of the façade system. Among

these developments, BAFs have been recognised as a potential design solution to enhance the energy efficiency of buildings. Through the literature review, it was found that the properties of BAFs should be incorporated with dynamic weather conditions in the energy simulation process. Furthermore, the interaction between thermal and visual performance also needs to be considered in the design and operation of BAFs.

In response to these requirements, a computational optimisation approach, which is built upon building energy modelling and optimisation techniques, is developed in Chapter 3 to explore the potential performance of BAFs for reducing the energy consumption of buildings. To streamline the design of BAFs, the building energy modelling (using EnergyPlus software) is linked with the optimisation process via a Python toolkit. This thesis formulates the operation of BAFs as an optimisation problem. It is different from conventional façade optimisation problems because the optimisation process needs to take into account whole sequences of time-varying BAF properties rather than find only one façade configuration. The proposed approach can find an optimal properties sequence of a BAF with various weather conditions, but still satisfy visual comfort requirements for building occupants.

Chapter 4 presented the design concept and solution of a BAF, which is inspired by the chameleon, for improving the energy efficiency of buildings. A comprehensive analysis of the similarities between the mechanism of a chameleon's skin and a BAF, namely electrochromic glazing, also was provided in this chapter. The computational optimisation approach, which is presented in Chapter 3, was extended with a decision-making assistance tool to design and assess the viability of BAF systems. The results showed that the BAF system could significantly reduce the total energy consumption (by 9.2% - 29.0%), compared to conventional façade systems. The case studies indicated that the BAF has great potential to improve energy efficiency in buildings, thereby reducing the GHG emission of the building sector. The results of this research can be used as a guide to discover future research and development processes

of BAFs. The computational optimisation approach can support the operation of current BAF products in the market (e.g., electrochromic window). This approach can be applied to both new and existing buildings. The proposed approach can be used for residential and non-residential buildings after modifying the model in EnergyPlus (e.g., thermostat setting, material properties of the components, and other characterises of the building). Future works can be conducted with a focus on the following aspects:

- The analysis of BAF systems can be expanded to other performance factors, including the cost of installation and operation or life cycle. Future works can also extend to different aspects of occupant behaviours. This thesis only considers the thermal and visual comfort of occupant behaviour.
- The application of the proposed approach can be expanded to various directions of BAFs such as kinetic components with actuation of movable parts via mechanical systems.

7.2 Data-driven approach

The advantages of data-driven approaches in predicting energy consumption in buildings are well-known. Data-driven approaches can improve existing limitations on modelling building energy consumption such as high time consumption and the requirement of expert experience. In this thesis, Chapter 5 was dedicated to the development of a data-driven approach to complement with the building energy simulation software in the proposed approach. For the first time, this study has developed and investigated a machine learning approach based on the electromagnetism-based firefly algorithm - artificial neural network (EFA-ANN) for predicting the energy consumption in buildings. Then, a sensitivity analysis was performed to identify the input with the most critical impact on the output of each dataset.

This study showed that the proposed model achieved both good results and a short computational time relative to other methods. Therefore, the EFA-ANN can help energy engineers to design energy-efficient buildings while reducing experimental requirements, and it could assist civil engineers and construction managers in the early design phase of energy-efficient buildings. The proposed data-driven approach can also be a useful tool for quickly and accurately solving many problems in engineering, including energy-efficient buildings, construction material strength, and structural strength. In this respect, future work can be conducted with a focus on the following aspects:

- More applications of data-driven methods can be discovered. One promising direction is to use data-driven methods to predict real-time weather conditions or occupant behaviours. It is expected that data-driven methods can handle this problem well as the capacity of machine learning was confirmed in several case studies. This work requires installing sensors inside and outside a building to collect weather conditions and occupant behaviours data. A data-driven model will then be used to analyse these data and provide a prediction for future events. Based on these future events, the proposed approach in the thesis can provide an approximate schedule for the BAF system in the building to minimise the energy consumption.
- It would be beneficial to implement the proposed data-driven approach to discover underlying relationships between thermal behaviour of the façade system and its energy consumption and translate them into useful and applicable rules. These rules then can be used to improve the energy efficiency of other buildings.

7.3 The computational data-driven platform for assisting biomimetic adaptive façade

A computational data-driven platform is proposed in this thesis to improve the effectiveness of the BAF system. The data-driven model is integrated into the design platform

of a BAF to overcome the drawbacks of building energy simulation software related to high time-consumption and the requirement of expert experience. After training energy data, the data-driven model can quickly predict the actual heating energy of the building. With the capacity of the data-driven approach, the computational data-driven platform can assist the design and operation of BAFs for energy-efficient buildings. The computational data-driven platform in this thesis can be a useful tool to solve other complex problems related to the façade system in buildings. In this respect, future work can be conducted with a focus on the following aspects:

- The data-driven approach can be used to understand occupants' behaviours. Therefore, it would be interesting to extend the computational data-driven platform to study the mutual interaction between the building residents and the BAF. In doing so, it is possible to operate BAFs in a direction that can lead to increased satisfaction from the building occupants.
- Future research can focus on the development and trial of actual BAF systems based on the outcome of the proposed computational, data-driven design platform. It is valuable to evaluate the performance of BAF systems to experimentally demonstrate its potential for improving building energy efficiency.

.

Appendix A

A modified firefly algorithm-artificial neural network expert system

[PUBLISHED JOURNAL[4]]

Abstract

The compressive and tensile strength of high-performance concrete (HPC) is a highly nonlinear function of its constituents. The significance of expert frameworks for predicting the compressive and tensile strength of HPC is greatly distinguished in material technology. This study aims to develop an expert system based on the artificial neural network (ANN) model in association with a modified firefly algorithm (MFA). The ANN model is constructed from experimental data while MFA is used to optimize a set of initial weights and biases of ANN to improve the accuracy of this artificial intelligence technique. The accuracy of the proposed expert system is validated by comparing obtained results with those from the literature. The result indicates that the MFA-ANN hybrid system can obtain a better prediction of the high-performance concrete properties. The MFA-ANN is also much faster at solving problems. Therefore, the proposed approach can provide an efficient and accurate tool to predict and design HPC.

1. Introduction

[4] Bui, D.-K., T. Nguyen, J.-S. Chou, H. Nguyen-Xuan, and T.D. Ngo, *A modified firefly algorithm-artificial neural network expert system for predicting compressive and tensile strength of high-performance concrete*. Construction and Building Materials, 2018. 180: p. 320-333.

Nowadays, high-performance concrete (HPC) has many applications in civil engineering, including high-rise buildings, high-speed railways, bridges and extreme loading (e.g., fire, blast, impact) resistance systems [1-11]. HPC has not only high compressive strength but also low permeability, and a high modulus of elasticity. Compared with ordinary concrete, which is composed of three main components including water, fine and coarse aggregates, and cement, HPC is supplemented by an additional cementitious material, for instance, silica fume, nano-silica, blast furnace slag and fly ash to enhance its compressive strength [12-14]. However, the properties of HPC depend on many elements such as mix proportions, material quality and the age of concrete [15].

Therefore, predicting the compressive and tensile strength of HPC is an important task because it can help to schedule operations in the early stages of structural design, thereby reducing experimental requirements. Thus, an accurate method for forecasting the compressive strength of HPC can significantly reduce time and cost. Many researchers have used mechanics-based simulation methods to quantify the strength of concrete [16-21]. Rabczuk *et al.* modeled the fracture of several reinforced concrete structures by using a three-dimensional mesh-free method [17]. Rabczuk and Belytschko applied particle methods to solve several fracture problems involving reinforced concrete structures and the computational results showed good agreement with experimental data [19]. Rabczuk *et al.* proposed a two-dimensional approach to model the fracture of reinforced concrete structures and took into account the interaction between the concrete and the reinforcement [21]. Drzymałaa used a testing method to investigate the effects of high temperatures on the properties of HPC [22]. Zhao *et al.* performed an experimental study on the shrinkage of HPC containing fly ash and ground granulated

blast-furnace slag [23]. In addition, several linear and nonlinear methods were carried out to find the relationship between the key factors, that may influence the compressive strength of HPC such as cement, fly ash, water, superplasticizer and age of testing [15, 24].

However, these methods make it difficult to obtain an accurate regression function because the compressive strength of HPC is affected by many factors. Also, the properties of concrete have a highly nonlinear relationship with its constituents, which poses difficulties in calculating the compressive strength of HPC from available data [25]. As a result, the common methods used for conventional concrete are often unsatisfactory for forecasting the compressive strength of HPC.

Many Artificial intelligence (AI) techniques have been proposed to solve the aforementioned problem. Chou and Pham introduced ensemble models to forecast the compressive strength of HPC [26]. This ensemble model was created by combining many individual AI techniques. Prasad *et al.* used an artificial neural network (ANN) model for predicting the compressive strength of self-compacting concrete and HPC [27]. Naderpour *et al.* predicted the compressive strength of recycled aggregate concrete by using ANN [28]. Ali *et al.* predicted the compressive strength of ordinary concrete and HPC by using the M5P model tree algorithm [29]. These AI techniques disregard any physical interaction between the input and output variables. In addition, the input parameters of the predictive data should be within the range of input parameters of the trained data, which is a shortcoming of these AI models [30]. These are all promising approaches but they are highly dependent on the initial parameters, which is a strong constraint that inhibits their performance.

Therefore, these AI techniques need to be combined with optimization algorithms and hybrid models [31]. Some authors have proposed these models to solve issues in many fields or areas. Nazari and Sanjayan optimized the parameters of a support vector machine to estimate the geopolymer, mortar and concrete compressive strengths [32]. In their research, five meta heuristic algorithms including the ant colony optimization algorithm, genetic algorithm, imperialist competitive algorithm, artificial bee colony optimization algorithm and particle swarm optimization algorithm, were used to optimize the parameters of the support vector machine (SVM). In another study, Marek applied Bayesian inference to a neural network for forecasting the compressive strength of HPC [33].

Among many optimization algorithms, the firefly algorithm is an efficient optimization tool, which was used to optimize machine learning models in many areas of research. Chou *et al.* used firefly algorithm-based least square support vector regression to solve many civil engineering prediction problems [34]. Ibrahim and Khatib optimized the random forests technique using the firefly algorithm and applied this model to forecast hourly global solar radiation [35]. However, using the firefly algorithm for enhancing the capability of artificial neural networks (ANN) has not received much attention, especially in civil engineering.

Therefore, this research seeks to apply the modified firefly algorithm (MFA) to optimize the weights and biases of ANN for effectively predicting the compressive strength of HPC. Specifically, the firefly algorithm has been modified for high dimensional optimization and combined with two smart components such as chaotic map and Lévy flights. Moreover, the parameters of ANN are updated, memorized and optimized by MFA during the training process, so the computing time is remarkably

reduced. This study also aims to validate the expert system by employing the k-fold cross-validation algorithm. Meanwhile, the performance of MFA-ANN will be compared with that of other techniques employed in similar work by hypothesis testing.

The remaining structure of the paper is divided into five sections. The next section presents a literature review on the current research related to prediction of the compressive and tensile strength of HPC by using machine learning technique. Section 3 describes the research methodology and performance evaluation methods. Section 4 outlines the properties that affected the compressive and tensile strength of high-performance concrete and two experimental datasets used in this study. Section 5 subsequently presents data preprocessing, model application, prediction of results of the MFA-ANN, and compares performance of the model with other methods based on the analytical results. The final section will summarize the research and provide concluding remarks.

2. Literature review

Forecasting the mechanical properties of concrete such as compressive strength is an important task in civil engineering because it requires many input parameters from various design practices [36, 37]. An efficient and reliable model for estimating the compressive strength in the early stages of a project can certainly shorten project duration [36]. In recent years, many studies using various approaches for estimating the compressive strength of concrete have been reported [38-41].

Erdal [42] used two-level and hybrid ensembles of decision trees for predicting the compressive strength of HPC. In this study, the author proposed three different ensemble approaches including single ensembles of decision trees, a two-level ensemble approach

and a hybrid ensemble approach. The obtained results demonstrate that the proposed ensemble models could significantly improve the prediction accuracy of the compressive strength of HPC. Another study was conducted by Yuvaraj *et al.* [43], who examined the applicability of support vector regression (SVR) to forecast the fracture characteristics of high strength and ultra-high strength concrete beams. The authors confirmed that SVR could obtain similar results with those from experiments.

Back in 1998, Yeh demonstrated the possibilities of using artificial neural networks (ANN) for predicting the compressive strength of HPC [25]. The author concluded that ANN obtained more accurate results than a model based on regression analysis, and ANN could be used as numerical experiments to review the effects of each ingredient in the concrete mix. In addition, Sobhani *et al.* compared adaptive network-based fuzzy inference systems and ANN models in terms of predicting the compressive strength of no-slump concrete [41]. This study indicated that ANN was more feasible in predicting the 28-day compressive strength of no-slump concrete than the traditional regression models.

However, the performance of ANN depends on the choice of initial weights and biases [44]. To this effect, many optimization algorithms were used to enhance the capability of ANN. Lee *et al.* proposed the harmony search algorithm to determine the near-global optimal initial weights in the training phase of ANN model [44]. Alavi and Gandomi proposed simulated annealing methods for determining the optimal initial weights of ANN [45]. Chang *et al.* used genetic algorithms to find the optimal set of initial weights to enhance the accuracy of ANN [46]. Liu *et al.* implemented the ensemble method to improve the accuracy of the ANN model [47].

The aforementioned studies agree that hybrid models achieve high-performance in solving prediction issues of many areas. Nevertheless, there are several studies on using hybrid models, or specifically, firefly algorithm (FA) based ANN to predict the compressive strength of HPC. FA was successfully used as an optimization algorithm in many studies and obtained high-performance [34, 35, 48, 49]. Moghaddam *et al.* used the support vector machine with FA to predict the fatigue life of polyethylene terephthalate modified asphalt mixtures [48]. Kazemivash and Moghaddam proposed FA based on the regression tree model for digital image watermarking [49]. Therefore, the objective of this study is to fill this gap by using MFA-ANN to predict the compressive and tensile strength of HPC via cross-fold validation and multiple performance measures. This hybrid expert system not only produces better accuracy but can also minimize computational costs compared to other methods reported in the literature.

3. Methodology

3.1 MFA-ANN expert system

3.1.1 Artificial Neuron Network

ANN simulates the function of the biological neuron by imitating the working principles of the human brain. ANN is based on a set of connected units called artificial neurons as illustrated in Figure 1. Each neuron transmits a signal to another neuron by a connection or synapse. Each connection is assigned a weight, which can modify the strength of the signal sent downstream [50, 51]. The construction of ANN can be divided into three main steps: (1) defining inputs and outputs of the problem; (2) training the network by modifying the weights and bias of the input, hidden and output layers; and (3) testing the network performance by comparing predicted values and actual values.

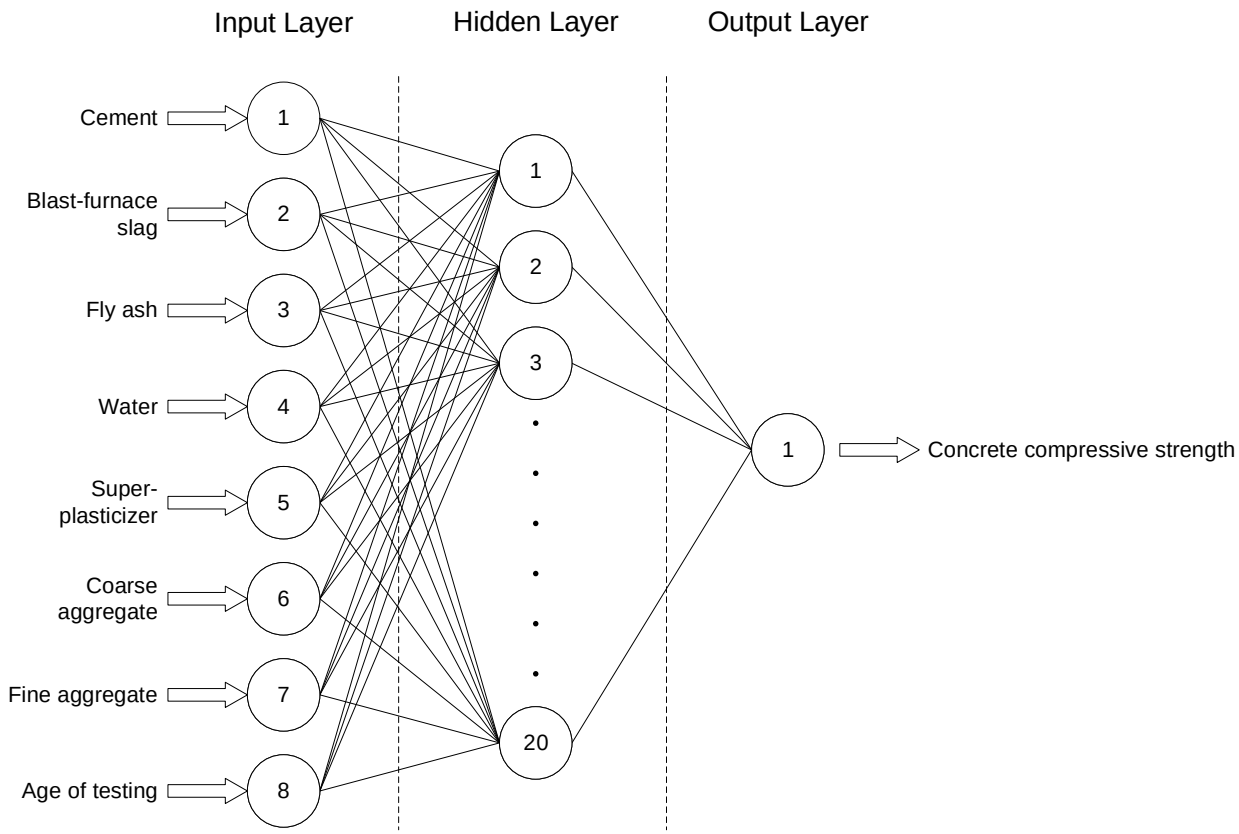

Figure 1. Schematic layout of an artificial neural network for forecasting the compressive strength of concrete.

The signals from the inputs are sent to the hidden nodes and calculated by a linear function (Eq. 1), which depends on the input weights and bias, before they are passed through a transfer function to produce the output of this hidden node [52] as depicted in Figure 2.

$$net_i = \sum_{i=1}^{8} w_{i,j} I_j + b_i \tag{1}$$

where net_i is the value of i^{th} net; I_j is the value of j^{th} input node; $w_{i,j}$ is the weight of the j^{th} input to the i^{th} hidden node; b_i is the bias parameter of the i^{th} hidden node. In this study, the sigmoid function is used as the transfer function (Eq. 2).

$$y_i = f\left(net_i\right) = \frac{1}{1 + exp(-net_i)} \tag{2}$$

where y_i is the output signal of the i^{th} hidden node; $exp(-net_i)$ is Euler's number to the power of $-net_i$.

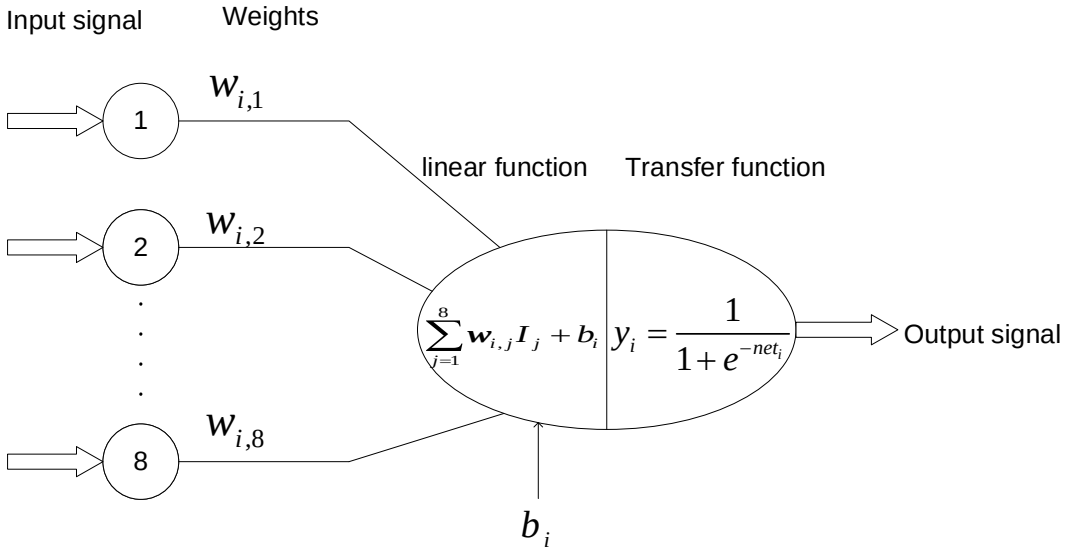

Figure 2. The simple structure of an artificial neuron.

The output from the hidden node is sent to the output layer and calculated by a linear function to output values. Mean square error (MSE) is used to evaluate the training process (objective function). The error E is calculated by:

$$E = \frac{1}{N \times N_{out}} \sum_{n=1}^{N} \sum_{o=1}^{N_{out}} (e_{n,o})^2 \tag{3}$$

where $e_{n,o} = \bar{y}_{n,o} - y_{n,o}$ is the training error at output o when applying instance n; n is the index of the training instance; N is number of instances; o is the index of the output, N_{out} is the number of outputs; is the predicted output by ANN and $\boldsymbol{y}$ is the actual output.

In the next step, the weights and bias parameter are modified to minimize the error E by the learning algorithm. The Levenberg–Marquardt algorithm, which was

independently developed by Kenneth Levenberg and Donald Marquardt [53, 54], is used as the learning algorithm in this study. This algorithm provides a numerical solution to a nonlinear function and is suitable for small and medium size training problems. The updated Levenberg–Marquardt algorithm can be presented as:

$$w^{k+1} = w^k - (J^{k^T} J^k + \mu \bar{I})^{-1} J^{k^T} e^k \tag{4}$$

where is the combination coefficient; $\bar{I}$ is the identity matrix; w^k is the weight matrix at k^{th} iteration and w is a vector of dimension $W \times 1$, with a total number of weights W; w^{k+1} is the weight matrix at $(k+1)^{th}$ iteration and J is Jacobian matrix [55]:

$$J = \overbrace{\quad\quad}^{\text{Node } 1} \cdots \overbrace{\quad\quad}^{\text{Node } i} \cdots$$

$$J = \left[\begin{array}{cccccc}
\frac{\partial e_{1,1}}{\partial w_{1,1}} & \frac{\partial e_{1,1}}{\partial w_{1,2}} & \cdots & \frac{\partial e_{1,1}}{\partial w_{i,1}} & \frac{\partial e_{1,1}}{\partial w_{i,2}} & \cdots \\
\frac{\partial e_{1,2}}{\partial w_{1,1}} & \frac{\partial e_{1,2}}{\partial w_{1,2}} & \cdots & \frac{\partial e_{1,2}}{\partial w_{i,1}} & \frac{\partial e_{1,2}}{\partial w_{i,2}} & \cdots \\
\cdots & \cdots & \cdots & \cdots & \cdots & \cdots \\
\frac{\partial e_{1,N_{out}}}{\partial w_{1,1}} & \frac{\partial e_{1,N_{out}}}{\partial w_{1,2}} & \cdots & \frac{\partial e_{1,N_{out}}}{\partial w_{i,1}} & \frac{\partial e_{1,N_{out}}}{\partial w_{i,2}} & \cdots \\
\cdots & \cdots & \cdots & \cdots & \cdots & \cdots \\
\frac{\partial e_{n,1}}{\partial w_{1,1}} & \frac{\partial e_{n,1}}{\partial w_{1,2}} & \cdots & \frac{\partial e_{n,1}}{\partial w_{i,1}} & \frac{\partial e_{n,1}}{\partial w_{i,1}} & \cdots \\
\cdots & \cdots & \cdots & \cdots & \cdots & \cdots \\
\frac{\partial e_{n,o}}{\partial w_{1,1}} & \frac{\partial e_{n,o}}{\partial w_{1,2}} & \cdots & \frac{\partial e_{n,o}}{\partial w_{i,1}} & \frac{\partial e_{n,o}}{\partial w_{i,1}} & \cdots \\
\cdots & \cdots & \cdots & \cdots & \cdots & \cdots \\
\frac{\partial e_{N,1}}{\partial w_{1,1}} & \frac{\partial e_{N,1}}{\partial w_{1,2}} & \cdots & \frac{\partial e_{N,1}}{\partial w_{i,1}} & \frac{\partial e_{N,1}}{\partial w_{i,2}} & \cdots \\
\frac{\partial e_{N,2}}{\partial w_{1,1}} & \frac{\partial e_{N,2}}{\partial w_{1,2}} & \cdots & \frac{\partial e_{N,2}}{\partial w_{i,1}} & \frac{\partial e_{N,2}}{\partial w_{i,2}} & \cdots \\
\cdots & \cdots & \cdots & \cdots & \cdots & \cdots \\
\frac{\partial e_{N,N_{out}}}{\partial w_{1,1}} & \frac{\partial e_{N,N_{out}}}{\partial w_{1,2}} & \cdots & \frac{\partial e_{N,N_{out}}}{\partial w_{i,1}} & \frac{\partial e_{N,N_{out}}}{\partial w_{i,1}} & \cdots
\end{array}\right]
\begin{array}{ll}
o = 1 & \\
o = 2 & \\
\cdots & n = 1 \\
o = N_{out} & \\
\cdots & \\
o = 1 & \\
\cdots & n = n \\
o = o & \\
\cdots & \\
o = 1 & \\
o = 2 & n = N \\
\cdots & \\
o = N_{out} &
\end{array} \tag{5}$$

where, the number of columns is equal to *W* and each row corresponds to a specified training instance *n* and output *o*; and the error vector *e* has the following form[52]:

$$e = \begin{bmatrix} e_{1,1} \\ e_{1,2} \\ \cdots \\ e_{1,N_{out}} \\ \cdots \\ e_{N,1} \\ e_{N,2} \\ \cdots \\ e_{N,N_{out}} \end{bmatrix} \quad (6)$$

3.1.2 Modified Firefly Algorithm

One recently developed nature-inspired metaheuristics method is the firefly algorithm (FA), which is inspired by the flashing characteristics and behavior of tropical fireflies [56]. This nature-inspired meta heuristic method accurately finds both global and local optima. FA follows three main idealized rules:

(i) Due to the gender of fireflies being unisex, one firefly can be attracted by other fireflies regardless of their gender;

(ii) Attractiveness and brightness are correlative to each other, so the less bright fireflies will be drawn to more brilliant ones. As distance increases, the attractiveness decreases and provided that there is no brighter one than a particular firefly, it will move randomly.

(iii) The brightness of a firefly is measured by the landscape of the objective function.

To solve minimization problems, the brightness can be determined by the objective function. The attractiveness of a firefly can be defined by Eq. (7) and is equivalent to the light intensity of neighboring fireflies

$$\beta^t = \beta_{\min} exp(-\gamma r^2) \tag{7}$$

where β^t is the firefly attractiveness at t^{th} iterations; $\beta_{\min}$ is the firefly attractiveness at $r = 0$; r is the distance between any two fireflies p and q, which is calculated by Eq. (8), and γ is the absorption coefficient ($0 \leq \gamma \leq 1$).

$$r_{pq} = \left\| x_p - x_q \right\| = \sqrt{\sum_{h=1}^{d} (x_{p,l} - x_{q,h})^2} \tag{8}$$

herein, $x_{p,l}$ ($x_{q,h}$) is the l^{th} (h^{th}) component of coordinate x_p (x_q) of the p^{th} (q^{th}) firefly; and d is the search space dimension.

To enhance the capability of the conventional FA, this study uses the Gauss/Mouse map (Eq. (9)) as the chaotic map for tuning the attractive parameters (β). Gandomi *et al.* indicated that the best technique for tuning attractive parameters (β) is the Gauss/Mouse map [57].

$$\text{The Gauss/Mouse map: } \beta_{chaotic}^{t+1} = \begin{cases} 0 & \beta_{chaotic}^{t} = 0 \\ 1/\beta_{chaotic}^{t} \bmod(1) & otherwise \end{cases} \tag{9}$$

where $\beta_{chaostic}^{t}$ is the chaotic number at t^{th} and t denotes the number of iterations, and $\beta_{chaostic}^{o}$ is randomly generated by a uniform distribution in [0, 1]. Eq. (7) is then updated to:

$$\beta^t = (\beta_{chaostic}^{t} - \beta_{\min}) exp(-\gamma r^2) + \beta_{\min} \tag{10}$$

where γ is the absorption coefficient, with γ=1 being the best result [34];

The movement of a firefly p that is attracted to another brighter firefly q is determined by:

$$x_p^{t+1} = x_p^t + \beta^t (x_q^t - x_p^t) + \alpha^t \varepsilon \times L(s) \tag{11}$$

where x_p (x_q) is the coordinate of the p^{th} (q^{th}) firefly; α is a trade-off coefficient to determine the random behavior; ε is a vector of random numbers determined from a Gaussian distribution or uniform distribution, and the simplest form of ε is:

$$\varepsilon = rand - 1/2 \tag{12}$$

where *rand* is a random number generated by a uniform distribution in [0, 1].

To improve the capacity of FA in finding global optima, this study tunes parameter α with an adaptive inertia weight. This effort can keep α within a reasonable range:

$$\alpha^t = \alpha_0 \theta^t \tag{13}$$

where α_0 is the initial trade-off coefficient, α^t is the trade-off coefficient at t^{th} iteration, and θ is the adaptive parameter ($0 < \theta < 1$).

The last component in Eq. 11 is the Lévy distribution, which can be calculated as follows:

$$L(s) \sim s = \frac{u}{|v|^{1/\tau}} \tag{14}$$

where $L(s)$ refers to the Lévy distribution at index τ, s is a power-law distribution, and u and v follow normal distribution and are determined by Eq. (15):

$$u \sim N(0, \sigma_u^2),\ v \sim N(0, \sigma_v^2) \tag{15}$$

where

$$\sigma_u = \left\{ \frac{\Gamma(1+\tau)\sin(\pi\tau/2)}{\Gamma[(1+\tau)/2]\tau 2^{(\tau-1)/2}} \right\}^{1/\tau}, \ \sigma_v = 1 \tag{16}$$

where $\Gamma(z)$ is the Gamma function, which is determined as follows:

$$\Gamma(z) = \int_0^\infty t^{z-1} e^{-t} dt \tag{17}$$

3.1.3 Implementing MFA on ANN

During the first stage, historical data are classified as learning and test data. A set of models are subsequently built from the learning data, and their performances are evaluated by the test data. The trained model in this research is ANN with a Levenberg–Marquardt learning function. The training process of ANN is optimization processing of the connection between neurons in different layers [47]. These connections are weights and biases, and different initial weight and bias values will result in different outputs. Therefore, this study develops an expert system that combines MFA and ANN. MFA is used to optimize the weight and bias vector of ANN and enhance its efficiency.

Before the model is trained, a logistic map is used to generate the initial weights and bias values. The logistic map can not only decrease the probability of a premature occurrence but also provide more diversity compared to randomly selected initial populations [58]. In the following Eq. (18), the logistic map is used instead of random parameters.

Logistic map: $\bar{x}^{t+1} = a\bar{x}^{t}(1-\bar{x}^{t})$ (18)

where $x^{\bar{t}}$ is a chaotic number at $\bar{t}$ and $\bar{t}$ denotes the number of iterations of this process; *a* is the biotic potential; *a* is fixed at 4 [59]; and $x \in (0,1)$, $x_0 \notin \{0.0; 0.25; 0.50; 0.75; 1.0\}$.

The range of the initial weights and bias also affects the search efficiency. The range of populations used in this study is [-0.5, 0.5] because Chang *et al.*[46] showed that this range can obtain better results compared to others employed in the literature. The optimization procedure is automated by using MFA-ANN for simultaneous optimization of ANN parameters and described in Figure 3. In MFA-ANN, the weights and biases of ANN are updated, memorized and optimized to minimize prediction errors. Therefore, MFA-ANN can significantly reduce the computing time in finding global optima. The fitness function of MFA-ANN is the root mean squared error (RMSE), which can be expressed as:

$$f = RMSE_{Validation-data} \tag{19}$$

In this study, the validation data are randomly chosen from 10% of the learning data.

3.2 Optimization Algorithm Evaluation

The optimization algorithm used in the proposed expert system should be evaluated for performance to confirm its capacity. In applied mathematics, a benchmark function is mostly used for the evaluation process. This method uses functions with known optimal solutions to test optimization algorithms. In other words, optimization algorithms try to find optimal solutions of the benchmark function and then compare these solutions with known solutions or those obtained from other algorithms.

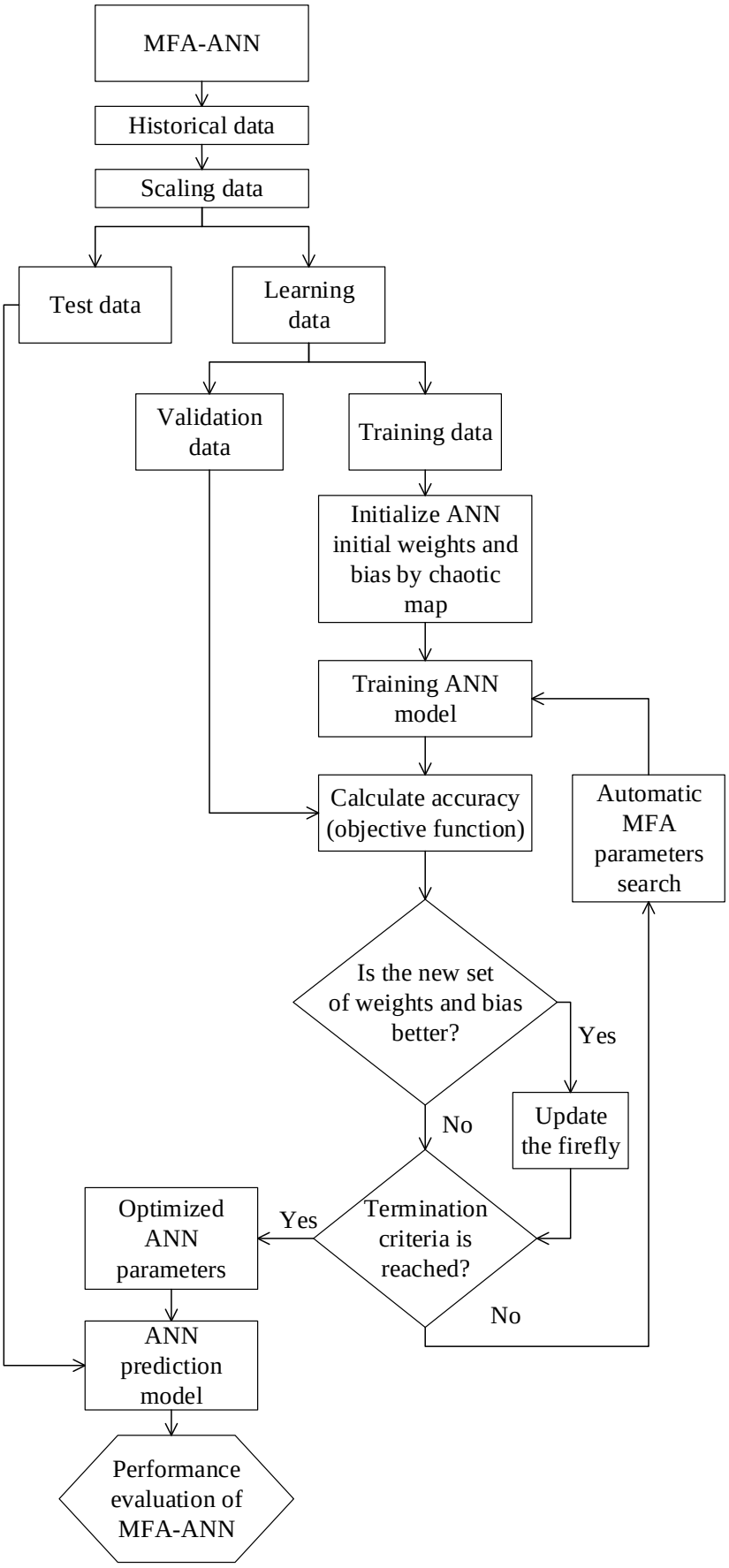
MFA-ANN
Historical data
Scaling data
Test data
Learning data
Validation data
Training data
Initialize ANN initial weights and bias by chaotic map
Training ANN model
Calculate accuracy (objective function)
Automatic MFA parameters search
Is the new set of weights and bias better?
Yes
No
Update the firefly
Termination criteria is reached?
Yes
No
Optimized ANN parameters
ANN prediction model
Performance evaluation of MFA-ANN

Figure 3. MFA-ANN hybrid expert system flowchart.

This study chooses four well-known functions to evaluate the performance of MFA among many widely recognized benchmark functions (Table 1). The performance of MFA is also compared with that of original FA and a notable optimization algorithm, namely the Artificial Bee Colony (ABC) algorithm. ABC is inspired from the intelligent foraging behavior of a honey bee swarm and proposed by Karaboga [60]. In other research, Karaboga and Basturk proved that the performances of ABC are better than those of particle swarm optimization, differential evolution and evaluation algorithms when solving high-dimensional problems [61]. Therefore, we can compare the performance of MFA with that of ABC.

Table 1. Optimized results of numerical benchmark functions.

Benchmark Function	Present MFA		FA [56]		ABC [60]	
	Mean	Standard deviation	Mean	Standard deviation	Mean	Standard deviation
Case 1: Population = 100, Iterations = 1000						
Rastrigin $f_1 = \sum_{i=1}^{D}(x_i^2 - 10\cos(2\pi x_i) + 10);$ $-5.12 \le x \le 5.12$	2.79E+01	4.56E+00	3.59E+01	1.29E+01	**6.20E+00**	**1.11E+00**
Sphere $f_2 = \sum_{i=1}^{D} x_i^2;$ $-100 \le x \le 100$	1.78E-04	6.20E-06	1.72E-02	2.10E-03	**1.11E-05**	**7.15E-06**
Griewank $f_3 = \frac{1}{4000}(\sum_{i=1}^{D}(x_i - 100)^2) - (\prod_{i=1}^{D}\cos(\frac{x_i - 100}{\sqrt{i}})) + 1;$ $-600 \le x \le 600$	**2.86E-04**	**2.24E-05**	6.18E-02	8.80E-03	3.30E-04	4.41E-04
Schwefel's 2.22	7.62E-03	1.06E-03	4.69E-01	1.72E-01	**1.37E-03**	**1.97E-04**

$f_4 = \sum_{i=1}^{D} \lvert x_i \rvert + \prod_{i=1}^{D} \lvert x_i \rvert;$ $-10 \le x \le 10$						
Case 2: Population = 15, Iterations = 15						
Rastrigin						
$f_1 = \sum_{i=1}^{D} (x_i^2 - 10\cos(2\pi x_i) + 10);$ $-5.12 \le x \le 5.12$	**4.09E+02**	**1.40E+01**	4.42E+02	3.44E+01	7.06E+02	3.57E+01
Sphere						
$f_2 = \sum_{i=1}^{D} x_i^2;$ $-100 \le x \le 100$	**1.10E+04**	**2.47E+03**	1.47E+04	4.97E+03	1.10E+05	8.17E+03
Griewank						
$f_3 = \frac{1}{4000}(\sum_{i=1}^{D}(x_i - 100)^2) - (\prod_{i=1}^{D}\cos(\frac{x_i - 100}{\sqrt{i}})) + 1;$ $-600 \le x \le 600$	**8.36E+02**	**1.23E+02**	2.12E+03	4.95E+02	1.02E+03	1.24E+02
Schwefel's 2.22						
$f_4 = \sum_{i=1}^{D} \lvert x_i \rvert + \prod_{i=1}^{D} \lvert x_i \rvert;$ $-10 \le x \le 10$	**6.37E+01**	**4.46E+00**	6.70E+01	9.01E+00	1.32E+02	5.27E+01

*__Bold__ is better

The results of MFA, FA, and ABC, which were used to optimize four benchmark functions under the same conditions, are compared in Table 1. Four functions were run 10 times with 50 dimensions because the study attempts to evaluate the performance of three algorithms for solving high-dimensional problems. In addition, the comparisons are based on two cases including: case #1, which has a population size and a number of iterations of 100 and 1000, respectively; and case #2, which has a population size and a number of iterations of 15 and 15, respectively. In case #1, ABC obtains the best result with the f_1, f_2, and f_4 function while MFA obtains the best result with the f_3 function. In contrast, MFA is the best algorithm for all four functions in case #2. The difference can

be explained by the rapid convergence of MFA to an optimal value, which is faster than ABC.

Fig.4 illustrates the convergence curve of MFA, FA, and ABC in a run of four benchmark functions in case #1. From the convergence curve, it is obvious that MFA can converge in very few iterations while ABC starts to converge after many iterations. Therefore, it can be concluded that MFA is suitable for solving complex problems such as optimizing ANN parameters, which cannot be run with a high population and iterations as case #1 is time-consuming. Besides, the results also demonstrate significant improvements of MFA compared with the original FA because the performance of MFA is much better than the original FA in all cases.

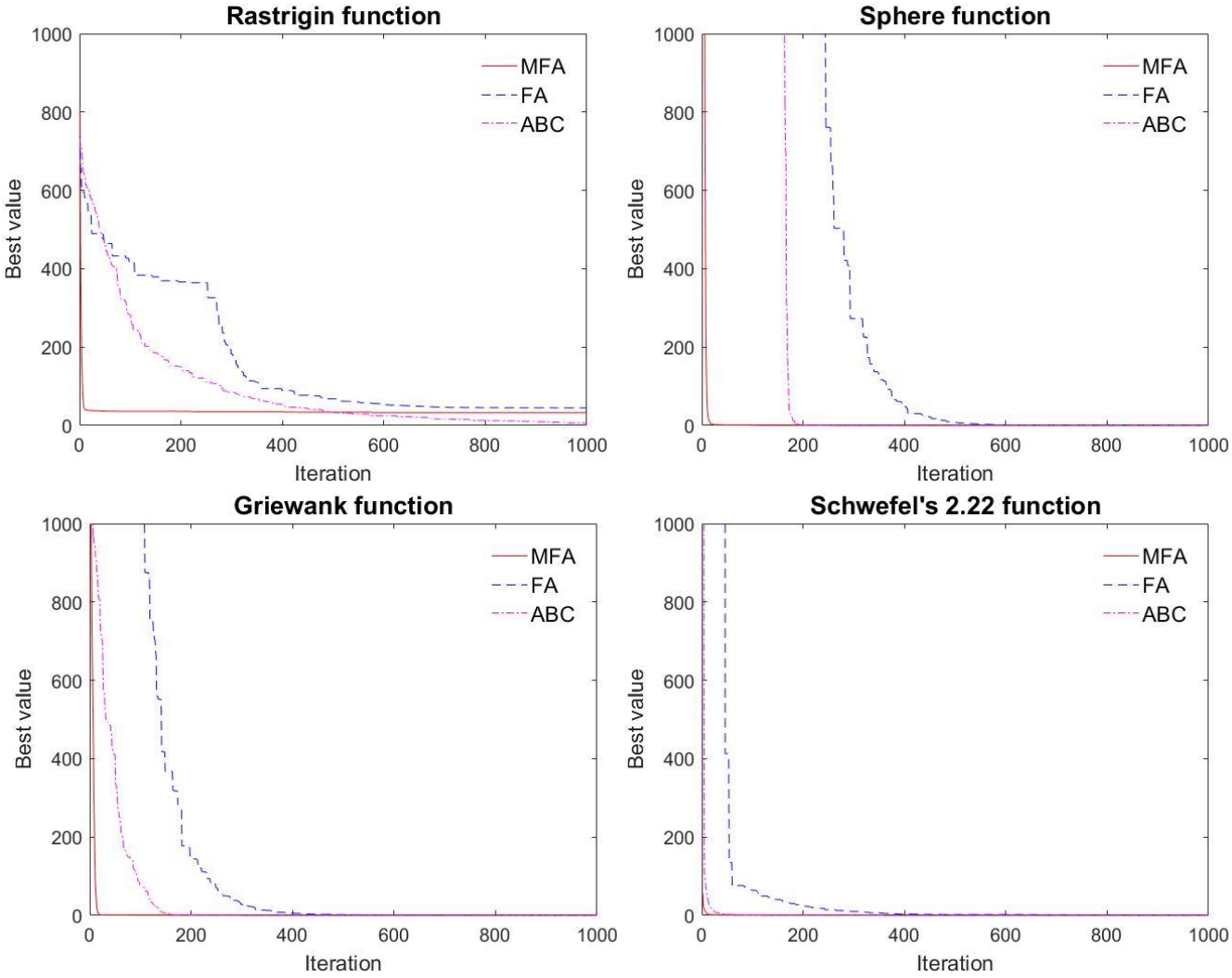

Figure 4. Convergence results of MFA, FA and ABC for four benchmark functions.

3.3 System performance evaluation methods

The performance of the proposed expert system is evaluated by the following performance measures:

- Linear Correlation Coefficient (*R*)

R is the common measure of correlation between the actual data and predicted data. When the actual and predicted data have the same propensity, *R* will equal to 1, which is

the maximum value. The mathematical formula of the linear correlation coefficient R can be represented as follows:

$$R = \frac{N \times N_{out} \sum_{n=1}^{N} \sum_{o=1}^{N_{out}} y_{n,o} . \bar{y}_{n,o} - (\sum_{n=1}^{N} \sum_{o=1}^{N_{out}} y_{n,o})(\sum_{n=1}^{N} \sum_{o=1}^{N_{out}} \bar{y}_{n,o})}{\sqrt{N \times N_{out} (\sum_{n=1}^{N} \sum_{o=1}^{N_{out}} y_{n,o}^2) - (\sum_{n=1}^{N} \sum_{o=1}^{N_{out}} y_{n,o})^2} \sqrt{N \times N_{out} (\sum_{n=1}^{N} \sum_{o=1}^{N_{out}} \bar{y}_{n,o}^2) - (\sum_{n=1}^{N} \sum_{o=1}^{N_{out}} \bar{y}_{n,o})^2}} \quad (20)$$

where y is the actual value; $\bar{y}$ is the predicted value; N is the number of instances; and N_{out} is the number of outputs

- Root Mean Square Error (RMSE):

$$RMSE = \sqrt{\frac{1}{N \times N_{out}} \sum_{n=1}^{N} \sum_{o=1}^{N_{out}} (\bar{y}_{n,o} - y_{n,o})^2} \quad (21)$$

- Mean Absolute Error (MAE):

$$MAE = \frac{1}{N \times N_{out}} \sum_{n=1}^{N} \sum_{o=1}^{N_{out}} \left| y_{n,o} - \bar{y}_{n,o} \right| \quad (22)$$

- Mean Absolute Percentage Error (MAPE):

$$MAPE = \frac{1}{N \times N_{out}} \sum_{n=1}^{N} \sum_{o=1}^{N_{out}} \left| \frac{y_{n,o} - \bar{y}_{n,o}}{y_{n,o}} \right| \quad (23)$$

3.4 Hypothesis Testing

A hypothesis test is a statistical test that is used to determine whether there is sufficient evidence to conclude an assumption. In this study, the assumption is that the results of the proposed method are better or identical to those obtained from other methods. The performance of MFA-ANN is evaluated by using four performance measures including *R*, RMSE, MAE and MAPE by hypothesis testing. In this study, the

null hypothesis *H0* correlated with the results of MFA-ANN ($\bar{\mu}$) is not statistically more accurate than the results from other studies ($\bar{\mu}_0$). Thus, the rejection region must be in the form $\{\bar{\mu} < \bar{\mu}_0\}$ or $\{\bar{\mu} > \bar{\mu}_0\}$ so that $P = (\bar{\mu} = \bar{\mu}_0 | H_0)$ doesn't reach the significance level in the test.

To compare RMSE, MAE and MAPE, this study assumes that the null hypothesis *H0* correlated with mean error rates of the proposed model ($\bar{\mu}$) is larger than those in other studies ($\bar{\mu}_0$). The rejection region must be in the form $\{\bar{\mu} < \bar{\mu}_0\}$ and $P = (\bar{\mu} = \bar{\mu}_0 | H_0)$ reaches the desired significance level in the test. In the correlation *R* comparison, the null hypothesis demonstrates that the mean correlation *R* ($\bar{\mu}$) in the proposed expert system is smaller than that in other works ($\bar{\mu}_0$), and the alternative hypothesis is the denial of *H0*.

4. Data collection

4.1 Dataset 1: Compressive strength of high-performance concrete

The efficiency of the proposed expert system is evaluated using published datasets [25, 62-66]. Database 1 includes a total of 1133 samples of high-performance concrete with one output variable and eight quantitative input variables. Eight inputs are investigated including the amount of cement, water, blast furnace slag, coarse aggregate, fine aggregate, super plasticizers, fly ash and the age of testing, while the compressive strength (in MPa) is the output.

Each input parameter has an effect on the compressive strength of concrete. For example, Johnson and Bawa showed that the compressive strength increases with the age of testing at a fixed water to cement ratio [67]. In addition, an increasing aggregate-

cement ratio will increase the density of concrete, which in turn affects the dynamic modulus and the compressive strength [67]. Furthermore, the effect of each input parameter on the output should also be investigated. For instance, Vu-Bac *et al.* proposed a software framework for quantifying the influence of input parameters on uncertain outputs [68]. Hamdia *et al.* evaluated the sensitivity of input parameters by using a polynomial chaos expansions surrogate model [69]. It is important to note that there are many other parameters that affect the compressive strength of concrete such as slump, forming conditions and curing conditions [15]. However, the main purpose of this research is to evaluate the performance of the proposed MFA-ANN in predicting the compressive strength of high-performance concrete. Hence, the study uses the same eight inputs, one output, and datasets from the literature to obtain appropriate comparisons.

Table 2 shows statistical information of all attributes of dataset 1. The relationship between these components and the compressive strength of HPC is highly nonlinear. Therefore, it is challenging to find the compressive strength of HPC based on these experimental datasets.

Table 2. Statistical parameters for the HPC datasets.

Parameter	Unit	Min.	Max.	Variable
Dataset 1: Compressive strength of high-performance **concrete**				
Cement	kg/m3	102.00	540.00	Input
Blast-furnace slag	kg/m3	0.00	359.40	
Fly ash	kg/m3	0.00	260.00	
Water	kg/m3	121.80	247.00	

Super-plasticizer	kg/m3	0.00	32.20	
Coarse aggregate	kg/m3	708.00	1145.00	
Fine aggregate	kg/m3	594.00	992.60	
Age of testing	Day	1.00	365.00	
Concrete compressive strength	MPa	2.30	82.60	Output
Dataset 2: Splitting tensile strength of concrete with manufactured sand				
Curing age	Day	1.00	388.00	Input
Cubic compressive strength	MPa	4.23	100.50	
splitting tensile strength	MPa	0.35	6.90	Output

The experimental dataset has been used and confirmed in part or in whole in many studies of predictive models (i.e., Gene Expression Programming (GEP), Multi-gene genetic programming (M-GGP), ensemble model between SVR and ANN, and the smart firefly algorithm based on least squares support vector regression). For example, Chou *et al.* used a nature-inspired metaheuristic regression system to estimate the compressive strength of HPC mixtures [34]. Their model obtained a reasonable similarity between predicted values and actual values of the compressive strength of HPC with R= 0.94 and RMSE = 5.62 MPa. They also indicated that their proposed model was better than other conventional methods. Alternatively, our work employs the MFA-ANN hybrid expert system to analyze this experimental dataset.

4.2 Dataset 2: Splitting tensile strength of concrete with manufactured sand

Dataset 2, which is shown in Table 2, consists of 714 data points of the splitting tensile strength of concrete with manufactured sand (MSC) at different curing days, which was collected from previous experimental studies [70]. The ingredients of MSC are ordinary silicate cement, an admixture consisting of fly ash, slag and silica fume, crushed stone and manufactured sand. Zhao *et al.* [71] proposed an empirical equation (Eq. 24) to predict the splitting tensile strength of MSC from the cubic compressive strength. Their model is suitable for predicting the tensile strength of MSC at different curing times.

$$f_{st,k} = \bar{a} f_{cu,\bar{k}}^{\bar{b}} \tag{24}$$

where f_{st} is the splitting tensile strength; f_{cu} is the cubic compressive strength; k is the curing time; and the values of $\bar{a}$ and $\bar{b}$ are listed in Table 3:

Table 3. Fitting values of $\bar{a}$ and $\bar{b}$.

Variable	Unit	Value					
Curing time $\bar{k}$	Days	3	7	28	90	180	1-338
Fit curves $\bar{a}$	-	0.102	0.076	0.166	0.202	0.695	0.217
Fit curves $\bar{b}$	-	0.886	0.982	0.778	0.734	0.450	0.716
Correlation R	-	0.897	0.970	0.924	0.945	0.954	0.926

Two inputs including the curing age and the cubic compressive strength are used to forecast the splitting tensile strength. The curing age ranges from 1 day to 388 days

while the compressive and tensile strength ranges are 4.23-100.5 MPa and 0.35-6.90 MPa, respectively. This study finds the relationship between the splitting tensile strength and the cubic compressive strength of MSC at different curing times including 3-day, 7-day, 28-day, 90-day, 180-day periods, and entire dataset.

5. Performance Evaluation and Discussion

5.1 Data Preprocessing and model application

The results of the performance tests used to predict the compressive and tensile strength of high strength concrete, which were obtained from the MFA-ANN expert system, will be discussed in this section. The K-fold cross-validation method is used in this research to reduce the over-fitting problem in model selection [72]. Kohavi demonstrated that 10-fold is the optimal number of folds that can obtain a good result within an acceptable timeframe [73]. There are several cross-validation methods such as leave-one-out cross-validation and scanning-test-set cross-validation, which could give similar results. For example, Badawy *et al.* used the scanning test set to elect the most representative training and test sample sets in their study [74]. However, several recent publications, which are compared with the results of this study, used the 10-fold cross-validation method in their research [26, 34]. Therefore, the 10-fold cross-validation method is also used in this research to evaluate the performance of the proposed model.

To develop the system for predicting the compressive and tensile strength of HPC, 1133 samples in dataset 1 are randomly selected and split into 10 distinct folds. In the first validation round, the first fold is used for testing while the nine remaining folds are used for training the model. The second fold is then used for testing in the following validation, and this is repeated until all ten validation rounds are completed to guarantee that all data samples are utilized in both the testing and training phases (Figure 5). The

performance of the model is then calculated by taking the average performance of the ten models in ten validation rounds. In order to make a reasonable comparison with the previous study, all data in dataset 2 are used for training and finding a relationship between the tensile and compressive strength of MSC. This study investigates six cases with a curing age of 3-days, 7-days, 28-days, 90-days and 180-days, as well as an entire dataset. The results will be compared with those in the previous study.

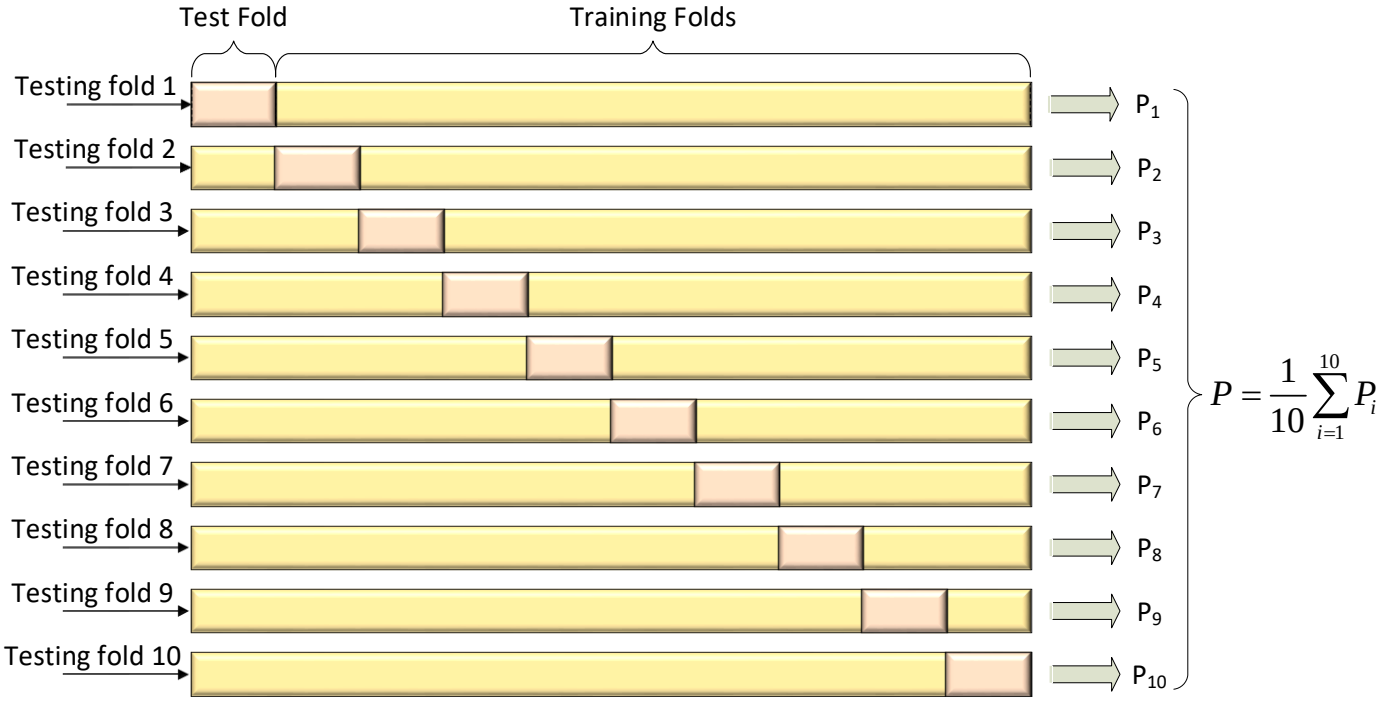

Figure 5. Ten-fold cross-validation.

In training ANN, scaling input and output data in the preprocessing step is essential. The major benefit of this work is to avoid attributes in larger numeric ranges that dominate those in smaller numeric ranges [75]. Another advantage is to prevent numerical difficulties during the calculation. In this study, the data is normalized to the range of [0, 1] using the min-max normalization algorithm, which is represented as follows:

$$x' = \frac{x - \min(x)}{\max(x) - \min(x)} \tag{24}$$

where x is the original value and x’ is the normalized value.

Table 4 lists the parameters for MFA-ANN hybrid expert system. The parameters used in this study are as follows:

- The number of fireflies is 15.
- The maximum generation is 15.
- The objective function is RMSE
- The size of training partition is 90%.
- The validation partition size is 10%.
- The number of hidden layers in ANN is 1.
- The number of nodes in the hidden layer is 20.
- The learning algorithm is Levenberg–Marquardt.
- The transfer function is sigmoid function.
- The parameters of ANN are the default parameters of ANN toolbox in Matlab R2016b software.

Table 4. The MFA-ANN hybrid expert system parameters.

Component	Parameter	Setting
MFA	Max generation	15
	β_{min}	0.1
	γ	1

	α_o	0.2
	Adaptive inertial weight θ	$(10^{-2}/0.9)^{1/MaxGeneration}$
	τ	1.5
	Objective function	RMSE
	Training partition	90%
	Validation partition	10%
	Cross validation	10 folds
ANN	No. of hidden layer	1
	No. of node in hidden layer	20
	Learning algorithm	Levenberg–Marquardt
	Transfer function	Sigmoid

The parameter θ in Table 4 is validated to find the optimal value for this system. In the original FA, Yang [56] proposed a value of $\theta = \left(10^{-5}/0.9\right)^{1/MaxGeneration}$. However, Chou *et al.* proved that $\theta=0.9$ can obtain the best result [34]. Therefore, the parametric test was carried out with several values of θ and Table 5 shows the experimental results obtained for seven case studies using the same dataset. Dataset 1 was used in this test, with 90% of data for learning and 10% of data for testing. From the result in Table 5, the best value of θ for the system is $\left(10^{-2}/0.9\right)^{1/MaxGeneration}$ for which the maximum generation in this study is 15. The reason that this value of θ was different to that of the original FA can be attributed to the difference between a number of generations. In the original FA, Yang used FA to solve simple problems so that the number of generations is high. However, this proposed expert system only used 15 generations thereby requiring a different value of θ, in this case $\theta = \left(10^{-2}/0.9\right)^{1/MaxGeneration}$.

Table 5. Comparison of analytical results using different values of θ.

θ	Performance measure			
	RMSE	MAE	MAPE	R
$(10^{-5}/0.9)^{1/MaxGeneration} \approx 0.47$	4.74	3.35	12.89%	0.958
$(10^{-4}/0.9)^{1/MaxGeneration} \approx 0.54$	5.24	3.70	13.11%	0.947
$(10^{-3}/0.9)^{1/MaxGeneration} \approx 0.64$	4.89	3.38	12.19%	0.954
$(10^{-2}/0.9)^{1/MaxGeneration} \approx 0.74$	**4.34**	**3.32**	**12.10%**	**0.963**
$(10^{-1}/0.9)^{1/MaxGeneration} \approx 0.86$	4.38	3.40	12.55%	0.962
0.9	4.47	3.41	12.10%	0.961
1	4.69	3.63	12.43%	0.956

5.2 Analytical discussion

Table 6 and Table 7 show the performance of the proposed expert system in the prediction of the compressive and tensile strength of HPC. This study also compares the results with other methods reported in previous works. The improvement of MFA-ANN, when compared with other methods, is validated by a hypothesis test.

Table 6. Prediction of performance and improvement rates of the MFA-ANN hybrid expert system for dataset 1.

Method	Performance measure				CT (minutes)	Improved by MFA-ANN system (%)			
	R (-)	RMSE (MPa)	MAE (MPa)	MAPE (%)		R (-)	RMSE (MPa)	MAE (MPa)	MAPE (%)
Dataset 1									
Gene Expression Programming (GEP) [76]	0.91	N/A	5.20	N/A	N/A	4.33*	-	34.30*	-

Multi-gene Genetic Programming (M-GGP) [77]	0.90	7.31	5.48	N/A	N/A	6.31*	33.70*	37.69*	-
Ensemble model (ANN + SVR) [26]	0.94	6.17	4.24	15.20	N/A	1.55**	21.50*	19.39*	23.01*
SFA-LSSVR [34]	0.94	5.62	3.86	12.28	15.90	1.34**	13.76*	11.54*	4.71**
MFA-ANN	0.95	4.85	3.41	11.70	4.60	-	-	-	-

Note: The MFA-ANN hybrid system was run 10 times, and the average result was taken to compare its efficacy with other methods;

CT stands for computing time (minutes).

*, ** indicates significance levels higher than (1%, 5%), respectively;

In dataset 1, Figure 6c shows that the proposed system obtains a lower MAE (3.41 MPa) compared to Gene Expression Programming (GEP) [76], Multi-gene genetic programming (M-GGP) [77], ensemble model (ANN+ SVR) [78] and the smart firefly algorithm-based Least Square Support Vector Regression (SFA-LSSVR) [34] (5.20 MPa, 5.48 MPa, 4.24 MPa and 3.86 MPa, respectively). MFA-ANN also achieves the lowest RMSE (4.85 MPa) and the lowest MAPE (11.70%) compared to other methods (Figure 6b and 6d).

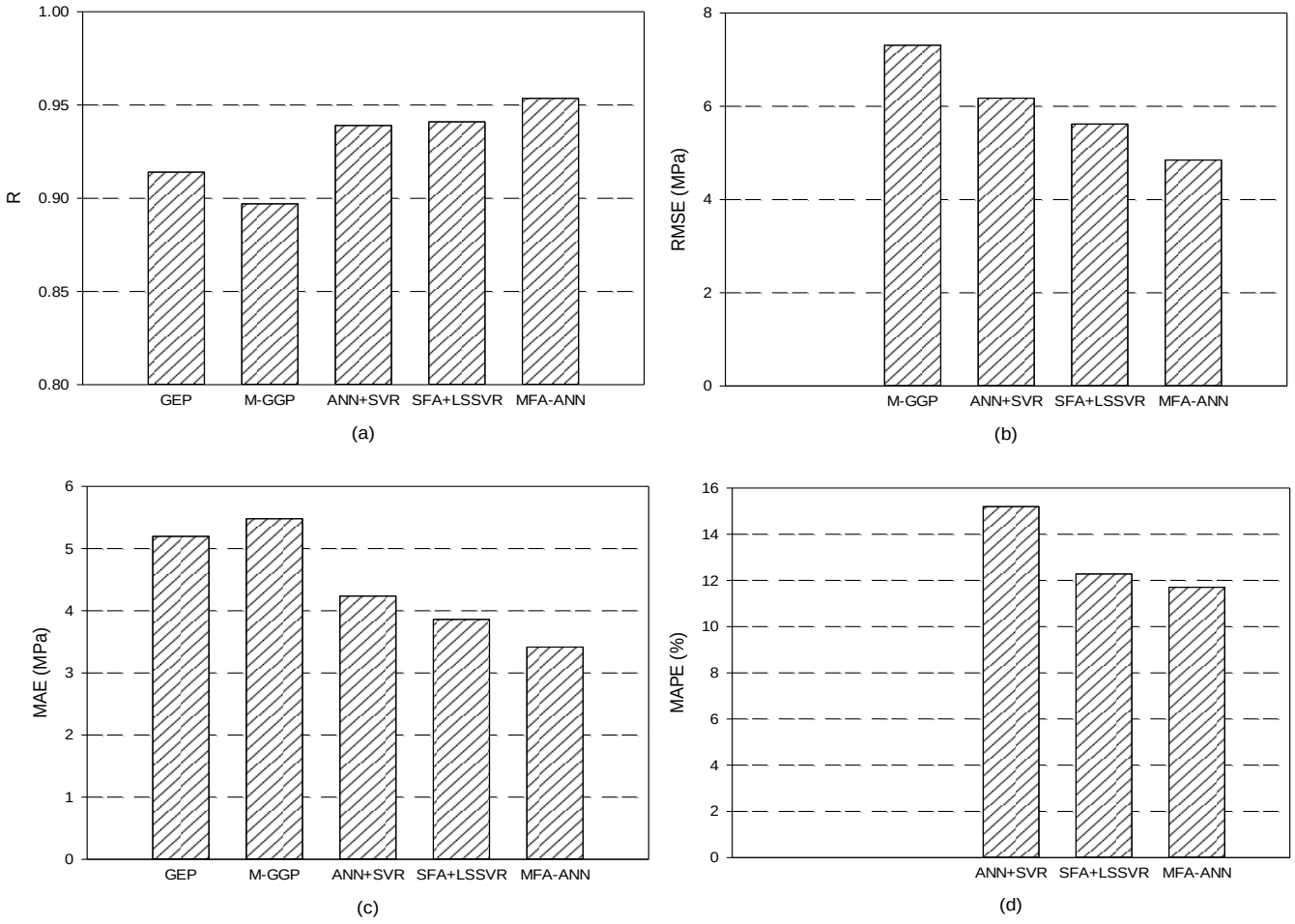

Figure 6. Performance comparison between MFA-ANN and other studies using dataset 1

Overall, the error rates of the proposed expert system are 4.71% - 37.69% better than those of other reported methods. The hypothesis tests also demonstrate that the results of MFA-ANN are significantly (1% - 5%) better than other methods. Also, MFA-ANN has a higher value of R (0.95) than other methods (Figure 6a). This means that the strength of association between the actual output and predicted output of the proposed methods is higher than those in previous studies. Figure 7 shows the correlation between the actual output and predicted output for one case in ten-cross folds.

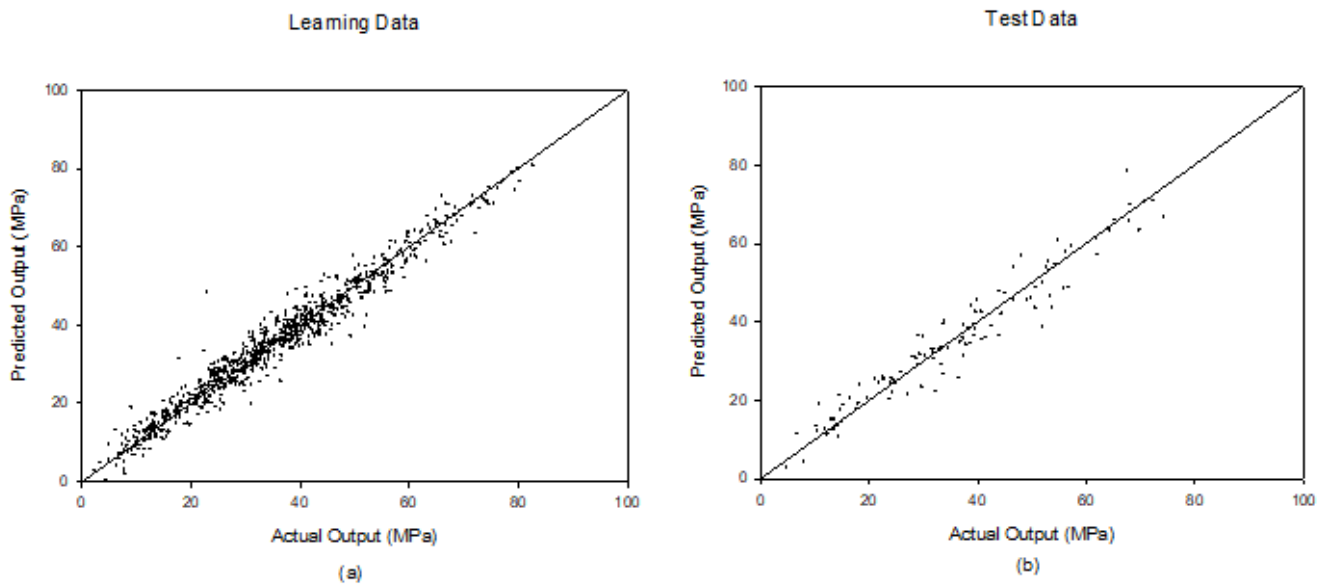

Figure 7. The correlation between actual output and predicted output in the learning data (a) and test data (b).

Moreover, the computing time in running one iteration of cross-fold validation is considerably reduced from 15.90 minutes (by using SFA-LSSVR) to 4.60 minutes (by using MFA-ANN). This time improvement can be attributed to the updating of weight and bias parameters of ANN in the training process. In SFA-LSSVR, the firefly algorithm was used to optimize the regularization and the sigma parameter of the RBF kernel. However, these two parameters are constant during the training process. Meanwhile, in MFA-ANN, the layer weight and bias parameters are updated during the training process of ANN. Moreover, MFA memorizes the updated layer weight and bias parameters, and optimizes them base on the updated value (Figure 3), such that the optimal value can be quickly obtained. Therefore, MFA-ANN is able to significantly reduce computing time when compared with SFA-LSSVR.

Table 7. Prediction performance and improvement rates of the MFA-ANN hybrid expert system for dataset 2.

Method	Performance measure				CT	Improved by MFA-ANN system (%)			
	R (-)	RMSE (MPa)	MAE (MPa)	MAPE (%)	(minutes)	*R* (-)	RMSE (MPa)	MAE (MPa)	MAPE (%)
Dataset 2									
3-day curing age (27 data)									
Fitting curve [71]	0.90	0.34	0.24	13.80	N/A	10.83*	74.74*	90.30*	94.80*
MFA-ANN	0.99	0.09	0.02	0.72	3.38	-	-	-	-
7-day curing age (130 data)									
Fitting curve [71]	0.97	0.32	0.22	12.98	N/A	2.44**	53.88*	59.44*	42.32*
MFA-ANN	0.99	0.15	0.09	7.49	3.75	-	-	-	-
28-days curing age (333 data)									
Fitting curve [71]	0.92	0.46	0.34	12.27	N/A	2.94*	19.18*	20.74*	16.96*
MFA-ANN	0.95	0.37	0.27	10.19	4.05	-	-	-	-
90-days curing age (83 data)									
Fitting curve [71]	0.94	0.35	0.28	10.37	N/A	5.21*	68.67*	77.90*	76.62*
MFA-ANN	0.99	0.11	0.06	2.43	3.50	-	-	-	-
180-day curing age (11 data)									
Fitting curve [71]	0.95	0.14	0.11	2.38	N/A	4.74*	92.51*	95.67*	95.21*
MFA-ANN	1.00	0.01	0.00	0.11	3.01	-	-	-	-
1-388-day curing age (714 data)									
Fitting curve [71]	0.93	0.45	0.35	15.99	N/A	3.62*	16.22*	21.46*	33.81*
MFA-ANN	0.96	0.38	0.28	10.59	4.40	-	-	-	-

Note: MFA-ANN hybrid system was run 10 times, and the average result was taken to compare its efficacy with other methods;

CT stands for computing time (minutes).

*, ** indicates significance levels higher than (1%, 5%), respectively;

In terms of dataset 2, Table 7 shows that the prediction results of MFA-ANN are superior to those of the fitting curve method in all six cases of curing age. The correlation coefficient *R* markedly improves by 2.44 – 10.83% when compared with the previous approach, especially for the 180-day curing period case, where the correlation coefficient *R* of MFA-ANN is almost 1 (the maximum value of R) (Figure 8). RMSE, MAE and MAPE are also better than the previous method by 16.22%-74.74%, 20.74% – 95.67%, and 16.96% - 95.21%, respectively. Figure 8 shows that MFA-ANN does not only have a higher correlation coefficient *R* but also has a smaller error rate than the fitting curve method. Therefore, MFA-ANN can be efficiently used for finding the relationship between the splitting tensile strength and the compressive strength of MSC. The computing time of MFA- ANN depends on a number of data and ranges from 3.01 – 4.40 minutes.

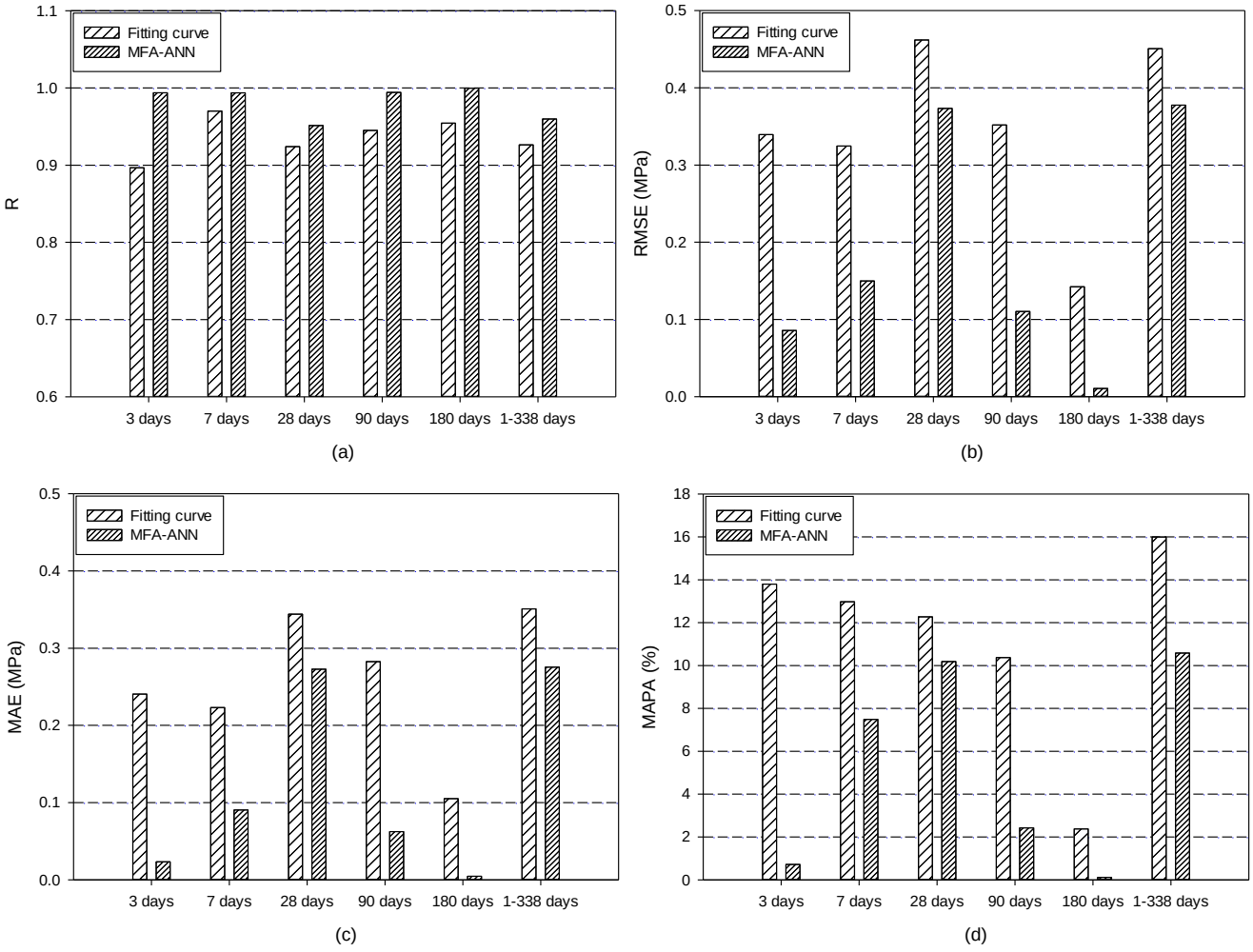

Figure 8. Performance comparison between MFA-ANN and another study in dataset 2.

6. Conclusions

We have for the first time investigated an efficient approach based on MFA-ANN for predicting the compressive and tensile strength of high-performance concrete. Two datasets of high-performance concrete samples from various laboratories are used to investigate the efficiency of the proposed expert system. The number of instances of the two datasets are 1133 and 714 samples, respectively. A 10-fold cross-validation method is used to reduce the overfitting problem of system performance. The accuracy of MFA-

ANN in forecasting the compressive and tensile strength of HPC is analyzed and compared with other methods from previous studies.

Compared to other methods in dataset 1, MFA-ANN has the lowest error rates in terms of RMSE, MAE and MAPE. Moreover, the strength of the relationship between actual outputs and predicted outputs for MFA-ANN is higher than that of other methods because MFA-ANN has the highest correlation R value (0.95). In dataset 2, MFA-ANN is better than the previous method for all six cases of curing age. The error rates improve by 16.96% - 95.67% compared to the fitting curve method while the correlation value R is higher than 0.95 in all cases. Therefore, this work confirms that the proposed system could adequately predict the compressive and tensile strength of HPC, and could substantially lessen the required facility work in the future.

The MFA-ANN hybrid expert system also markedly reduces computing time. This proposed approach can not only improve the accuracy but also run about 3.5 times faster than SFA-LSSVR [34]. The information of fireflies, weight and bias parameters in MFA-ANN are continuously updated, memorized and optimized, which helps the system to quickly converge to an optimal value. Therefore, the proposed expert system can be used as an efficient tool for providing speedy and truthful forecasting.

In addition, this research used one hidden layer with twenty nodes. A higher number of hidden layers or nodes results in more effective training of ANN, but the optimization of weight and bias parameters will take more time. In this study, the proposed expert system achieved not only good results but also short running times. Hence, the number of hidden layer and nodes is acceptable. The proposed approach provides an effective alternative tool for making fast and accurate predictions and thereby suitable for a wide range of problems in engineering.

Acknowledgements

The first author would like to thank the University of Melbourne for offering the Melbourne Research Scholarship. This work was also supported by The ARC Training Centre for Advanced Manufacturing of Prefabricated Housing (CAMP.H) at the University of Melbourne.

References

1. Bezgin, N.Ö., *High performance concrete requirements for prefabricated high speed railway sleepers.* Construction and Building Materials, 2017. 138: p. 340-351.
2. Ng, K.W., J. Garder, and S. Sritharan, *Investigation of ultra high performance concrete piles for integral abutment bridges.* Engineering Structures, 2015. 105: p. 220-230.
3. Nguyen, K.T.Q., T. Ngo, P. Mendis, and D. Heath, *Performance of high-strength concrete walls exposed to fire.* Advances in Structural Engineering, 2017.
4. Ngo, T., S. Fragomeni, P. Mendis, and B. Ta, *Testing of normal-and high-strength concrete walls subjected to both standard and hydrocarbon fires.* ACI Structural Journal, 2013. 110(3): p. 503-503.
5. Ngo, T., P. Mendis, and A. Whittaker, *A Rate Dependent Stress-Strain Relationship Model for Normal, High and Ultra-High Strength Concrete.* International Journal of Protective Structures, 2013. 4(3): p. 451-466.

6. Ngo, T. and P. Mendis, *Modelling the dynamic response and failure modes of reinforced concrete structures subjected to blast and impact loading.* Structural Engineering and Mechanics, 2009. 32(2): p. 269-282.

7. Popa, M., Z. Kiss, H. Constantinescu, and G. Bolca, *Case Study: Designing a 40 Storey High Office Building Using two Variants, with Regular Concrete Columns and with Compound Ultra-High Performance Concrete Columns and Regular Concrete Columns.* Procedia Technology, 2016. 22: p. 40-47.

8. Tanapornraweekit, G., N. Haritos, P. Mendis, and T. Ngo, *Finite element simulation of FRP strengthened reinforced concrete slabs under two independent air blasts.* International Journal of Protective Structures, 2010. 1(4): p. 469-488.

9. Ngo, T., P. Mendis, and T. Krauthammer, *Behavior of ultrahigh-strength prestressed concrete panels subjected to blast loading.* Journal of Structural Engineering, 2007. 133(11): p. 1582-1590.

10. Ngo, T., P. Mendis, A. Gupta, and J. Ramsay, *Blast loading and blast effects on structures–an overview.* Electronic Journal of Structural Engineering, 2007: p. 76-91.

11. Plotzitza, A., T. Rabczuk, and J. Eibl, *Techniques for Numerical Simulations of Concrete Slabs for Demolishing by Blasting.* Journal of Engineering Mechanics, 2007. 133(5): p. 523-533.

12. Papadakis, V.G. and S. Tsimas, *Supplementary cementing materials in concrete: Part I: efficiency and design.* Cement and Concrete Research, 2002. 32(10): p. 1525-1532.

13. Rupasinghe, M., R.S. Nicolas, P. Mendis, M. Sofi, and T. Ngo, *Investigation of strength and hydration characteristics in nano-silica incorporated cement paste.* Cement and Concrete Composites, 2017. 80: p. 17-30.

14. Rupasinghe, M., P. Mendis, T. Ngo, T.N. Nguyen, and M. Sofi, *Compressive strength prediction of nano-silica incorporated cement systems based on a multiscale approach.* Materials & Design, 2017. 115: p. 379-392.

15. Ni, H.-G. and J.-Z. Wang, *Prediction of compressive strength of concrete by neural networks.* Cement and Concrete Research, 2000. 30(8): p. 1245-1250.

16. Rabczuk, T., G. Zi, S. Bordas, and H. Nguyen-Xuan, *A simple and robust three-dimensional cracking-particle method without enrichment.* Computer Methods in Applied Mechanics and Engineering, 2010. 199(37): p. 2437-2455.

17. Rabczuk, T., G. Zi, S. Bordas, and H. Nguyen-Xuan, *A geometrically non-linear three-dimensional cohesive crack method for reinforced concrete structures.* Engineering Fracture Mechanics, 2008. 75(16): p. 4740-4758.

18. Rabczuk, T. and T. Belytschko, *A three-dimensional large deformation meshfree method for arbitrary evolving cracks.* Computer Methods in Applied Mechanics and Engineering, 2007. 196(29): p. 2777-2799.

19. Rabczuk, T. and T. Belytschko, *Application of Particle Methods to Static Fracture of Reinforced Concrete Structures.* International Journal of Fracture, 2006. 137(1): p. 19-49.

20. Rabczuk, T. and T. Belytschko, *Cracking particles: a simplified meshfree method for arbitrary evolving cracks.* International Journal for Numerical Methods in Engineering, 2004. 61(13): p. 2316-2343.

21. Rabczuk, T., J. Akkermann, and J. Eibl, *A numerical model for reinforced concrete structures.* International Journal of Solids and Structures, 2005. 42(5): p. 1327-1354.

22. Drzymała, T., W. Jackiewicz-Rek, M. Tomaszewski, A. Kuś, J. Gałaj, and R. Šukys, *Effects of High Temperature on the Properties of High Performance Concrete (HPC).* Procedia Engineering, 2017. 172: p. 256-263.

23. Zhao, Y., J. Gong, and S. Zhao, *Experimental study on shrinkage of HPC containing fly ash and ground granulated blast-furnace slag.* Construction and Building Materials, 2017. 155: p. 145-153.

24. Erdal, H.I., O. Karakurt, and E. Namli, *High performance concrete compressive strength forecasting using ensemble models based on discrete wavelet transform.* Engineering Applications of Artificial Intelligence, 2013. 26(4): p. 1246-1254.

25. Yeh, I.C., *Modeling of strength of high-performance concrete using artificial neural networks.* Cement and Concrete Research, 1998. 28(12): p. 1797-1808.

26. Chou, J.-S. and A.-D. Pham, *Enhanced artificial intelligence for ensemble approach to predicting high performance concrete compressive strength.* Construction and Building Materials, 2013. 49(0): p. 554-563.

27. Prasad, B.K.R., H. Eskandari, and B.V.V. Reddy, *Prediction of compressive strength of SCC and HPC with high volume fly ash using ANN.* Construction and Building Materials, 2009. 23(1): p. 117-128.

28. Naderpour, H., A.H. Rafiean, and P. Fakharian, *Compressive strength prediction of environmentally friendly concrete using artificial neural networks.* Journal of Building Engineering, 2018. 16: p. 213-219.

29. Behnood, A., V. Behnood, M. Modiri Gharehveran, and K.E. Alyamac, *Prediction of the compressive strength of normal and high-performance concretes using M5P model tree algorithm.* Construction and Building Materials, 2017. 142: p. 199-207.

30. Hamdia, K.M., T. Lahmer, T. Nguyen-Thoi, and T. Rabczuk, *Predicting the fracture toughness of PNCs: A stochastic approach based on ANN and ANFIS.* Computational Materials Science, 2015. 102: p. 304-313.

31. Mosavi, A., T. Rabczuk, and A.R. Varkonyi-Koczy, *Reviewing the Novel Machine Learning Tools for Materials Design*, in *Recent Advances in Technology Research and Education: Proceedings of the 16th International Conference on Global Research and Education Inter-Academia 2017*, D. Luca, L. Sirghi, and C. Costin, Editors. 2018, Springer International Publishing: Cham. p. 50-58.

32. Nazari, A. and J.G. Sanjayan, *Modelling of compressive strength of geopolymer paste, mortar and concrete by optimized support vector machine.* Ceramics International, 2015. 41(9): p. 12164-12177.

33. Słoński, M., *A comparison of model selection methods for compressive strength prediction of high-performance concrete using neural networks.* Computers & Structures, 2010. 88(21): p. 1248-1253.

34. Chou, J.-S., W.K. Chong, and D.-K. Bui, *Nature-Inspired Metaheuristic Regression System: Programming and Implementation for Civil Engineering Applications.* Journal of Computing in Civil Engineering, 2016. 30(5).

35. Ibrahim, I.A. and T. Khatib, *A novel hybrid model for hourly global solar radiation prediction using random forests technique and firefly algorithm.* Energy Conversion and Management, 2017. 138: p. 413-425.

36. Behnood, A., J. Olek, and M.A. Glinicki, *Predicting modulus elasticity of recycled aggregate concrete using M5′ model tree algorithm.* Construction and Building Materials, 2015. 94: p. 137-147.

37. Yuan, Z., L.-N. Wang, and X. Ji, *Prediction of concrete compressive strength: Research on hybrid models genetic based algorithms and ANFIS.* Advances in Engineering Software, 2014. 67: p. 156-163.

38. Thomas, R.J. and S. Peethamparan, *Stepwise regression modeling for compressive strength of alkali-activated concrete.* Construction and Building Materials, 2017. 141: p. 315-324.

39. Dogan, G., M.H. Arslan, and M. Ceylan, *Concrete compressive strength detection using image processing based new test method.* Measurement, 2017. 109: p. 137-148.

40. Rebouh, R., B. Boukhatem, M. Ghrici, and A. Tagnit-Hamou, *A practical hybrid NNGA system for predicting the compressive strength of concrete containing natural pozzolan using an evolutionary structure.* Construction and Building Materials, 2017. 149: p. 778-789.

41. Sobhani, J., M. Najimi, A.R. Pourkhorshidi, and T. Parhizkar, *Prediction of the compressive strength of no-slump concrete: A comparative study of regression, neural network and ANFIS models.* Construction and Building Materials, 2010. 24(5): p. 709-718.

42. Erdal, H.I., *Two-level and hybrid ensembles of decision trees for high performance concrete compressive strength prediction.* Engineering Applications of Artificial Intelligence, 2013. 26(7): p. 1689-1697.

43. Yuvaraj, P., A. Ramachandra Murthy, N.R. Iyer, S.K. Sekar, and P. Samui, *Support vector regression based models to predict fracture characteristics of high strength and ultra high strength concrete beams.* Engineering Fracture Mechanics, 2013. 98: p. 29-43.

44. Lee, A., W.Z. Geem, and K.-D. Suh, *Determination of Optimal Initial Weights of an Artificial Neural Network by Using the Harmony Search Algorithm: Application to Breakwater Armor Stones.* Applied Sciences, 2016. 6(6).

45. Alavi, A.H. and A.H. Gandomi, *Prediction of principal ground-motion parameters using a hybrid method coupling artificial neural networks and simulated annealing.* Computers & Structures, 2011. 89(23): p. 2176-2194.

46. Chang, Y.-T., J. Lin, J.-S. Shieh, and M.F. Abbod, *Optimization the Initial Weights of Artificial Neural Networks via Genetic Algorithm Applied to Hip Bone Fracture Prediction.* Advances in Fuzzy Systems, 2012. 2012: p. 9.

47. Liu, Q., X. Cui, Y.-C. Chou, M.F. Abbod, J. Lin, and J.-S. Shieh, *Ensemble artificial neural networks applied to predict the key risk factors of hip bone fracture for elders.* Biomedical Signal Processing and Control, 2015. 21: p. 146-156.

48. Moghaddam, T.B., M. Soltani, H.S. Shahraki, S. Shamshirband, N.B.M. Noor, and M.R. Karim, *The use of SVM-FFA in estimating fatigue life of polyethylene terephthalate modified asphalt mixtures.* Measurement, 2016. 90: p. 526-533.

49. Kazemivash, B. and M.E. Moghaddam, *A predictive model-based image watermarking scheme using Regression Tree and Firefly algorithm.* Soft Computing, 2017.

50. Singh, T.N., S. Sinha, and V.K. Singh, *Prediction of thermal conductivity of rock through physico-mechanical properties.* Building and Environment, 2007. 42(1): p. 146-155.

51. Lee, S., J. Ha, M. Zokhirova, H. Moon, and J. Lee, *Background Information of Deep Learning for Structural Engineering.* Archives of Computational Methods in Engineering, 2017: p. 1-9.

52. Yu, H. and B. Wilamowski, *Levenberg-Marquardt Training*, in *Intelligent Systems*. 2011, CRC Press. p. 1-16.

53. Levenberg, K., *A METHOD FOR THE SOLUTION OF CERTAIN NON-LINEAR PROBLEMS IN LEAST SQUARES.* Quarterly of Applied Mathematics, 1944. 2(2): p. 164-168.

54. Marquardt, D., *An Algorithm for Least-Squares Estimation of Nonlinear Parameters.* Journal of the Society for Industrial and Applied Mathematics, 1963. 11(2): p. 431-441.

55. Wilamowski, B.M. and Y. Hao, *Neural Network Learning Without Backpropagation.* IEEE Transactions on Neural Networks, 2010. 21(11): p. 1793-1803.

56. Yang, X.-S., *Nature-Inspired Metaheuristic Algorithms*. 2008: Luniver Press. 128.

57. Gandomi, A.H., X.S. Yang, S. Talatahari, and A.H. Alavi, *Firefly algorithm with chaos.* Communications in Nonlinear Science and Numerical Simulation, 2013. 18(1): p. 89-98.

58. Li, Y., S. Deng, and D. Xiao, *A novel Hash algorithm construction based on chaotic neural network.* Neural Computing and Applications, 2011. 20(1): p. 133-141.

59. Hong, W.-C., Y. Dong, L.-Y. Chen, and S.-Y. Wei, *SVR with hybrid chaotic genetic algorithms for tourism demand forecasting.* Applied Soft Computing, 2011. 11(2): p. 1881-1890.

60. Karaboga, D., *An idea based on honey bee swarm for numerical optimization*, in *Technical Report-Tr06*. 2005. p. 1-10.

61. Karaboga, D. and B. Basturk, *On the performance of artificial bee colony (ABC) algorithm.* Applied Soft Computing, 2008. 8(1): p. 687-697.

62. Lim, C.-H., Y.-S. Yoon, and J.-H. Kim, *Genetic algorithm in mix proportioning of high-performance concrete.* Cement and Concrete Research, 2004. 34(3): p. 409-420.

63. Yeh, I.-C., *Modeling slump of concrete with fly ash and superplasticize.* Computers and Concrete, 2008. 5(6): p. 559-572.

64. Carlos, V. and G. Cristian, *Modeling Portland Blast-Furnace Slag Cement High-Performance Concrete.* Materials Journal. 101(5).

65. Pala, M., E. Özbay, A. Öztaş, and M.I. Yuce, *Appraisal of long-term effects of fly ash and silica fume on compressive strength of concrete by neural networks.* Construction and Building Materials, 2007. 21(2): p. 384-394.

66. Siddique, R., P. Aggarwal, and Y. Aggarwal, *Prediction of compressive strength of self-compacting concrete containing bottom ash using artificial neural networks.* Advances in Engineering Software, 2011. 42(10): p. 780-786.

67. de Graft-Johnson, J.W.S. and N.S. Bawa, *Effect of mix proportion, water-cement ratio, age and curing conditions on the dynamic modulus of elasticity of concrete.* Building Science, 1969. 3(3): p. 171-177.

68. Vu-Bac, N., T. Lahmer, X. Zhuang, T. Nguyen-Thoi, and T. Rabczuk, *A software framework for probabilistic sensitivity analysis for computationally expensive models.* Advances in Engineering Software, 2016. 100: p. 19-31.

69. Hamdia, K.M., M. Silani, X. Zhuang, P. He, and T. Rabczuk, *Stochastic analysis of the fracture toughness of polymeric nanoparticle composites using polynomial chaos expansions.* International Journal of Fracture, 2017. 206(2): p. 215-227.

70. Zhao, S., F. Hu, X. Ding, M. Zhao, C. Li, and S. Pei, *Dataset of tensile strength development of concrete with manufactured sand.* Data in Brief, 2017. 11: p. 469-472.

71. Zhao, S., X. Ding, M. Zhao, C. Li, and S. Pei, *Experimental study on tensile strength development of concrete with manufactured sand.* Construction and Building Materials, 2017. 138: p. 247-253.

72. Bishop, C., *Pattern Recognition and Machine Learning*. Information Science and Statistics. 2006, New York: Springer-Verlag.

73. Kohavi, R., *A Study of Cross-Validation and Bootstrap for Accuracy Estimation and Model Selection*. 1995. 1137-1143.

74. Badawy, M.F., M.A. Msekh, K.M. Hamdia, M.K. Steiner, T. Lahmer, and T. Rabczuk, *Hybrid nonlinear surrogate models for fracture behavior of polymeric nanocomposites.* Probabilistic Engineering Mechanics, 2017. 50: p. 64-75.

75. Lin, C.-w.H.a.C.-c.C.a.C.-j., *A practical guide to support vector classification*. 2010: Department of Computer Science, National Taiwan University,Taipei, Taiwan.

76. Mousavi, S.M., P. Aminian, A.H. Gandomi, A.H. Alavi, and H. Bolandi, *A new predictive model for compressive strength of HPC using gene expression programming.* Advances in Engineering Software, 2012. 45(1): p. 105-114.

77. Gandomi, A.H., A.H. Alavi, D.M. Shadmehri, and M.G. Sahab, *An empirical model for shear capacity of RC deep beams using genetic-simulated annealing.* Archives of Civil and Mechanical Engineering, 2013. 13(3): p. 354-369.

78. Chou, J.-S. and A.-D. Pham, *Enhanced artificial intelligence for ensemble approach to predicting high performance concrete compressive strength.* Construction and Building Materials, 2013. 49: p. 554-563.